Journal of Paleontology, 90(5), 2016, p. 854–887

0022-3360/16/0088-0906
doi: 10.1017/jpa.2016.49

Journal of PALEONTOLOGY
A JOURNAL OF THE PALEONTOLOGICAL SOCIETY

Organic-walled microfossils of the mid-Neoproterozoic Alinya Formation, Officer Basin, Australia

Leigh Anne Riedman,[1,2] and Susannah Porter[1]

[1]Department of Earth Science, University of California, Santa Barbara, CA 93106, USA ⟨lriedman@umail.ucsb.edu⟩, ⟨porter@geol.ucsb.edu⟩
[2]New address: Department of Earth and Planetary Sciences, Harvard University, Cambridge, MA 02138, USA ⟨lriedman@fas.harvard.edu⟩

Abstract.—Estimates of Precambrian eukaryotic diversity and disparity indicate broad trends of increase in the Mesoproterozoic Era, leading to a peak and then rapid decline by ca. 750 Ma. The organic-walled microfossil assemblage presented here is representative of that mid-Neoproterozoic height of eukaryotic species richness. Organic-rich shales and siltstones of the mid-Neoproterozoic upper Alinya Formation, eastern Officer Basin, Australia, preserve an abundant and diverse assemblage of organic-walled microfossils deposited in a low-latitude, shallow marine setting. Use of scanning electron microscopy (SEM) revealed an unexpected level of morphological detail not visible in transmitted light microscopy. This led to the recognition of new species as well as establishment of degradational sequences, which aid in fossil recognition. In total, 26 taxa are described here; these include 21 previously named forms, four newly described species (*Caelatimurus foveolatus, Culcitulisphaera revelata*, *Karenagare alinyaensis*, and *Morgensternia officerensis*), and one new combination (*Vidalopalla verrucata*).

Introduction

The Neoproterozoic Era was marked by fluctuations in oceanic and atmospheric chemistry (Meyer and Kump, 2008; Canfield, 2014), dynamic shifts in climate (Pierrehumbert et al., 2011) and carbon cycling (e.g., Rothman et al., 2003; Swanson-Hysell et al., 2010), formation and rifting of the supercontinent Rodinia (Li et al., 2008), and major biological innovations such as the advent of biomineralization and multicellularity (reviewed in Javaux, 2011; Knoll, 2011). Molecular clock analyses suggest divergences of major eukaryotic clades occurred in the middle Mesoproterozoic to early Neoproterozoic (Berney and Pawlowski, 2006; Zimmer et al., 2007; Lücking et al., 2009; Parfrey et al., 2011), and compilations of fossil data (Huntley et al., 2006; Knoll et al., 2006; Cohen and Macdonald, 2015) indicate that eukaryotic diversity and disparity increased steadily during this time, preceding the dramatic drop and biotic turnover that appears to have foreshadowed the Cryogenian snowball Earth glaciations (Riedman et al., 2014).

These eukaryotic diversity trends are based largely upon the fossil record of the acritarchs, a polyphyletic group of spheroidal organic-walled microfossils that compose the bulk of the Precambrian fossil record. As a group, acritarchs are prone to taxonomic problems such as inflation (multiple names given to ontogenetic or taphonomic variants of a single biological taxon) or deflation (a lack of differentiation between similar, often simple, forms). Such taxonomic difficulties lead to uncertainty in the interpretations of eukaryotic diversity trends based upon this record. Early and middle Neoproterozoic acritarchs seem particularly prone to these taxonomic issues, often appearing to lack diagnostic morphological features.

Traditionally, organic-walled microfossils have been studied mainly by use of transmitted light microscopy. A number of studies of Proterozoic acritarchs (e.g., Vidal, 1976, 1979; Butterfield et al., 1994; Arouri et al., 1999; Javaux et al., 2003; Moczydłowska and Willman, 2009; Peng et al., 2009; Pang et al., 2013; Tang et al., 2013; Agić et al., 2015) have utilized other techniques such as scanning and transmission electron microscopy (SEM and TEM) to gather morphological and ultrastructural information, and during the course of this study the taxonomic importance of characterizing micron-scale fossil morphology by SEM quickly became apparent. A number of taxa were found to have micro- and nano-scale morphological details that would have gone undetected by transmitted light. Those specimens (e.g., *Culcitulisphaera revelata* n. gen. n. sp. and *Lanulatisphaera laufeldii* [= *Trachysphaeridium laufeldii*] [Vidal, 1976] Porter and Riedman, 2016, p. 827) might have been counted within form taxa such as *Leiosphaeridia* or mistakenly split into several separate taxa based on taphonomic alteration. Thus, it appears that early to middle Neoproterozoic acritarchs do, in fact, possess taxonomically important morphological details, but they are manifest on a smaller scale than seen in many younger forms. This offers hope that acritarch taxonomic difficulties can be ameliorated, although perhaps not eliminated, leading to more robust assessments of Precambrian eukaryotic diversity trends.

An additional benefit to the increased use of SEM in acritarch studies is the opportunity to characterize taphonomic sequences of these taxa. This not only allowed poorly preserved specimens to be assigned to their proper taxonomic groups but also provided additional information about the structure of the vesicle walls (e.g., remarks in *C. revelata*).

Here we present a systematic description of the organic-walled microfossils of the upper Alinya Formation, an early to middle Neoproterozoic siliciclastic unit from eastern Officer Basin, Australia. This fossil assemblage includes common and long-ranging taxa such as *Valeria lophostriata* Jankauskas, (1979) 1982, taxa such as *C. revelata* that are known from just a few other units, and new taxa for which additional occurrences are equivocal. The Alinya assemblage provides a glimpse of a diverse ecosystem inhabiting a low-latitude (Pisarevsky et al., 2001, 2007), shallow intertidal marine environment during the early to middle Neoproterozoic Era.

Geological setting and age

The Officer Basin (Fig. 1) spans more than 3.5×10^5 km^2 in the states of Western and South Australia and contains ~7 km of Proterozoic sedimentary rocks partially overlain by ~1 km of Phanerozoic deposits including the modern Gibson and Great Victoria Deserts (Grey, 2005). The Officer Basin composes the southwestern portions of a large depositional system known as the Centralian Superbasin (Walter et al., 1995), sedimentation within which initiated in the early Neoproterozoic Era during intracratonic subsidence, perhaps related to rifting associated with break-up of Rodinia (Lindsay and Leven, 1996). The late Neoproterozoic to early Cambrian Petermann Orogeny and Paleozoic Alice Springs Orogeny led to fragmentation of the Centralian Superbasin into the present-day Officer, Amadeus, Ngalia, and Georgina basins (Walter et al., 1995).

The Alinya Formation is a predominantly fine-grained siliciclastic unit that prior to the drilling of the Giles 1 wildcat petroleum well in 1985 was known only from sporadic and deeply weathered outcrops along the northeastern margins of Officer Basin (Zang and McKirdy, 1994). Seismic interpretations suggest the Alinya Formation is 230 m thick in the northern reaches of the basin, thins to ~57 m in the area of Giles 1, and may extend into the Nullarbor Plain to the south (Morton, 1997). Together with the underlying Pindyin Sandstone and locally overlying Coominaree Dolomite and Cadlareena Volcanics, the Alinya Formation is considered an equivalent of the Callanna Group of the Adelaide Rift Complex and Stuart Shelf (Morton, 1997).

The Pindyin Sandstone fines upward from a pebble conglomerate with trough cross bedding and large-scale, low-angle cross bedding indicative of a fluvial setting to finer sands with herringbone cross bedding suggestive of transgression into a peritidal environment (Zang, 1995; Lindsay and Leven, 1996; Morton, 1997). Zang (1995) divided the Alinya Formation into two units, the lower of which is characterized by red-brown to pale green siltstones with sandstone interbeds and common anhydrite, and the upper unit (from which the samples discussed here were collected) comprises stacked cycles of organic-rich siltstones grading into black shales and siltstones with interbedded evaporite deposits and terminating in aeolian sandstones. The upper unit of the Alinya Formation is interpreted to have been deposited in a shallow subtidal to repeatedly inundated coastal sabkha setting (Zang, 1995; Morton, 1997). Zang (1995) also described an assemblage of acritarchs from the Alinya Formation; comparisons with that study are discussed in the following.

Samples of the Alinya Formation were collected from the Giles 1 drill core, currently housed in the Glenside Core Facility, Adelaide. Giles 1 was drilled by Comalco Ltd. as a wildcat exploratory petroleum well in eastern Officer Basin (Fig. 1), South Australia (28°25'54"S, 132°23'12"E) and reached a total depth of 1,326.8 meters, terminating in the Tonian (Grey et al., 2011) aeolian Pindyin Sandstone. In the Giles 1 drill core, the Alinya Formation conformably overlies the Pindyin Sandstone and is, in turn, unconformably overlain by the Ediacaran Tarlina Sandstone; no Cryogenian glacial units are preserved.

Age constraints

There are no direct age constraints on the Alinya Formation. Deposition preceded the onset of the Cryogenian glaciations (ca. 716.5 Ma; Macdonald et al., 2010a), and although absent from the Giles 1 drill core, the Sturtian Chambers Bluff Tillite is found higher in the sequence elsewhere in eastern Officer Basin. Debris of the late Neoproterozoic Acraman bolide impact (Hill et al., 2004) and distinctive Ediacaran acritarch taxa (Willman and Moczydłowska, 2008) are found in the Ungoolya Group stratigraphically above the Alinya Formation within the Giles 1 drill core, providing additional, if broad, minimum age constraints.

According to lithological correlations, the upper unit of the Alinya Formation is considered a lateral facies equivalent of the Coominaree Dolomite, a unit restricted to the Manya Trough in the eastern part of Officer Basin (Fig. 1) and to the western portions of the Adelaide Rift Complex (Morton, 1997; Hill, 2005). Rocks from the Coominaree Dolomite (Manya 5 drill core) have been correlated with those of the lower Bitter Springs Formation of the Amadeus Basin (upper Gillen Member + lower Loves Creek Member by Hill and Walter [2000] and with the lower two-thirds of the Loves Creek Member by Grey and colleagues [2011]) according to carbon and strontium isotopes and stromatolite biostratigraphy (*Acaciella australica* assemblage). The Bitter Springs negative carbon isotope anomaly occurs at the boundary of the Gillen and Loves Creek members of the Bitter Springs Formation (Halverson et al., 2005; Swanson-Hysell et al., 2010) and has been constrained to be no older than 811.5 Ma (Macdonald et al., 2010a). Although no geochemical studies have yet sought the Bitter Springs anomaly in the Alinya Formation, correlation with the Coominaree Dolomite suggests a broad age of 811 to 716.5 Ma for the Alinya Formation.

Discussion

Comparison with previous study of the Alinya Formation.—A previous study of the Alinya Formation by Zang (1995) revealed some of the diversity documented here. Certain forms are held in common between these works and others are not; newly discovered forms include *Caelatimurus foveolatus* n. gen. n. sp., *Culcitulisphaera revelata* n. gen. n. sp., *Karenagare alinyaensis* n. gen. n. sp., *Morgensternia officerensis* n. gen. n. sp., and *Volleyballia dehlerae* Porter and Riedman, 2016. Biostratigraphically significant forms reported by Zang (1995) but not recovered in this study include *Trachyhystrichosphaera aimika* Hermann, 1976 (in Timofeev et al., 1976) emended

https://doi.org/10.1017/jpa.2016.49 Published online by Cambridge University Press

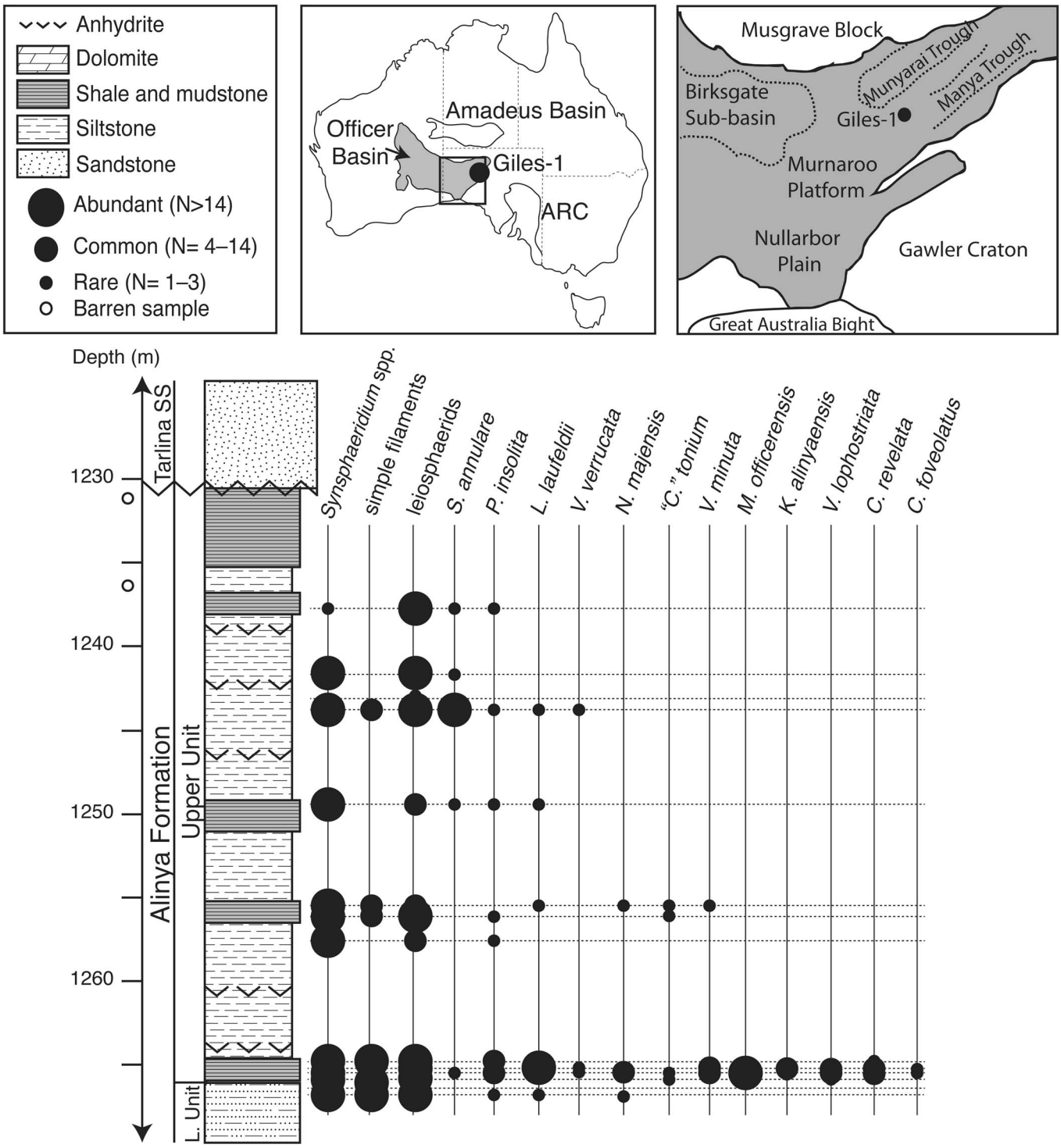

Figure 1. Maps and stratigraphic column of Alinya Formation from Giles 1 drill core and fossil occurrences by sample depth. National map at center top; black box is map of eastern Officer Basin, expanded at right. Amadeus Basin is seen to the north and Adelaide Rift Complex (ARC) to the east (Modified from Zang, 1995; Gravestock, 1997).

by Butterfield et al., 1994, *T. stricta* Hermann, 1989 (in Jankauskas et al., 1989), *T. vidalii* Knoll, 1984, *Cymatiosphaeroides kullingii* Knoll, 1984, and *Vandalosphaeridium* sp. cf. *V. reticulatum* (Vidal, 1976) as well as the vase-shaped microfossils (VSM) *Melanocyrillium* sp.

One of the forms recovered in both studies is '*Comasphaeridium' tonium*, a species named by Zang (1995) from Alinya Formation (the generic assignment is considered dubious by the present authors and placed in quotation marks). Some authors (Willman and Moczydłowska, 2008; Grey et al., 2011)

https://doi.org/10.1017/jpa.2016.49 Published online by Cambridge University Press

have expressed concern about the occurrence of this fossil in the early to middle Neoproterozoic Alinya Formation, arguing that its acanthomorphic ornamentation is more consistent with acritarchs of the Ediacaran Period. However, the specimens illustrated do not conform to any recognized Ediacaran acritarch taxa (Grey et al., 2011), and the concern over these fossils may speak more to an unwarranted assumption that certain morphological characters—rather than monophyletic taxa—define chronostratigraphic intervals (cf. Xiao et al., 1997).

Zang (1995, p. 147) reported large acritarchs attributed to *Trachyhystrichosphaera aimika* with vesicle diameters from 50 to 400 µm and hollow processes up to 70 µm in length, as well as the occurrence of *T. stricta* (synonymized with *T. aimika* by Butterfield et al., 1994), which exhibits vesicle diameters up to 800 µm. No specimens attributable to the genus *Trachyhystrichosphaera,* or with such great dimensions, were observed during the present study. Specimens Zang (1995) attributed to *T. vidalii* (in part; fig. 23C) and *T. stricta* (fig. 25H–J; both synonymized with *T. aimika* by Butterfield et al., 1994) appear to be forms comparable to *Pterospermopsimorpha* sp.; the 'processes' appear to be folds of the outer envelope. Other specimens attributed to *T. vidalii* (fig. 23A, B, D, E) and some left in open nomenclature as *Trachyhystrichosphaera* sp. cf. *T. aimika* (fig. 26E–G) may bear processes but share no similarity with *Trachyhystrichosphaera* spp. The remainder of those left as *T.* sp. cf. *T. aimika* (fig. 26A, B) appear to be fragments of smooth-walled acritarchs overlain by filaments of *Siphonophycus* spp. Similarly, in contrast to Zang's study, no specimens attributable to the genus *Vandalosphaeridium* were observed. Those figured by Zang (*Vandalosphaeridium* sp. cf. *V. reticulatum*; fig. 23F–H) do not conform to the specific diagnosis provided by Vidal (1981) and Vidal and Ford (1985), who described a vesicle bearing widely spaced, funnel-shaped processes supporting an outer membrane. Rather, they appear to be degraded leiosphaerids or portions of aggregates of small spheroidal cells.

Another fossil group recorded in Zang's (1995) study that is of great potential biostratigraphic and paleoecological significance is the vase-shaped microfossil (VSM) *Melanocyrillium* sp. (fig. 25E, F). As a group, VSMs, allied with modern amoebozoan and, possibly, rhizarian testate amoebae (Porter and Knoll, 2000; Porter et al., 2003), are found abundantly and globally in Tonian-age (1 Ga to 720 Ma) rocks. Work by Nagy and colleagues (2009; as well as others cited therein) indicates the acritarch assemblage associated with VSMs is a taxonomically depauperate one dominated by long-ranging taxa such as small leiosphaerids. This is true not only for the Chuar Group, but for other globally distributed assemblages as well where VSMs are seen in association with simple filaments and smooth-walled acritarchs but not with ornamented or acanthomorphic acritarchs. This pattern applies to all reported occurrences of VSMS with the apparent exception of the Draken Formation of Spitsbergen (Knoll et al., 1991; figs. 5.4, 5.5, 7.6) where VSM casts are seen in thin section with fossils identified as *Trachyhystrichosphaera vidalii* (= *T. aimika*). It is possible that a lack of co-occurrences could be due to differences in preferred habitats, but at least in the case of the Chuar Group fossils, VSMs are seen from peritidal to distal subtidal depositional environments, habitats typical of diverse acritarch assemblages. Nagy et al. (2009) suggest the shift seen from a diverse acritarch assemblage to one dominated by smooth-walled leiosphaerids and VSMs is indicative of a major, possibly global biotic signal. Thus the discovery of VSMs in the diverse acritarch assemblage of the Alinya Formation would be noteworthy for paleoecological as well as biostratigraphic reasons. Zang (1995) reported recovery of three *Melanocyrillium* sp. specimens in association with spiny acritarchs from a chert of the lower Alinya Formation collected in outcrop at North Pindyin Hills, northeastern Officer Basin. Although it is possible that the specimens reported by Zang do represent VSMs, it seems more likely (judging from the two figured specimens) that these are torn elongate acritarchs such as *Navifusa* sp. No specimens of any VSM species were recovered during the present study; note, however, this study was restricted to the upper Alinya Formation of the Giles 1 drill core, and comparison of the stratigraphic position of Zang's outcrop chert sample with depths in the Giles 1 drill core is not straightforward.

Biostratigraphy.—Those taxa from the Alinya Formation that have biostratigraphic potential (i.e., they are morphologically distinctive and confidently identified in other units) include *Valeria lophostriata, Culcitulisphaera revelata*, *Caelatimurus foveolatus*, and *Lanulatisphaera laufeldii*. However, all but one of these taxa have long stratigraphic ranges: *V. lophostriata* is seen in the ca. 1.8 Ga Changcheng Group, China (Yan and Liu, 1993), and the 770–742 Ma Chuar Group, USA (Vidal and Ford, 1985; Nagy et al., 2009), and *C. revelata* occurs in the ca. 1 Ga Lakhanda Group, Siberia (Schopf, 1992), and the 770–742 Ma Chuar Group (Nagy et al., 2009; Porter and Riedman, 2016). *C. foveolatus* is a new species described here, but was reported as a sphere with a reticulated surface from the Mesoproterozoic Roper Group of Australia (Peat et al., 1978) and under the name *Turuchanica maculata* from the poorly constrained but probably Mesoproterozoic Muhos Formation of Finland (Tynni and Uutela, 1984). *L. laufeldii* may have the shortest range as it has not been recorded in units older than the middle Neoproterozoic in age; it is seen in the Visingsö Group (Vidal, 1976), the Chuar and Uinta Mountain groups (Vidal and Ford, 1985; Nagy et al., 2009; Porter and Riedman, 2016), and the Kildinskaya Group (Samuelsson, 1997).

Also noteworthy is the absence of certain taxa considered to be index fossils, in particular, *Cerebrosphaera globosa* (= *C. buickii*; see Sergeev and Schopf, 2010 and Porter and Riedman, 2016 for nomenclatural details; Hill and Walter, 2000; Hill et al., 2000; Grey et al., 2011), *Trachyhystrichosphaera aimika* (Butterfield et al., 1994; Samuelsson and Butterfield, 2001; Tang et al., 2013), and *Cymatiosphaeroides kullingii* (Kaufman et al., 1992; Butterfield et al., 1994). Of these, however, *T. aimika* is the least useful as an index taxon as it has a very long stratigraphic range, occurring in the 811–717 Ma upper Fifteenmile Group (formerly Tindir Group; Allison and Awramik, 1989; Macdonald et al., 2010a, b) as well as the >1,005 ± 4 Ma Lakhanda Group (Hermann in Timofeev et al., 1976; Rainbird et al., 1998). *C. kullingii* also occurs in the upper Fifteenmile Group and may be present (noted as only *Cymatiosphaeroides* sp.) in the 900–800 Ma Miroyedikha Formation (Veis et al., 1998). The distinctively wrinkled

https://doi.org/10.1017/jpa.2016.49 Published online by Cambridge University Press

ornamented acritarch *C. globosa* appears to have the shortest ranges of these possible index taxa; its first appearance in Australia is constrained to be ca. 800 Ma (Grey et al., 2011), and the youngest occurrence is in the lower Chuar Group (770–742 Ma; Nagy et al., 2009; Porter and Riedman, 2016).

The biostratigraphic use of the absence of index taxa is complicated by the potential for preservational bias. Although the absence of VSMs from the Alinya assemblage could potentially be caused by laboratory processing, the lack of *C. globosa*, *T. aimika*, and *C. kullingii* from the Alinya assemblage likely reflect primary absence from the biota due to either environmental or stratigraphic reasons. These fossils are relatively large (usually > 100 µm, often as large as 700 µm) and conspicuous, and even fragments of them are recognizable. This argument is particularly apt with regard to *C. globosa,* which is both robust and distinctive; even very small fragments of *C. globosa* can be identified.

Diversity patterns from this study.—Fossil abundance and taxonomic diversity covary throughout the sample suite (Fig. 2), suggesting diversity changes may simply be artifacts of changes in fossil abundance. However, standardized diversity—measured as the taxonomic diversity of a subsample composed of the first twenty specimens encountered during light microscopy—is also positively correlated with sample diversity. This suggests that fluctuations in diversity are genuine.

The greatest taxonomic diversity was found in the lowest part of the upper Alinya Formation (1,265.36–1,265.71 m; Figs. 1, 2). Samples from the uppermost parts of this formation host a greater proportion of smooth-walled spheroids (leiosphaerids), colonies of cells, and simple filaments; few ornamented acritarchs occur in these rocks. We suspect that the absence of ornamented acritarchs in younger samples is primary rather than taphonomically driven given that they appear to be relatively robust (i.e., thicker walled) compared to many of the leiosphaerids that are present in these samples. Whether this shift reflects local factors such as a change in water depth or global factors such as extinction is not known. The whole unit is interpreted to record deposition in a shallow marine to sabkha environment, and forms considered to have been benthic mat formers (i.e., *Synsphaeridium* spp. and the various filamentous species) are seen throughout the unit, thus any change in water depth is likely to have been relatively little.

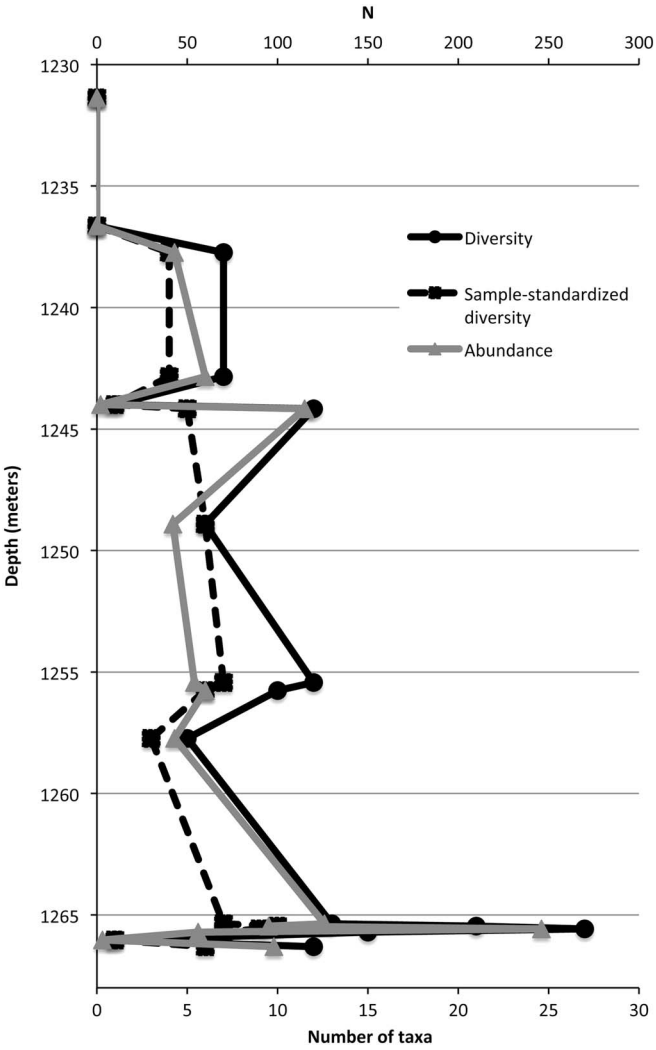

Figure 2. Abundance, taxonomic diversity, and standardized diversity of upper Alinya Formation of Giles 1. Y-axis is sample depth; lower X-axis is number of taxa (sample diversity and standardized diversity); upper X-axis is number of specimens recorded (abundance). Standardized diversity reflects taxonomic diversity of subsamples consisting of the first 20 specimens recorded in light microscopy of strewn slides.

Materials and methods

All samples for this study were processed by standard hydrofluoric maceration by Waanders Palynology Consulting, following protocols outlined by Grey (1999). Macerate samples are stored in 200 proof ethyl alcohol to discourage fungal and bacterial growth.

For SEM study, drops of sample macerate were strewn on glass slides or on SEM stubs and allowed to air dry. Transmitted light microscopy (using a Zeiss Axioskop 40) was performed on the glass slide preparations in order to locate specimens, note coordinates, and circle them with a fine-point marker so they could be located during SEM study. A 20- to 30-nm-thick carbon coat was applied with a high-vacuum carbon coater to reduce the effects of charge build-up. SEM was performed with a FEI Quanta 400 field-emission, environmental SEM using a voltage of 5 kV and working distances from 7 to 9 mm. After SEM analyses, glass coverslips were epoxied to the glass slides (using Petropoxy 154) and photographed under high magnification transmitted light microscopy using QImaging camera and Qcapture software. This allowed comparison of the same specimens in SEM and light microscopy.

Cross sectioning by Focused Ion Beam Electron microscopy (FIB-EM) was performed on *Culcitulisphaera revelata* n. gen. n. sp. specimens partially embedded in epoxy using FEI DB235 Dual-Beam FIB. Samples were prepared by applying a drop of epoxy (Petropoxy 154) to an SEM stub and then holding the stub with the stem in contact with a hot plate in order to begin curing before a drop of fossil macerate was applied. The goal was to apply the fossils to epoxy that was not completely cured but would cure by virtue of residual heat of the stub. When the epoxy reached a tacky texture, the stub was

https://doi.org/10.1017/jpa.2016.49 Published online by Cambridge University Press

removed from the heat and a drop of fossil macerate was applied by pipette. The stub was then allowed to cool. After carbon coating (20 to 30 nm), fossils were located by SEM. Relocation of fossils for FIB sectioning was expedited by creation of high-resolution montages of stubs during SEM. FIB is most efficient and least likely to produce slicing artifacts when used on smooth surfaces; this was achieved by selecting regions of low topographic relief and applying a ~500 nm coat of platinum to the 10 µm x 10 µm square region to be sliced. Near the target region, a 2 × 2 µm square of platinum was applied and an 'X' marked into the surface to act as a fiducial marker, used after sectioning was complete in order to align images. The FIB milled away 80 ~120-nm-thick sections of the fossil; after each slice, an electron image of the milled edge of the fossil was captured.

Systematic paleontology

All illustrated specimens have been reposited in the collections of the South Australian Museum (SAM), Adelaide, under the accession numbers SAM P49464–P49558. Slide numbers in captions begin with depth (in meters) in the Giles 1 drill core and are followed by a forward slash mark and specimen coordinates and then accession number in parentheses. Fossil coordinates were generated using England Finder graticule with sample slide label to the left for all slides except 1265.46-Feb6 and 1265.46-2_28B, for which the label is to the right. A table of all specimens, their accession numbers, slides or stubs, and coordinates is available in the supplemental data file. Coordinates are unavailable for specimens on stubs. The International Code of Nomenclature for Algae, Fungi, and Plants (Melbourne Code, 2011) is followed.

Acritarchs Evitt, 1963
Genus *Caelatimurus* new genus

Type species.—*Caelatimurus foveolatus*, n. sp., by monotypy.

Diagnosis.—As for type species.

Etymology.—From the Latin, *caelatum,* meaning 'embossed or engraved' and *murus*, meaning 'wall' for the embossed appearance of the vesicle. Pseudocompounding is intentional (recommendation 60G.1(c) of the ICN) and used to indicate etymological difference with the Latin *caelum*, meaning sky or heaven.

Remarks.—The diagnostic feature of this genus, the embossed ellipsoids upon the vesicle wall, is not seen in previously named genera, thus a new genus is erected here for the new species, *Caelatimurus foveolatus*.

Caelatimurus foveolatus new species
Figure 3.6–3.8

1978 Sphere with type I reticulate surface; Peat, Muir, Plumb, McKirdy, and Norvick, p. 5, fig. 3A.

1978 Sphere with type II reticulate surface; Peat, Muir, Plumb, McKirdy, and Norvick, p. 5, fig. 3B, 3D–F.

1984 *Turuchanica maculata* Tynni and Uutela, p. 24, ?fig. 175, fig. 176, non 177, nec 178–179, ?180–182, nec 183–186 (in part).

2016 *Caelatimurus foveolatus*; Porter and Riedman, p. 819, fig. 3.1.

Holotype.—(Fig. 3.6, 3.7), SAM Collection number P49508, slide 1265.57-19A, coordinate G27-2, depth of 1,265.57 m Giles 1 drill core, Alinya Formation, Officer Basin, Australia.

Diagnosis.—Optically dense spheroidal to ellipsoidal organic-walled microfossils ~30 to 60 µm in diameter, bearing frequent (~40 per 100 μm^2), small (0.9 to 1.2 µm wide and ~2 µm long), light-colored ellipsoidal depressions upon the vesicle.

Occurrence.—This form has been reported from the Neoproterozoic Chuar Group (Porter and Riedman, 2016), the Mesoproterozoic Roper Group (Peat et al., 1978), and in the poorly constrained, but probably Mesoproterozoic, Muhos Formation of Finland (Tynni and Uutela, 1984).

Description.—Optically dense spheroidal to ellipsoidal organic-walled microfossils ranging in diameter from 30.6 to 59.2 µm ($\overline{x} = 41.3\,\mu m$, $s = 15.6$, $N = 3$) bearing lighter-colored ellipsoidal marks 0.9 to 1.2 µm wide and typically ~2 µm in length that appear to be impressions in the vesicle wall.

Etymology.—From the diminutive of the Latin *fovea*, meaning 'minutely pitted.'

Material examined.—Three specimens from the Alinya Formation, Giles 1 drill core depth 1,265.46 and 1,265.57 m.

Remarks.—Peat and colleagues (1978) reported two morphotypes of reticulated spheroids from the McMinn Formation of the Mesoproterozoic Roper Group (fig. 3A, 3B, 3C–F; we do not include fig. 3C in the preceding synonymy because distortion due to crystalline growth makes identification of that specimen equivocal). These two morphotypes are distinguished by width of the ellipsoidal impressions. Measurements from the images of the Roper Group specimens indicate similar vesicle diameters, ranging from 45 to 50 µm; the type I reticulated spheroids bear ellipsoidal markings 0.5 to 1 µm in width and 1.5 to 4 µm in length, and type II reticulated spheroids bear ellipsoidal markings 1.8 to 2 µm in width and 2 to 3.2 µm in length. Specimens from the Alinya Formation range from 30.6 to 59.2 µm in diameter and bear ellipsoidal markings 0.9 to 1.2 µm in width and ~2 µm in length, and the single specimen recovered from the Chuar Group (Porter and Riedman, 2016) is 29 µm in diameter with ellipsoidal markings 1 to 1.5 µm in width and 1 to 3 µm in length. Thus, the specimens from the Alinya and Chuar assemblages bridge the morphological distance between the two morphotypes described by Peat et al. (1978). Because of this, we interpret the differences in ellipsoidal dimensions as intraspecific rather than indicative of separate species.

This species also occurs in the Muhos Formation of Finland (Tynni and Uutela, 1984), but the name assigned in that paper, *Turuchanica maculata*, is not employed here. This is because

https://doi.org/10.1017/jpa.2016.49 Published online by Cambridge University Press

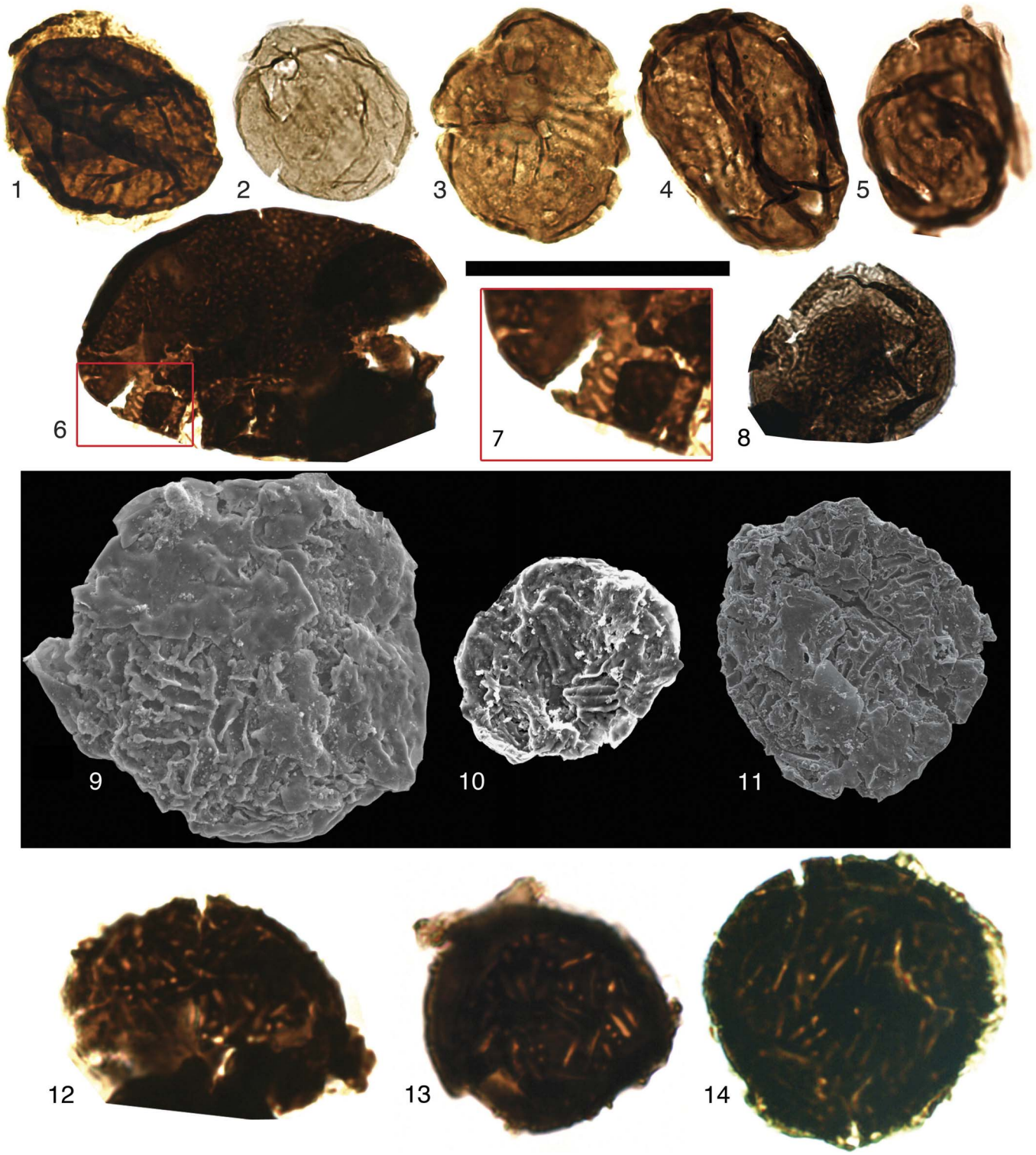

Figure 3. (**1–5**) *Karenagare alinyaensis* n. gen. n. sp.; (**4**) holotype. (**6–8**) *Caelatimurus foveolatus* n. gen. n. sp.; (**6, 7**) holotype. (**9–14**) *Volleyballia dehlerae*. Note that on (**2, 3**) striations are visible on only a portion of vesicle; (**1**) possible outer vesicle visible; (**4**) ridges suggestive of external ornamentation visible on the lower-most portions. Images (**1–8, 12–14**) are from transmitted light microscopy; (**9–11**) are from scanning electron microscope. Scale bar below (**3**) is 50 µm for (**1–6, 8**) and is 25 µm for (**7, 9–11**). Slides and coordinates: (**1**) 1265.46-18B/M28-2 (P49491); (**2**) 1265.57-19A/N38-1 (P49506); (**3**) 1265.46-18B/W31-0 (P49492); (**4**) 1265.46-18B/H18-3 (P49493); (**5**) 1265.57-19A/Y40-2 (P49507); (**6, 7**) 1265.57-19A/G27-2 (P49508); (**8**) 1265.57-19A/L16-4 (P49509); (**9**) 1265.46-2_28B (P49504); (**10**) 1265.57-March8StubA (P49545); (**11**) 1265.57-March20_epoxyA (P49546); (**12**) 1265.57-19A/H38-2 (P49510); (**13**) 1265.57-19A/M40-0 (P49511); (**14**) 1265.57-19A/M15-4 (P49512).

although Tynni and Uutela (1984) mentioned a patterned wall in their description, this feature—considered here to be a diagnostic feature—is not apparent in the holotype (pl. 8, fig. 175). It is clearly visible in only one (pl. 8, fig. 176) and possibly present in another three (pl. 8, fig. 180–182) of the twelve specimens figured.

https://doi.org/10.1017/jpa.2016.49 Published online by Cambridge University Press

Due to the frequency and regularity of these markings in all occurrences as well as their absence from any other taxa, the embossed vesicle ornamentation of *C. foveolatus* is interpreted to be of primary biological origin rather than a taphonomic one—either by distortions caused by crystal growth or movement (cf. Xiao and Knoll, 1999) or by borings of microbial degradation of the vesicle (cf. Grey and Willman, 2009).

Genus *Comasphaeridium* Staplin, Jansonius, and Pocock, 1965

Type species.—*Comasphaeridium cometes* (Valensi, 1949) Staplin, Jansonius and Pocock, 1965.

'*Comasphaeridium*' *tonium* Zang, 1995
Figure 4.2–4.4

1995 *Comasphaeridium tonium* Zang, p. 162, fig. 24A–G.

Holotype.—(Zang, 1995; fig. 24B), slide 5341RS308-8 from 1,237.9 m of Giles 1 drill core, Alinya Formation, Officer Basin, Australia.

Occurrence.—The Neoproterozoic Alinya Formation (Zang, 1995). Singh and Babu (2013) also reported *C. tonium* from the Neoproterozoic Raipur Group of India; however, the fossil figured is too poorly preserved to provide an unequivocal identification.

Description.—Spheroidal organic-walled microfossils ranging in vesicle diameter from 42.5 to 57.9 µm ($\overline{x} = 51.3\,\mu$m, s = 5 µm, N = 7) and bearing frequent (12–20 visible in 10 µm section of vesicle perimeter) short, simple, unbranching fine processes (length range 0.8–2.4 µm, $\overline{x} = 1.5\,\mu$m, s = 0.6; width range 0.4 to 0.7 µm, $\overline{x} = 0.5\,\mu$m, s = 0.1 µm). No outer envelope has been observed. Processes appear to be solid, as determined from the consistent optical density of processes viewed from the side and head-on; they do not appear to be a lighter shade in the center of the process.

Material examined.—Seven specimens from the Alinya Formation, Giles1 drill core depths 1,255.43, 1,255.76, 1,265.57 and 1,265.71 m.

Remarks.—The specimens recovered in this study conform to Zang's (1995) description of *C. tonium* from the Alinya Formation. However, the generic assignment of this species to the Mesozoic genus *Comasphaeridium* is considered dubious due to its overly broad diagnosis ("spherical to ellipsoidal, sometimes of large size with densely crowded, thin, solid, usually simple, more or less flexible hair-like spines"; Staplin et al., 1965, p. 192). Unfortunately, the current fossil material is not sufficient to recommend a new nomenclatural combination or erection of a new genus.

Genus *Culcitulisphaera* new genus

Type species.—*Culcitulisphaera revelata* n. sp., by monotypy.

Diagnosis.—As for type species.

Etymology.—From the Latin *culcitula*, meaning 'small pillow,' and *sphaera*; a sphere covered by small pillows.

Remarks.—The distinctiveness of the pillow elements of the vesicle exterior warrants the erection of a new genus. No existing genus is known that can accommodate the features diagnostic of *Culcitulisphaera revelata*, thus a new genus is established here.

Culcitulisphaera revelata new species
Figures 5, 6.4–6.6, 7, 8

Non 1966 *Trachyhystrichosphaera laminaritum* Timofeev, p. 36, pl. 7, fig.3.

1979 *Kildinella* sp.; Vidal, pl. 4, figs. C, D.

?1985 *Trachysphaeridium* sp. A; Vidal and Ford, p. 377, figs. 8B, 8D.

1992 *Trachysphaeridium laminaritum*; Schopf, pl. 14, fig. A.

2009 *Trachysphaeridium laminaritum*; Nagy, Porter, Dehler, and Shen, fig. 1H.

2016 *Culcitulisphaera revelata*; Porter and Riedman, p. 822, figs. 5.1–5.7.

Holoype.—(Fig. 5.1), SAM Collection number P49519, slide 1265.57-19A, coordinate N24-1, depth of 1,265.56 m, Giles 1 drill core, Alinya Formation.

Diagnosis.—Optically dense spheromorphic organic-walled microfossil distinguished by a surface ornament of tightly packed 1 to 3 µm cushion-shaped outpockets of the vesicle that may appear only as ~1 µm diameter light spots or alveolae under transmitted light microscopy.

Occurrence.—Appears in late Mesoproterozoic to middle Neoproterozoic units: the uppermost Limestone Dolomite 'series' (beds 19–20) of the Eleonore Bay Group of East Greenland (Vidal, 1979), the Chuar Group of southwestern United States (Nagy et al., 2009; Porter and Riedman, 2016), and the Lakhanda Group of Siberia (Schopf, 1992; however, see the following).

Description.—Optically dense organic vesicle circular to ellipsoidal in outline, ranging in diameter from 34.6 to 88.4 µm ($\overline{x} = 60.3\,\mu$m, s = 15.6, N = 24); reflecting an originally spherical to subspherical shape. Vesicle surface consists of small circular to subcircular outpockets. The outpocket elements range in diameter from 1.3 to 2.7 µm ($\overline{x} = 1.8\,\mu$m, s = 0.6, N = 17; measurement unavailable in specimens viewed only by transmitted light microscopy). Vesicular elements are unlikely to have been surficial scales as none has yet been found separated from the vesicle surface, and inspection of all specimens suggests full attachment to the vesicle. Thus far, these vesicular elements have been recognized only under SEM. When specimens are viewed with transmitted light microscopy, the surface appears to have small (~0.7 µm) alveolae or hemispherical depressions in the vesicle, which are in fact the centers of the outpockets where light passes through fewer layers of vesicle. Occasionally, these structures

https://doi.org/10.1017/jpa.2016.49 Published online by Cambridge University Press

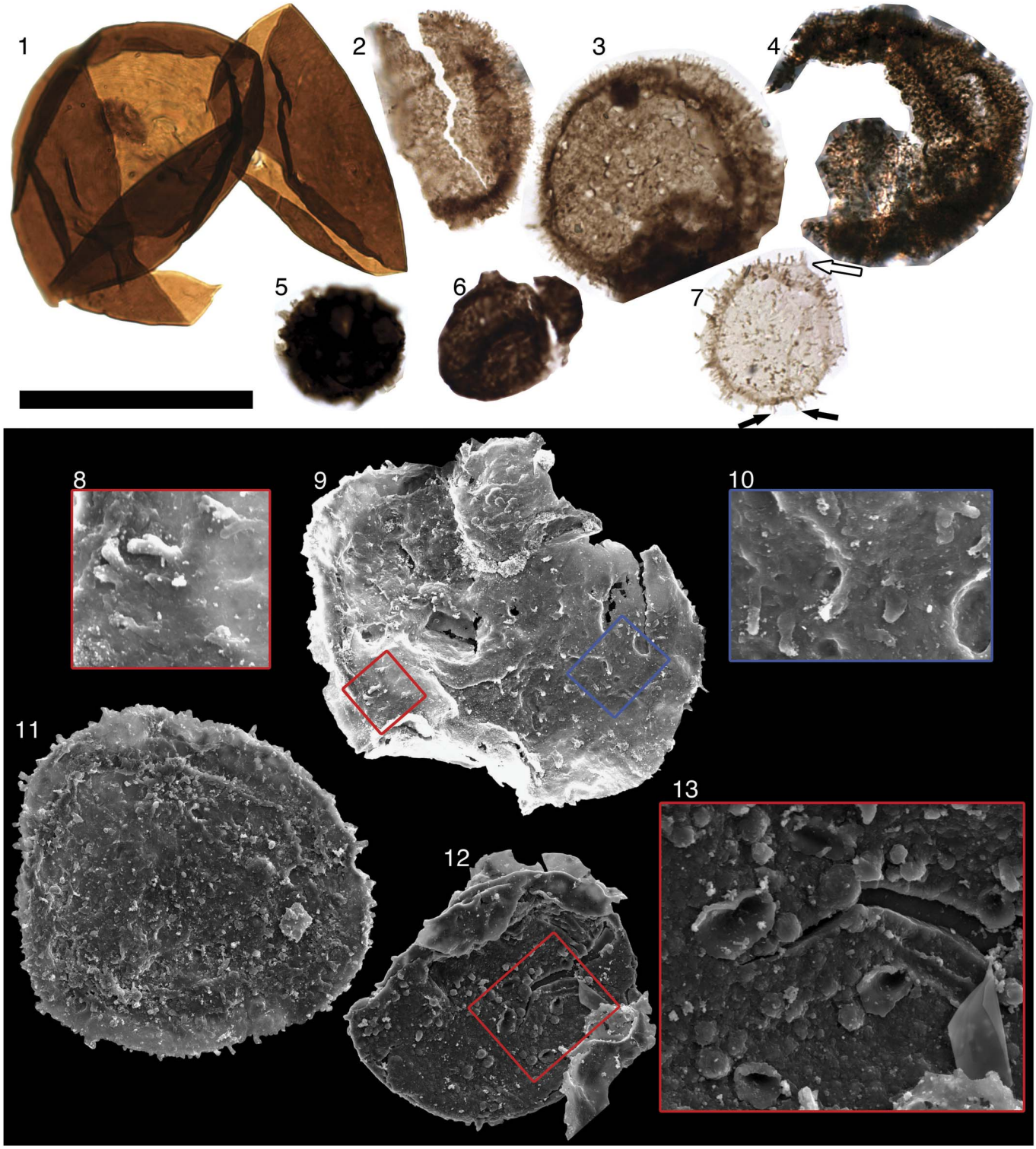

Figure 4. (**1**) *Valeria lophostriata*. (**2–4**) '*Comasphaeridium*' *tonium*. (**5**) Unnamed Acritarch sp. B. (**6**) Unnamed Acritarch sp. C. (**7–11**) Unnamed Acritarch sp. D: (**7**) white arrow indicates conical extension of vesicle below process; left black arrow indicates process bifurcation; right black arrow indicates process overlap. (**12**) Unnamed Acritarch sp. E. Black scale bar is 50 µm for (**1–7**), 33 µm for (**9**), 25µm for (**11, 12**), 10 µm for (**8, 10**), and 8 µm for (**13**). Slide and coordinates: (**1**) 1265.57-19A/L38-0 (P49517); (**2**) 1255.76-16B/G22-1 (P49484); (**3**) 1265.57-19A/L18-3 (P49518); (**4**) 1255.76-16B/M34-3 (P49485); (**5**) 1242.84-13A/L16-1 (P49467); (**6**) 1255.43-15A/Q20-1 (P49478); (**7**) 1255.76-16A/T13-0 (P49482); (**8–10**) 1265.46-Feb6/on top of other fossils, unavailable (P49499); (**11**) 1265.57-1_29BigStubB (P49538), (**12**) 1265.57-1_29BigStubB (P49539).

can be recognized as cushion-shaped elements along the periphery of a specimen as viewed under light microscopy (Fig. 5.1–5.5).

A spectrum of taphonomic variation is seen in *C. revelata* specimens. Study of these variants has been informative for developing an understanding of the vesicle morphology

https://doi.org/10.1017/jpa.2016.49 Published online by Cambridge University Press

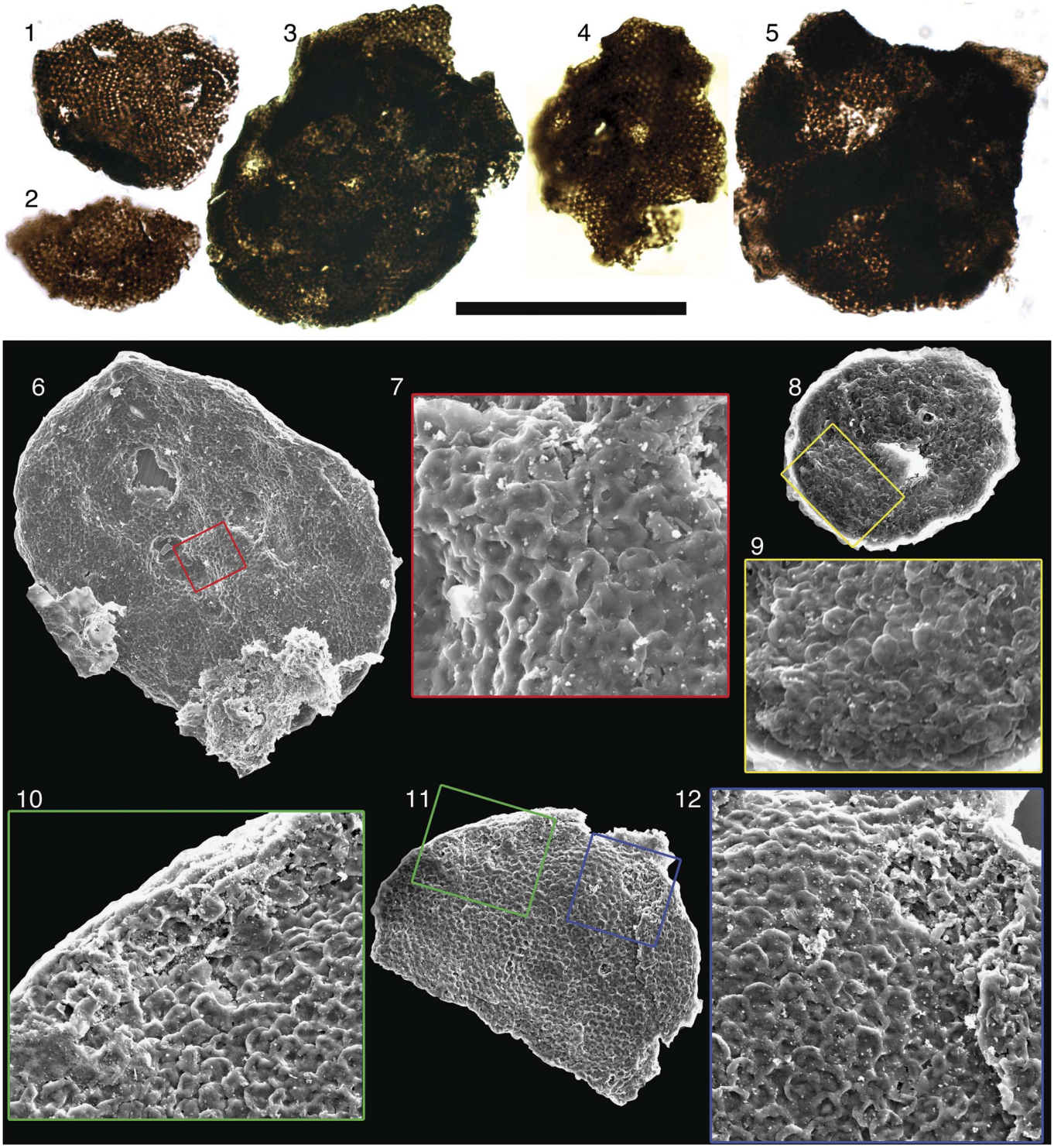

Figure 5. *Culcitulisphaera revelata* n. gen. n. sp.: (**1–5**) transmitted light images; (**6–12**) scanning electron microscope images; (**1**) holotype. Scale bar is 50 µm for (**1–6, 8, 11**), 8 µm for (**7**), and 16 µm for (**9, 10, 12**). Slide and coordinates: (**1**) 1265.57-19A/N24-1 (P49519); (**2**) 1265.26-18B/S34-2 (P49494); (**3**) 1265.46-18A/L38-3 (P49487); (**4**) 1265.46-18B/G30-3 (P49495); (**5**) 1265.46-18A/L26-2 (P49488); (**6, 7**) 1265.57-LittleStubB (P49541); (**8, 9**) 1265.57-1_17BigStubA (P49534); (**10–12**) 1265.46-Feb6/Z34-0 (P49500).

(for example, by providing evidence of the hollow nature of the pillow-shaped elements and indication that the wall is composed of individual pillow elements rather than bearing only a textured surface). The flexibility of the vesicle wall is indicated in the folding that occurs in the elements along the perimeter of the flattened fossil, giving an imbricated appearance (Fig. 7.4). During degradation, the pillow elements of the vesicle appear to 'deflate'; the outer wall of the element sinks into the underlying cavity (Figs. 5.7, 5.12, 7.3), creating a honeycomb-like appearance. Occasionally, the outermost skin of the pillows

https://doi.org/10.1017/jpa.2016.49 Published online by Cambridge University Press

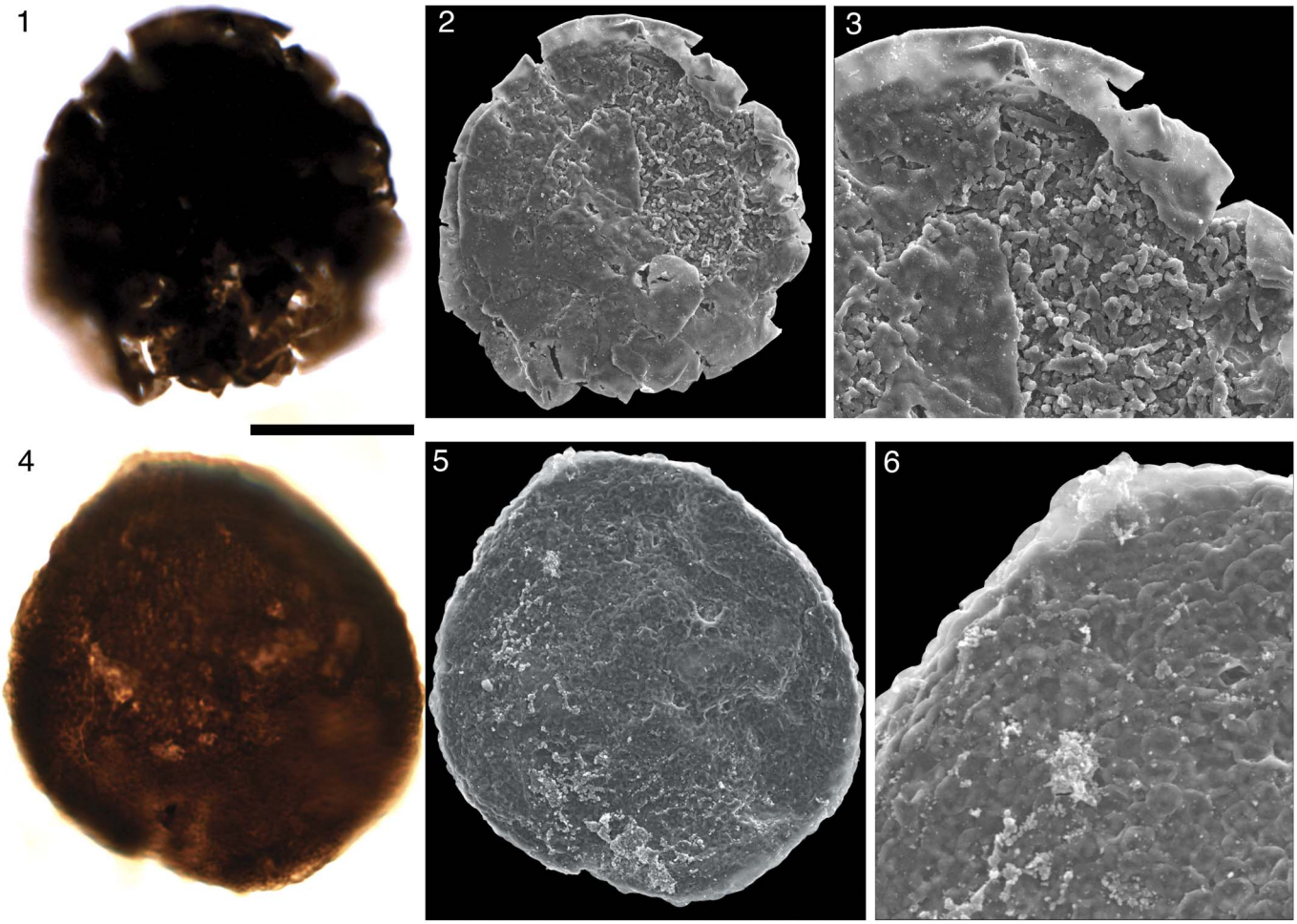

Figure 6. Transmitted light and scanning electron microscope images of *Lanulatisphaera laufeldii* and *Culcitulisphaera revelata* n. gen n. sp. specimens: (**1–3**) are same specimen of *L. laufeldii*; (**4–6**) are same specimen of *C. revelata.* (**1, 4**) Transmitted light microscope images; (**2, 3, 5, 6**) scanning electron microscope images. Scale bar is 20 µm for (**1, 2, 4, 5**), 10 µm for (**3**), and 7 µm for (**6**). Slide and coordinates: (**1–3**) 1265.46-Feb6/E29-0 (P49498); (**4–6**) 1265.46-2_28B/AA55-4 (P49503).

shows rupture (Fig. 7.1, 7.2) or appears to have been sheared away from the fossil (arrows in Fig. 7.5), revealing a smooth surface within. Several of the fossils studied here also show a wart-like crater that excavates through the vesicle layers (Fig. 5.6, 5.11, 5.12); this feature is not interpreted as an excystment structure, but more likely represents postmortem degradation.

FIB-EM sectioning and analysis by energy-dispersive X-ray spectroscopy (EDS) of *C. revelata* specimens (Fig. 8) indicates a homogeneous carbon composition with no discernable boundaries between vesicle layers, likely to be a product of compaction and diagenesis. FIB-EM nanotomography of these samples did, however, reveal the presence of frequent 30 to 600 nm nanopores within the vesicle (Fig. 8.4, 8.5). Similar nanopores are seen in FIB serial sections of the Mesoproterozoic acritarch, *Shuiyousphaeridium macroreticulatum* (Du, 1988 in Guan et al., 1988) Yan 1992 (in Yan and Zhu, 1992) (Schiffbauer and Xiao, 2009; Pang et al., 2013). The occurrence of these features is unlikely to represent artifacts of processing and may speak to a spongy, woven, or reticulated subsurface in this taxon. A particularly clear example of this spongy, woven substructure is seen in a specimen of the Chuar Group (fig. 5.4a, 5.5a of Porter and Riedman, 2016).

Etymology.—From the Latin *revelatum*, meaning 'revealed,' referring to the fact that the pillow elements of the vesicle were unknown until revealed by SEM.

Material examined.—Twenty-seven specimens from the Alinya Formation, Giles 1 drill core depths 1,265.36, 1,265.46, and 1,265.57 m.

Remarks.—*C. revelata* is not considered here to be conspecific or congeneric with *Trachysphaeridium laminaritum,* although this was thought a likely taxonomic home for these specimens due to similarities with specimens figured by Schopf et al. (1992) and Nagy et al. (2009). The original diagnosis and description of *T. laminaritum* (Timofeev, 1966) are vague and do not mention features considered diagnostic of *C. revelata* (i.e., alveolae or circular to cushion-shaped vesicular elements), instead describing a thick-walled vesicle with a chagrinate texture ranging from 70 to 250 µm in diameter (typically 120 to 200 µm)—larger than the 35- to 88-µm-diameter specimens recovered from the Alinya Formation. In addition, the fossil images of *T. laminaritum* (pl. 7, fig. 3; hand-drawn illustrations) do not conclusively illustrate diagnostic features of this taxon.

https://doi.org/10.1017/jpa.2016.49 Published online by Cambridge University Press

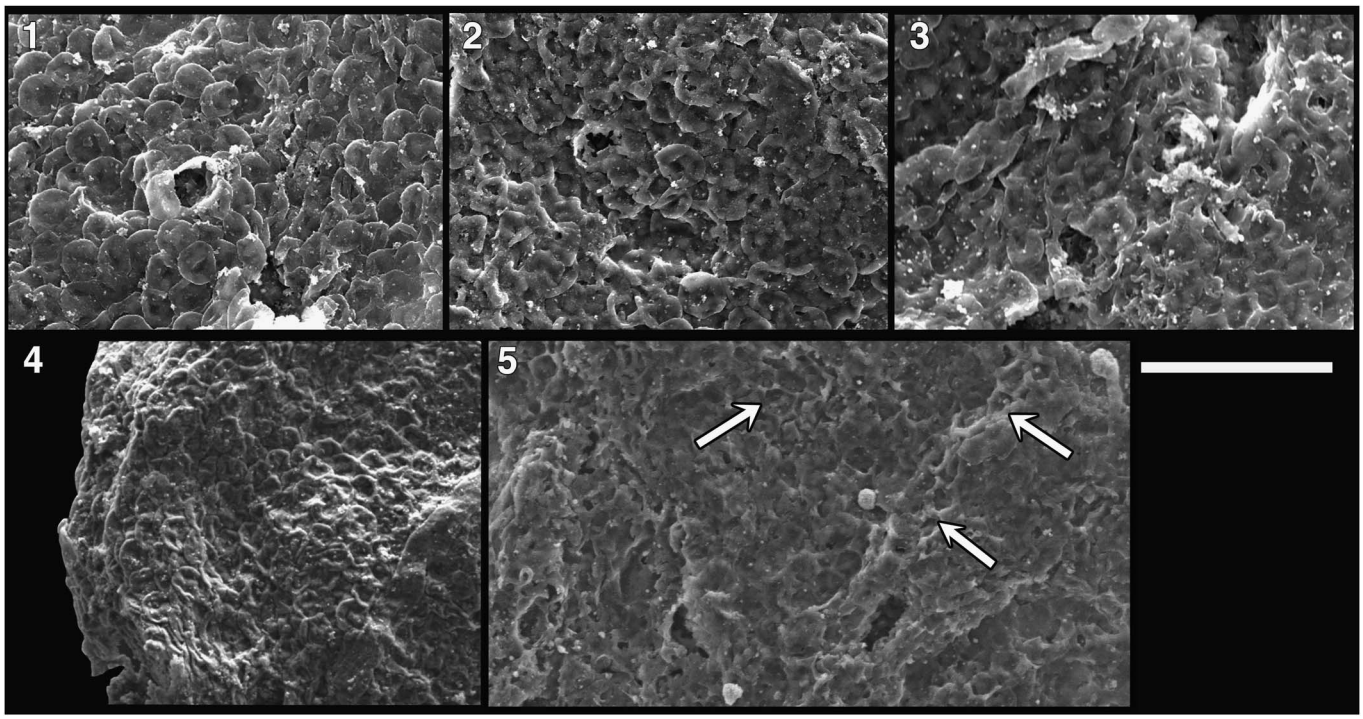

Figure 7. (**1–5**) Sequence of taphonomic degradation of *Culcitulisphaera revelata* n. gen. n. sp. Note pillow-like elements of *C. revelata* (**1**) become progressively sunken (**2–4**). In parts of (**5**) the top layer of the pillow element is sheared away (white arrows). Scale bar = 10 µm. Slide/stub and coordinates: (**1**) 1265.57-1_17BigStubA (P49534); (**2**) 1265.46-Feb6/on top of other fossils, unavailable (P49497); (**3**) 1265.57-1_17BigStubA (P49535); (**4**) 1265.57-4_15/N45-2 (P49549); (**5**) 1265.46-2_28B/O50-2 (P49502).

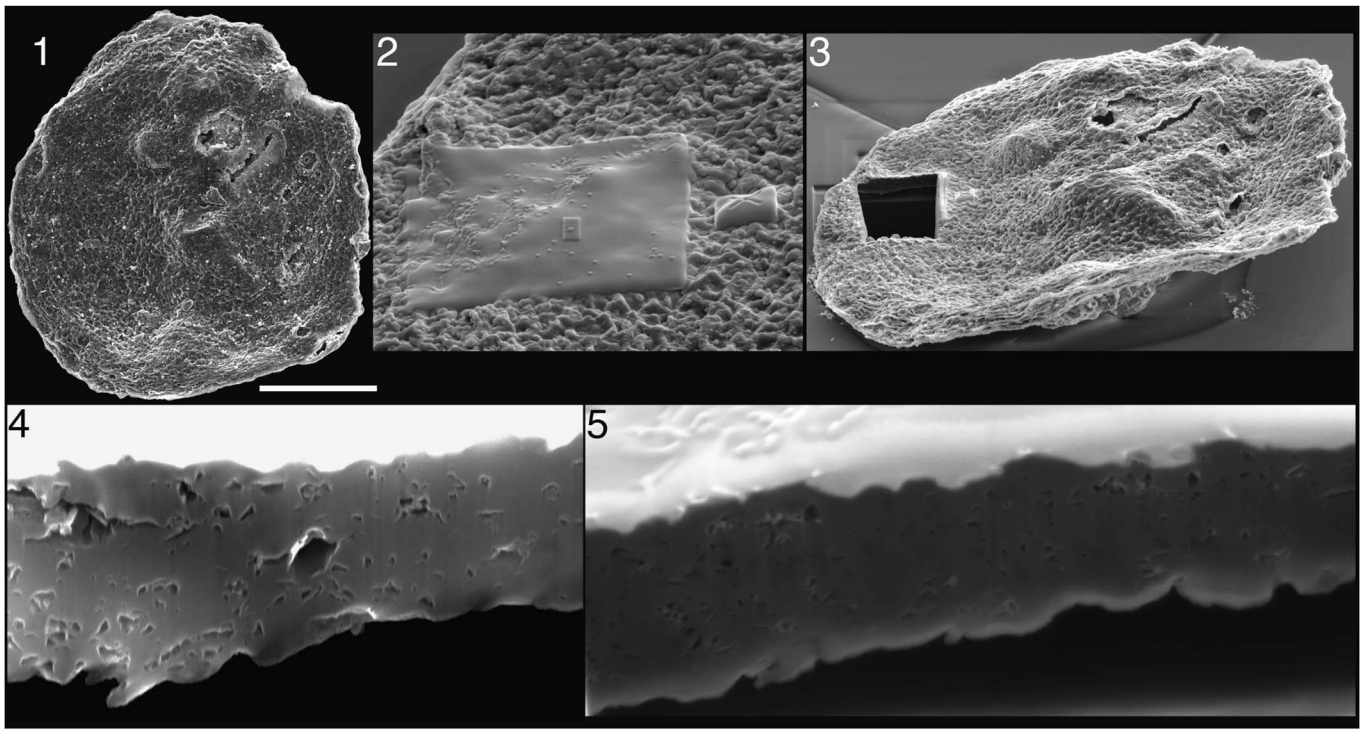

Figure 8. FIB-EM sectioning of *Culcitulisphaera revelata* n. gen. n. sp. All images of same specimen. (**2**) Platinum coating and nearby fiducial marker applied to fossil before FIB sectioning. (**3**) Fossil after sectioning complete. (**4, 5**) Acritarch wall with nanopores. Scale bar is 20 µm for (**1**), 4 µm for (**2**), 13 µm for (**3**), 1 µm for (**4, 5**). Stub: 1265.57 March20_epoxyA (P49547).

The fossil imaged in plate 14, figure A, p. 1075 of Schopf (1992) appears to be *C. revelata*. The caption reads, "*Trachysphaeridium laminaritum* Timofeev in press HOLOTYPE" and the fossil is indicated as being from the Lakhanda Group of Siberia (the publication "in press" is unclear and not listed in the bibliography). The "holotype" designation in the caption is

https://doi.org/10.1017/jpa.2016.49 Published online by Cambridge University Press

apparently incorrect as the holotype Timofeev (1966) designated for *T. laminaritum* was from a drill core taken from northern Moldova, not from the Lakhanda Group of Siberia. Differences in diameter and outline indicate these are two distinct specimens. There would have been no need to designate a neotype in 1992 as Timofeev's original specimens were still available for study as of 1996 (Knoll, 1996; contra Jankauskas et al., 1989). In any case, the specimen figured by Schopf (1992) indicates that *C. revelata* was a part of the ca. 1 Ga Lakhanda biota, extending this form's geographic and stratigraphic range.

Genus *Karenagare* new genus

Type species.—*Karenagare alinyaensis* n. sp., by monotypy

Diagnosis.—As for type species.

Etymology.—*Karenagare* is from the Japanese name for the element of raked sand or gravel in Zen rock gardens forming impressionistic waterless streams. It applies here to the resemblance of the fossil's ridged ornament to the lines of sand or gravel composing the 'stream.'

Remarks.—These fossils are distinguished from other striated acritarch taxa by the undulating nature of the striations rather than sharp grooves as seen in *Volleyballia dehlerae* or narrow ridges (~0.5 µm from crest to crest) as in *Valeria lophostriata*. In addition, these undulations are seen on the exterior of the vesicle as opposed to the interior linear ornamentations of *V. lophostriata* (Javaux et al., 2004). Although these species share superficial similarity, there is no reason to presume they may have been closely related. Thus, the decision to erect a new genus for this species (rather than a new species within *Valeria* or *Volleyballia*) is based on intent to create a biologically meaningful generic concept.

Karenagare alinyaensis new species
Figure 3.1–3.5

?1996 Unnamed acritarch, Knoll, pl. 4, fig 11.

Holotype.—(Fig. 3.4), SAM Collection number P49493, slide 1265.46-18B, coordinate H18-3, depth of 1,265.46 m, Giles 1 drill core, Alinya Formation.

Diagnosis.—Spheroidal to ellipsoidal organic-walled microfossils bearing 2–3 µm wide, parallel, undulatory, ripple-like external striations.

Occurrence.—Neoproterozoic Alinya Formation of Officer Basin, South Australia, and perhaps an unspecified Neoproterozoic unit of Russia (Knoll, 1996).

Description.—Spheroidal to ellipsoidal organic-walled microfossils with vesicles of varying opacity and distinctive ornamentation of wide, parallel, undulating, ripple-like striations measuring 2–3 µm from crest to crest of ridges (the darker lineations). Vesicles range in diameter from 32.2 to 86.7 µm ($\overline{x} = 42.7\,\mu m$, s = 16.2 µm, N = 10). On certain specimens (Fig. 3.2, 3.3), the striations are visible on only a small part of the vesicle, but others exhibit striations over the entire visible vesicle surface; whether this is indicative of ontogenetic or taphonomic variation is not yet clear. One specimen may exhibit an outer envelope (Fig. 3.1). Striations appear to ornament the external surface of the vesicle as suggested by their appearance along the periphery of the vesicle (lower portion of Fig. 3.4).

Etymology.—For the fossil's discovery in the Alinya Formation of Officer Basin, South Australia.

Material examined.—Ten specimens from the Alinya Formation, Giles 1 drill core depths 1,265.46 and 1,265.57 m.

Remarks.—The 'unnamed acritarch' of Knoll (1996) appears similar to *K. alinyaensis* but as measured from the image is ~25 µm in diameter with striations ~1 µm from crest to crest, somewhat smaller with more closely spaced ridges than those recovered here.

There is an intriguing morphological similarity between *K. alinyaensis* and species of *Moyeria*, early Paleozoic organic-walled microfossils interpreted as possible euglenoids (Gray and Boucot, 1989). The size and curvature of the undulations in the vesicle of *K. alinyaensis* are consistent with the appearance of the ridges in *Moyeria* sp.; these have been interpreted as pellicle strips in the latter (Gray and Boucot, 1989). At this time nothing more than a mention of morphological similarity is possible, but if further study were to establish a euglenoid affinity for *K. alinyaensis*, this would be the oldest known record of this clade.

Genus *Lanulatisphaera* Porter and Riedman 2016

Type species.—*Lanulatisphaera laufeldii* (Vidal, 1976) Porter and Riedman 2016.

Lanulatisphaera laufeldii (Vidal, 1976) Porter and Riedman 2016
Figures 6.1–6.3, 9.9–9.12, 10

1976 *Trachysphaeridium laufeldi* Vidal, p. 36, fig. 21A–N.
1985 *Trachysphaeridium laufeldi*; Vidal and Ford, p. 375, fig. 7A, B.
?1985 *Trachysphaeridium laufeldi*; Vidal and Ford, p. 375, fig. 7D, F.
?1985 *Trachysphaeridium laminaritum*; Vidal and Ford, p. 373, fig. 8A, C.
1997 *Lophosphaeridium laufeldii*; Samuelsson, p. 174, fig, 7F, H, I.
2009 *Lophosphaeridium laufeldi*; Nagy, Porter, Dehler, and Shen, fig. 1J.
2016 *Lanulatisphaera laufeldii*; Porter and Riedman, p. 828–831, figs. 9.1–9.6, 10.1–10.7, 11.1–11.4, 12.1–12.7, ?12.8.

Holotype.—(Vidal, 1976; fig. 21A–E), Specimen BV/83.60—1: X/53.3 middle unit, Kumlaby bore hole, Neoproterozoic Visingsö Group, Sweden. Designated by Vidal (1976).

https://doi.org/10.1017/jpa.2016.49 Published online by Cambridge University Press

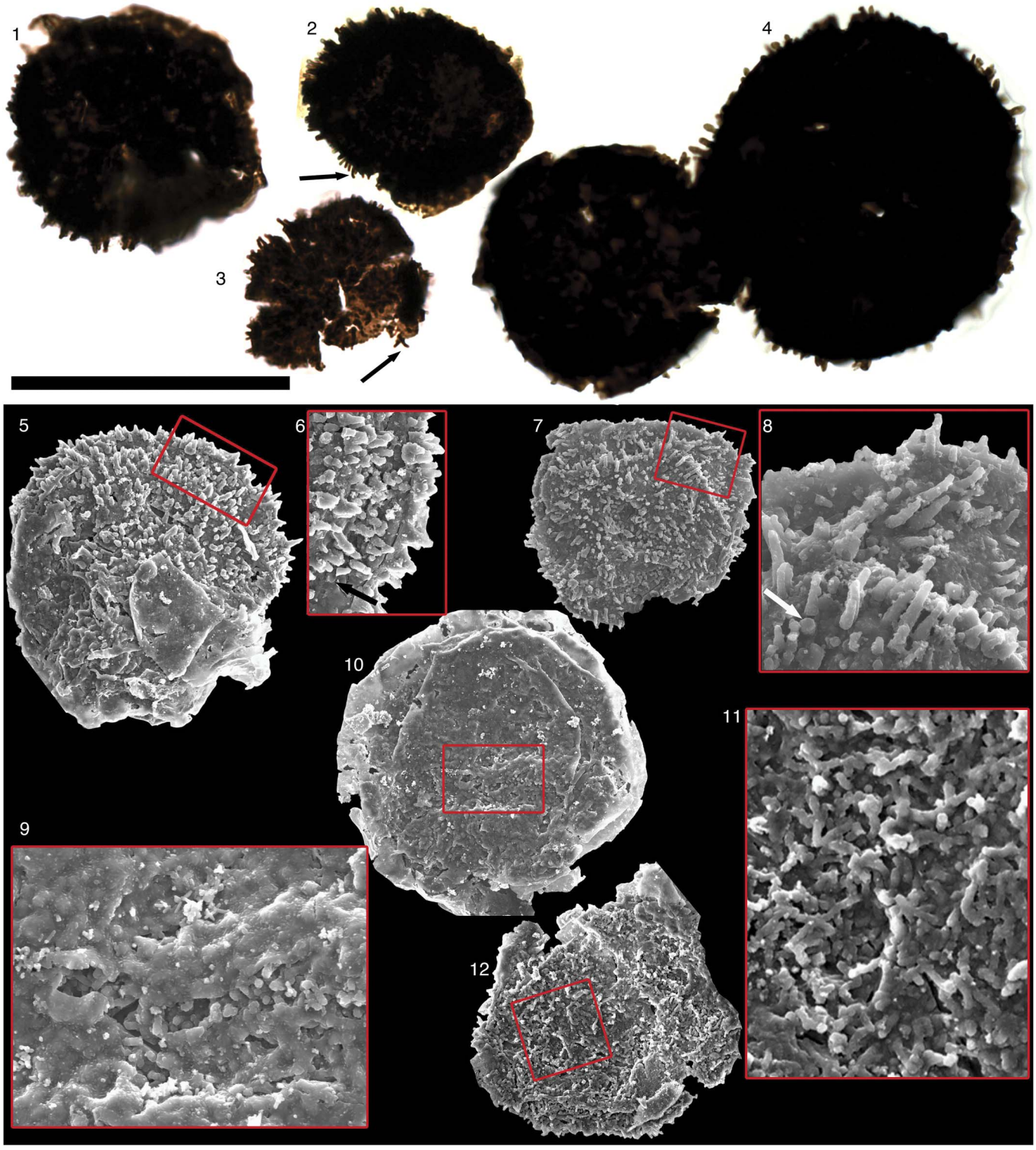

Figure 9. (**1–8**) *Morgensternia officerensis* n. gen. n. sp.: (**1**) holotype; (**2, 3**) arrows indicate rare bent processes; (**6, 8**) arrows indicate stump of a broken process revealing solid character. (**9–12**) *Lanulatisphaera laufeldii*: (**9**) close-up on nano-scale mammillary ornament upon vesicle; (**11**) close-up on anastomosing filaments beneath outer envelope (absent from this specimen). Scale bar is 50 μm for (**1–4**), 35 μm for (**5, 7, 10, 12**), 18 μm for (**6**), and 9 μm for (**8, 9, 11**). Slide and coordinates: (**1**) 1265.57-19A/V32-4 (P49520); (**2**) 1265.46-18B/N19-1 (P49496); (**3**) 1265.57-19A/S38-0 (P49521); (**4**) 1265.71-105A/U27-2 (P49550); (**5, 6**) 1265.57-LittleStubB (P49542); (**7, 8**)–1265.57-LittleStubA (P49536); (**9, 10**) 1265.57-LittleStubB (P49543); (**11, 12**) 1265.46-Feb6/missing after epoxy (P49501).

Occurrence.—Occurs in early Neoproterozoic units including Visingsö Group of southern Sweden (Vidal, 1976), the Kildinskaya Group, northwestern Russia (Samuelsson, 1997), and the Chuar and Uinta Mountain groups of southwestern United States (Vidal and Ford, 1985; Nagy et al., 2009; Porter and Riedman, 2016).

https://doi.org/10.1017/jpa.2016.49 Published online by Cambridge University Press

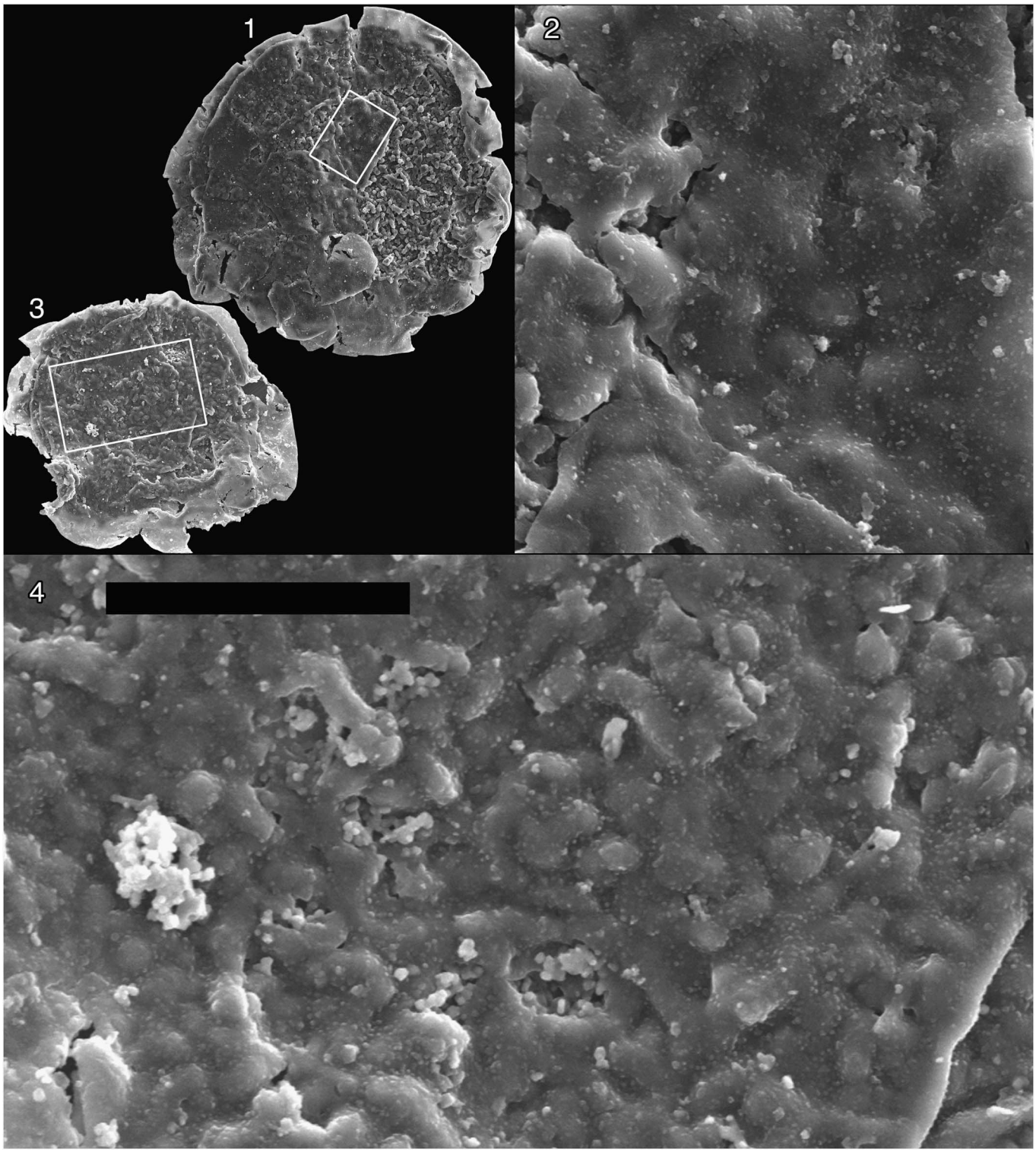

Figure 10. Vesicle detail of *Lanulatisphaera laufeldii*: (**2**) detail of inset in (**1**); (**4**) detail of inset in (**3**); note nano-scale mammillary ornamentation. Scale bar is 5 µm for (**2, 4**) and 40 µm for (**1, 3**). Slide/Stub and coordinates: (**1, 2**) 1265.46-Feb6/E29-0 (P49498); (**3, 4**) 1265.57-1_29LittleStubA (P49537).

Description.—Small, spheroidal, organic-walled microfossils ranging in diameter from 26.5 to 46.1 µm ($\overline{x} = 33.1\,\mu$m, s = 4.6 µm, N = 21) and bearing abundant, solid, thin ($\overline{x} = 0.4\,\mu$m, s = 0.1 µm, N = 21), filamentous structures that emanate from the external surface of the inner vesicle and fuse distally. Outer vesicle envelops—but does not appear to make contact with—the inner vesicle or reticulate filamentous structures. Outer vesicle exhibits a fine-scale (~50 to 100 nm diameter) mammillar ornament (Figs. 9.9, 10.2, 10.4; see also fig. 10.4, 10.5a, 10.6a in Porter and Riedman, 2016).

https://doi.org/10.1017/jpa.2016.49 Published online by Cambridge University Press

Filamentous processes not typically visible in transmitted light microscopy but are easily identifiable by SEM. In transmitted light, fossils appear very dark and often mottled; double-vesicle construction not always easily determined due to optical density of outer vesicle.

During taphonomic degradation the filaments become flattened and shortened by breakage, but still visibly fused (Fig. 6.3).

The occasional spiny protuberances and circular openings surrounded by raised rims reported by Vidal (1976) and Vidal and Ford (1985) and seen in Nagy et al. (2009, fig. 1j) were not observed in the present material.

Material examined.—Twenty-one specimens from the Alinya Formation, Giles 1 drill core depths 1,265.46 and 1,265.57 m.

Remarks.—Similarities are seen between *L. laufeldii* and *Morgensternia officerensis* n. gen. n. sp. (both Fig. 9); these species may be distinguished by differences in process character. Whereas the conical processes of *M. officerensis* are easily viewed in transmitted light, the reticulated filaments of *L. laufeldii* do not project as far from the surface and may be difficult to recognize in transmitted light. In addition, as viewed by SEM, processes of *L. laufeldii* are constant in diameter and anastomose distally with neighboring processes whereas *M. officerensis* processes are conical, tapering distally, and do not anastomose. Both forms possess external envelopes; however, the nano-scale mammillar ornament of *L. laufeldii* has not been observed on specimens of *M. officerensis*.

Genus *Leiosphaeridia* Eisenack, 1958b, emend. Downie and Sarjeant, 1963

Type Species.—*Leiosphaeridia baltica* Eisenack, 1958b.

Remarks.—*Leiosphaeridia* is a form genus comprising morphologically simple, smooth, organic-walled microfossils. Recent ultrastructural analyses have illustrated the polyphyletic nature of this group (e.g., Talyzina and Moczydłowska, 2000; Javaux et al., 2004; Willman, 2009).

The formal designations of *Leiosphaeridia* species given by Jankauskas and colleagues (1989) are followed here. Species are differentiated on the basis of diameter and opacity of the vesicle. *L. crassa* and *L. jacutica* possess an optically dense vesicle and are differentiated by being less than (*L. crassa*) or greater than (*L. jacutica*) 70 µm in diameter. Similarly, *L. minutissima* and *L. tenuissima* possess vesicles of low optical density and are differentiated on the basis of being less than (*L. minutissima*) or greater than (*L. tenuissima*) 70 µm in diameter.

Leiosphaeridia crassa (Naumova, 1949) Jankauskas (in Jankauskas et al., 1989)
Figure 11.5

1949 *Leiotriletes crassus* Naumova, p. 54, pl.1, figs. 5, 6, pl.2, figs. 5, 6.
1989 *Leiosphaeridia crassa*; Jankauskas in Jankauskas, Mikhailova, and Hermann, p. 75, pl. 9, figs. 5–10 (see for additional synonymy).
1994 *Leiosphaeridia crassa*; Butterfield, Knoll, and Swett, p. 40, figs. 16F, 23K.
1994 *Leiosphaeridia crassa*; Hofmann and Jackson, p. 22, figs. 13.3, 15.19–15.29.
1999 *Leiosphaeridia crassa*; Buick and Knoll, p. 756, fig. 5.2–5.4.
2005 *Leiosphaeridia crassa*; Grey, 2005, p. 179, figs. 63A–C, 64 A, ?B, ?C, D.
2008 *Leiosphaeridia crassa*; Moczydłowska, p. 84, figs. 7A, 8G.
2016 *Leiosphaeridia crassa*; Porter and Riedman, p. 830, fig. 11.2

Holotype.—No holotype was designated by Naumova (1949). Jankauskas (in Jankauskas et al., 1989, p. 75) designated a specimen (pl. 1, fig. 3) from Naumova (1949) as lectotype. However, this specimen was not of a species they synonymized with *Leiosphaeridia crassa,* but was instead *Leiotriletes simplicissimus*, a species Jankauskas and colleagues (1989) synonymized with a different species of *Leiosphaeridia*, *L. minutissima*.

Occurrence.—Ubiquitous in Precambrian and Phanerozoic organic-walled microfossil assemblages.

Description.—Solitary, spheroidal, smooth, single-walled vesicles 18 to 70 µm in diameter ($\bar{x} = 36.5\,\mu$m, s = 13.4 µm, N = 132). Vesicle dark but translucent.

Material examined.—One hundred sixty-seven specimens measured (many more present but uncounted) from the Alinya Formation, Giles 1 drill core depths 1,237.74, 1,242.84, 1,244.17, 1,248.91, 1,255.43, 1,255.76, 1,257.73, 1,265.36, 1,265.46, 1,265.57, 1,265.71, and 1,266.31 m.

Leiosphaeridia jacutica (Timofeev, 1966) Mikhailova and Jankauskas (in Jankauskas et al., 1989)
Figure 11.6

1966 *Kildinella jacutica* Timofeev, p. 30, pl. 7, fig. 2.
1989 *Leiosphaeridia jacutica*; Mikailova and Jankauskas in Jankauskas, Mikhailova, and Hermann, p. 77, pl. 12, figs. 3, 7, 9 (see for additional synonymy).
1994 *Leiosphaeridia jacutica*; Butterfield, Knoll, and Swett, p. 42, fig. 16H.
1994 *Leiosphaeridia jacutica*; Hofmann and Jackson, 1994, p. 22, fig. 17.1–17.4.
2005 *Leiosphaeridia jacutica*; Grey, 2005, p. 183, fig 63G.
2009 *Leiosphaeridia jacutica*; Vorob'eva, Sergeev, and Knoll, p. 185, fig. 14.13.
2016 *Leiosphaeridia jacutica*; Porter and Riedman, p. 830, fig. 11.3

Holotype.—(Timofeev, 1966; pl. 7, fig. 2), preparation number 452/1, Biostratigraphy Laboratory, ЛАГЕД АН СССР Maya River Collection, Mesoproterozoic to Neoproterozoic Lakhanda Group, Russia.

Occurrence.—Ubiquitous in Precambrian and Phanerozoic organic-walled microfossil assemblages.

https://doi.org/10.1017/jpa.2016.49 Published online by Cambridge University Press

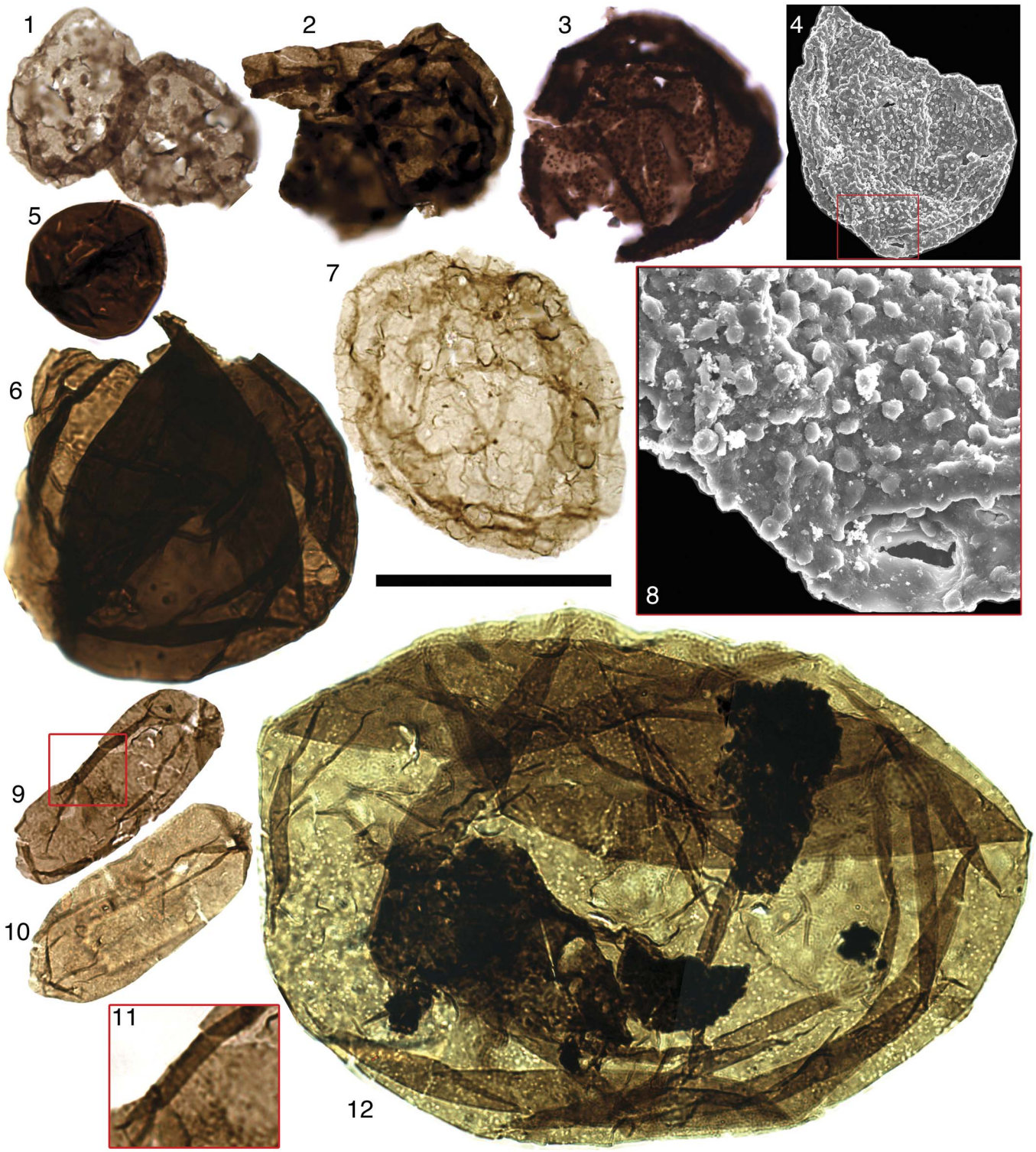

Figure 11. (**1, 2**) Unnamed Acritarch sp. A. (**3, 4, 8**) *Vidalopalla verrucata* n. comb. (**5**) *Leiosphaeridia crassa*. (**6**) *Leiosphaeridia jacutica*. (**7**) *Leiosphaeridia minutissima*. (**9, 10**) *Navifusa majensis*. (**12**) *Leiosphaeridia tenuissima*. (**8**) Shows detail of (**4**). (**11**) Shows transverse annulations of (**9**). Scale bar is 50 µm for (**1–7, 9, 10, 12**), 10 µm for (**8**), and 25 µm for (**11**). Slide and coordinates: (**1**) 1255.43-15A/E25-1 (P49477); (**2**) 1265.71-105A/L17-4 (P49479); (**3**) 1265.57-19A/H32-1 (P49513); (**4, 8**) 1265.57- LittleStubB (P49540); (**5**) 1265.57-19A/T40-2 (P49514); (**6**) 1265.57- 19A/M43-0 (P49515); (**7**) 1237.74-12/J34-1 (P49464); (**9, 11**) 1265.57-19A/T28-3 (P49516); (**10**) 1266.31-20/P35-0 (P49556); (**12**) 1265.46-18A/N17-0 (P49486).

Description.—Solitary, spheroidal, smooth, single-walled vesicles 70 to 317 µm in diameter ($\overline{x}$ = 137.3 µm, s = 48.4 µm, N = 35). Vesicle dark but translucent.

Material examined.—Thirty-six specimens from the Alinya Formation, Giles 1 drill core depths 1,242.84, 1,244.17, 1,248.91, 1,255.76, 1,265.36, 1,265.46, and 1,265.57 m.

https://doi.org/10.1017/jpa.2016.49 Published online by Cambridge University Press

Leiosphaeridia minutissima (Naumova, 1949) Jankauskas (in Jankauskas et al., 1989)
Figure 11.7

1949 *Leiotriletes minutissimus* Naumova, p. 52, pl. 1, figs. 1, 2, pl. 2, figs. 1, 2.
1989 *Leiosphaeridia minutissima*; Jankauskas in Jankauskas, Mikhailova, and Hermann, p. 79, pl. 9, figs. 1–4, 11 (see for additional synonymy).
1994 *Leiosphaeridia minutissima*; Hofmann and Jackson, p. 21, figs. 15.9–15.15.
1999 *Leiosphaeridia minutissima*; Buick and Knoll, p. 756, fig. 5.3–5.6.
2005 *Leiosphaeridia minutissima*; Grey, p. 184, fig. 63D.
2008 *Leiosphaeridia minutissima*; Moczydłowska, p. 84, fig. 8H.
2016 *Leiosphaeridia minutissima*; Porter and Riedman, p. 830, fig. 11.1, 11.5, 11.6.

Holotype.—No holotype was designated by Naumova (1949). Jankauskas (in Jankauskas et al., 1989, p. 80) designated a specimen of *Leiotriletes minutissimus* (pl. 1, fig. 1) from Naumova (1949) as lectotype. Lower Cambrian Blue Clay, Baltic States.

Occurrence.—Ubiquitous in Precambrian and Phanerozoic organic-walled microfossil assemblages.

Description.—Solitary, spheroidal, smooth, single-walled vesicles 10 to 70 µm in diameter ($\overline{x} = 35.7\,\mu$m, s = 13.4 µm, N = 79).

Material examined.—One hundred specimens measured (many more present but uncounted) from the Alinya Formation, Giles 1 drill core depths 1,237.74, 1,242.84, 1,244, 1,244.17, 1,255.76, 1,257.73, 1,265.36, 1,265.46, 1,265.57, 1,265.71, and 1,266.31 m.

Leiosphaeridia tenuissima Eisenack, 1958a
Figure 11.12

1958a *Leiosphaeridia tenuissima* Eisenack, p. 391, pl. 1, figs. 2, 3.
1989 *Leiosphaeridia tenuissima*; Jankauskas in Jankauskas, Mikhailova, and Hermann, p. 81, pl. 9, figs. 12, 13.
1994 *Leiosphaeridia tenuissima*; Butterfield, Knoll, and Swett, p. 42, fig. 16I.
1994 *Leiosphaeridia tenuissima*; Hofmann and Jackson, 1994, p. 22, fig. 15.16–15.18.
2005 *Leiosphaeridia tenuissima*; Grey, p. 184, fig. 63H.
2016 *Leiosphaeridia tenuissima*; Porter and Riedman, p. 830, fig. 11.4.

Holotype.—(Eisenack, 1958a; pl. 1, fig. 2), preparation A_3, 3 number 4 from the *Dictyonema*-shales of the Ordovician Baltic.

Occurrence.—Ubiquitous in Precambrian and Phanerozoic organic-walled microfossil assemblages.

Description.—Solitary, spheroidal, smooth, single-walled vesicles 70 to 144 µm in diameter ($\overline{x} = 95.9\,\mu$m, s = 23.1 µm, N = 11).

Material examined.—Seventeen specimens from the Alinya Formation, Giles 1 drill core depths 1,237.74, 1,244.17, 1,255.76, 1,265.36, 1,265.46, 1,265.57, and 1,265.71 m.

Genus *Morgensternia* new genus

Type Species.—*Morgensternia officerensis* n. sp., by monotypy.

Diagnosis.—As for type species.

Etymology.—The German, *morgenstern*, referring to the fossil's resemblance to the medieval weapon of that name composed of a metal ball bearing frequent spikes.

Remarks.—Similar fossils have been assigned in open nomenclature to the genus *Gorgonisphaeridium*; however, due to significant differences in diagnostic characters, the new genus *Morgensternia* is erected here for the new species *M. officerensis* rather than including this species in the existing genus *Gorgonisphaeridium*. *M. officerensis* processes are straight rather than sinuous and consistently conically tipped, rather than the occasional branched processes seen in species of *Gorgonisphaeridium,* including the type species, *G. winslowiae* Staplin, Jansonius, and Pocock, 1965. In addition, *M. officerensis* possesses an outer vesicle, a feature not found in *Gorgonisphaeridium* species. The combination of diagnostic characters seen in *M. officerensis* is not found in previously erected genera.

Morgensternia officerensis new species
Figure 9.1–9.8

?1991 *Gorgonisphaeridium maximum* Knoll, Swett, and Mark, p. 557, fig. 21.12.
?1992 *Baltisphaeridium* sp. A; Zang and Walter, p. 280, pl. 5, figs. A–J.
?1992 *Baltisphaeridium* sp. B; Zang and Walter, p. 281, pl. 5, figs. K–L, (non M–O).
?1994 *Gorgonisphaeridium* sp.; Butterfield, Knoll, and Swett, p. 40, figs. 14I–J.
?2009 *Cymatiosphaeroides* cf. *C. kullingii*; Nagy, Porter, Dehler, and Shen, fig. 1.I.

Holotype.—(Fig. 9.1), SAM collection number P49520, slide 1265.57-19A, coordinate V32-4, depth of 1,265.57 m, Giles 1 drill core, Alinya Formation.

Diagnosis.—Optically dense, organic-walled microfossils with abundant (7 to 10 processes visible in a 10 µm section of vesicle periphery) processes that are ~2 µm long, solid, and conical, narrowing from a ~0.8 µm diameter base to a ~0.4 µm diameter tip. Smooth-walled outer envelope occasionally preserved. Processes do not support or connect to the outer envelope.

Occurrence.—See Remarks section for details of possible occurrences.

https://doi.org/10.1017/jpa.2016.49 Published online by Cambridge University Press

Description.—Organic-walled microfossils with optically dense vesicles ranging in diameter from 23.7 to 59.6 µm ($\bar{x}$ = 36.3 µm, s = 8 µm, N = 37), bearing abundant short, solid, conical processes that range in length from 1.0 to 3.3 µm ($\bar{x}$ = 1.9 µm, s = 0.6 µm, N = 37). Solid character was determined in SEM by observation of stumps upon the vesicle left by broken processes (e.g., arrow in Fig. 9.8). Processes narrow from the base (0.8 µm) to a blunt tip (~0.4 µm); rarely, specimens are seen to possess processes with bulbous terminations in addition to conical processes (Fig. 9.4). Processes are typically straight, but rarely a few are seen to be bent (not broken; arrows in Fig. 9.2, 9.3), possibly indicating a plastic, rather than brittle, character. Smooth outer envelope is occasionally preserved (Fig. 9.1, 9.2).

Etymology.—In reference to the fossil's discovery in units of Officer Basin, Australia.

Material examined.—Thirty-seven specimens from the Alinya Formation, Giles 1 drill core depths 1,265.46, 1,265.57, and 1,265.71 m.

Remarks.—The specimens described here from the Alinya Formation resemble fragmentary acritarch fossils from the Draken (Knoll et al., 1991) and Svanbergfjellet formations (Butterfield et al., 1994) in that all of these forms bear small, solid, conical processes. The Draken and Svanbergfjellet specimens were assigned to the genus *Gorgonisphaeridium,* an almost entirely Paleozoic genus with a broad diagnosis that indicates the spines are "solid, usually sinuous, slender or broad … tips simple or distally branched, flexible, bases may be slightly bulbous" (Staplin et al., 1965). Knoll and colleagues (1991) created a new combination, *Gorgonisphaeridium maximum,* based on the single, solid-process bearing Draken specimen and seemingly similar fossils from the Ediacaran age Doushantuo Formation. However, subsequent study of the Doushantuo specimens revealed a hollow character to the processes, and the combination was recognized as invalid (Knoll, 1992, p. 765). The genus *Echinosphaeridium* (later renamed *Knollisphaeridium* by Willman and Moczydłowska, 2008) was then erected for large acritarchs with densely arranged, hollow processes, excluding the solid-process-bearing Draken specimen. Butterfield and colleagues (1994) left a similar form in open nomenclature, *Gorgonisphaeridium* sp. Both the Draken and Svanbergfjellet specimens resemble those described here, save the near order-of-magnitude difference in vesicle diameters.

The new genus *Morgensternia* is erected here to accommodate the new species *M. officerensis* due to dissimilarity with species of *Gorgonisphaeridium* such as the presence of an outer envelope, a general lack of flexibility to the spines, an absence of branching, and shorter and more numerous processes in this new species.

Cymatiosphaeroides kullingii is another form bearing short, thin, solid processes and having an outer envelope (up to twelve envelopes according to the emended diagnosis of Butterfield and colleagues, 1994). However, *C. kullingii* differs from *Morgensternia officerensis* not only by its tendency toward much greater vesicle dimensions (30–350 µm) but, more important, by its diagnostic thickening of its processes at both the base and apex and the connection of the processes to the outer vesicle (Knoll et al., 1991). *M. officerensis* specimens do not indicate connection between the processes and outer vesicle.

Certain specimens illustrated from the Neoproterozoic Liulaobei and Gouhou formations of North China (pl. 5, figs. A–L; Zang and Walter, 1992) appear comparable to the forms described here as *M. officerensis*. Zang and Walter describe the processes as hollow in character and communicating freely with the vesicle interior, an interpretation difficult to reconcile with the images provided. This interpretation contrasts with that of solid processes in *M. officerensis* of the Alinya Formation. In addition, Yin and Sun (1994) suggest, because of a lack of flattening, that the Liulaobei and Gouhou specimens may actually be modern contaminants. These fossils would be placed in synonymy only if future investigation assures a Neoproterozoic provenance and reveals a shared hollow or solid character for processes of both the Australian and Chinese forms.

M. officerensis is considered to fall outside of *Lanulatisphaera laufeldii* due to its conical and nonfusing processes, more optically dense vesicle, and somewhat smaller vesicle diameter of the former. In addition, the nano-scale mammillar ornament of *L. laufeldii* (Figs. 9.9, 10) is not seen in *M. officerensis*.

Genus *Navifusa* Combaz, Lange, and Pansart, 1967 ex Eisenack, 1976

Type species.—*Navifusa navis* (Eisenack 1938) Eisenack, 1976

Navifusa majensis Pyatiletov, 1980
Figure 11.9–11.11

1980 *Navifusa majensis* Pyatiletov, p. 144, fig. 1.
1994 *Navifusa majensis*; Hofmann and Jackson, p. 20, fig. 15.1–15.4.
1995 *Lakhandinna dilatata*; Zang, p. 165, fig. 29A, ?D, ?G.
1995 *Archaeoellipsoides karatavicus*; Zang, p. 162, fig. 29H, J, K.
1999 *Navifusa majensis*; Samuelsson, Dawes, and Vidal, fig. 5A.
2001 *Navifusa majensis*; Samuelsson and Butterfield, fig. 5A.
2005 *Navifusa majensis*; Prasad, Uniyal, and Asher, figs. 3.10, 5.15, ?7.1.
2011 *Navifusa majensis*; Couëffé and Vecoli, fig. 6.7.
2013 *Navifusa majensis*; Tang et al., fig. 5H.
2016 *Navifusa majensis*; Porter and Riedman, p. 833, fig. 13.1.

Holotype.—(Pyatiletov, 1980; fig. 1a), ИГиГ СО АН СССР, preparation number 685 from Khabarovsk Krai, left bank of Maya River, Mesoproterozoic to Neoproterozoic Lakhanda Group, third subsuite, Russia.

Occurrence.—*Navifusa majensis* is widely distributed in units of late Mesoproterozoic to early Neoproterozoic age, including the Lakhanda Group of Siberia (Pyatiletov, 1980), the Bylot Supergroup of Arctic Canada (Hofmann and Jackson, 1994), the Thule Supergroup of Greenland (Samuelsson et al., 1999), the Lone Land Formation of northwestern Canada (Samuelsson and

https://doi.org/10.1017/jpa.2016.49 Published online by Cambridge University Press

Butterfield, 2001), the Vindhyan Supergroup of Central India (Prasad et al., 2005), the Kwahu Group of Ghana (Couëffé and Vecoli, 2011), and the Liulaobei Formation of North China (Tang et al., 2013).

Description.—Ellipsoidal organic-walled microfossils with a mean length of 63.3 µm and mean width of 28.0 µm (length range 39.9 to 118.0 µm, width range 16.2 to 78.9 µm). Mean length-to-width ratio is 2.5, varying from 1.5 to 4.1 (N = 9).

Material examined.—Nine specimens from the Alinya Formation, Giles 1 drill core depths 1,255.43, 1,265.57, and 1,266.31 m.

Remarks.—One specimen (Fig. 11.9, 11.11) bears subtle transverse annulations in its center, a feature suggestive of *Pololeptus rugosus* described from the Liulaobei Formation (Yin and Sun, 1994; Tang et al., 2013). The genus *Pololeptus* was erected by Yin (in Yin and Sun, 1994) to accommodate oval-shaped, organic-walled microfossils with patches of characteristic "worm-like or netted sculptures" (p. 101). Tang and colleagues (2013) synonymized the three species of this genus and emended the diagnosis of the remaining species, *P. rugosus*, to include the newly discovered character of transverse annulations. The single annulated specimen recovered from the Alinya Formation does not bear the characteristic terminal sculpture described by Yin and Sun (1994) and Tang et al. (2013) and is narrower than the Liulaobei specimens (19 µm wide, 53 µm long as compared to 30–145 µm wide and 40–280 µm long in Liulaobei Formation). For these reasons, we are hesitant to assign the name *P. rugosus* to this one specimen.

Genus *Pterospermopsimorpha* Timofeev, 1966 emend. Mikhailova and Jankauskas (in Jankauskas et al., 1989)

Type Species.—*Pterospermopsimorpha pileiformis* Timofeev, 1966.

Remarks.—The diagnosis followed here is from Jankauskas and colleagues (1989). The fossils are described as consisting of two spheroidal to ellipsoidal vesicles, one within the other. The diameter of the inner vesicle is not less than two-thirds the diameter of the outer. Vesicle diameters range from 10 to 500 µm for the outer and 8 to 400 µm for the inner.

This genus, like many morphologically simple acritarch genera, is almost certainly polyphyletic. Thus, interpretations of biological or ecological significance of the presence or absence of members of this genus warrant caution.

Pterospermopsimorpha, a dispheromorph, is often confused with the pteromorph genus, *Simia*. See *Simia* remarks section for details.

Pterospermopsimorpha insolita Timofeev, 1969 emend. Mikhailova (in Jankauskas et al., 1989)
Figure 12.6–12.9

1969 *Pterospermopsimorpha insolita* Timofeev, p. 16, pl. 3, fig. 8.

1989 *Pterospermopsimorpha insolita*; Mikhailova in Jankauskas, Mikhailova, and Hermann, p. 49, pl. 3, figs. 5, 6 (see for additional synonymy).

1994 *Pterospermopsimorpha insolita*; Hofmann and Jackson, p. 24, fig. 17.10–17.13.

?1997 ?*Pterospermopsimorpha* sp.; Cotter, p. 266, fig. 8H.

1999 *Pterospermopsimorpha insolita*; Cotter, p.76, fig. 7B.

?1999 *Simia annulare*; Samuelsson, Dawes, and Vidal, fig. 7A.

2005 *Pterospermopsimorpha insolita*; Prasad, Uniyal, and Asher, pl. 3, figs. 7, 9, pl. 5, fig. 17.

2009 *Pterospermopsimorpha insolita*; Nagy, Porter, Dehler, and Shen, fig. 1E.

?2011 *Pterospermopsimorha insolita*; Couëffé and Vecoli, fig. 6.6.

Holotype.—Holotype designated by Timofeev (1969, p. 16, pl. 3, fig. 8 from Turukhansk area on Tunguska River, preparation number 16/5, Biostratigraphy Laboratory ИГТД АН СССР) was reported by Jankauskas and colleagues (1989, p. 49) as lost; they selected preparation number 16/42 from the same location for the lectotype (Jankauskas, 1989; p. 49, pl. 3, fig. 6).

Occurrence.—A common and widely distributed component of organic-walled microfossil assemblages ranging from Mesoproterozoic to early Paleozoic in age (discussed in Hofmann and Jackson, 1994). Reported occurrences include units of Siberia (Timofeev, 1969; Jankauskas et al., 1989), the Bylot Supergroup of Canada (Hofmann and Jackson, 1994), the Vindhyan Supergroup of India (Prasad et al., 2005), the Chuar Group of western United States (Nagy et al., 2009); and Kanpa, Hussar, and Browne formations of western Officer Basin, Australia (Cotter, 1999).

Description.—Spheroidal organic-walled microfossils of vesicle-within-vesicle construction. Diameters of inner vesicles range from 16.9 to 64.3 µm ($\bar{x}$ = 35.7 µm, s = 12.7 µm), diameters of outer vesicles from 25.0 to 97.4 µm ($\bar{x}$ = 42.5 µm, s = 16.9 µm).

Material examined.—Thirty-seven specimens from Alinya Formation, Giles 1 drill core depths 1,237.74, 1,244.17, 1,248.91, 1,255.76, 1,257.73, 1,265.36, 1,265.57, 1,265.71, and 1,266.31 m.

Genus *Simia* Mikhailova and Jankauskas (in Jankauskas et al., 1989)

Type Species.—*Simia simica* (Jankauskas, 1980) Jankauskas et al., 1989.

Description.—Organic-walled microfossils with spheroidal to discoidal central bodies 20 to 300 µm in diameter and bearing an equatorial flange of widths 5 to 30 µm.

Remarks.—There is much confusion in the literature regarding the genus *Simia* and how it differs from the genus *Pterospermopsimorpha*. The main difference between these two genera is easily recognized in principle; *Simia* is a spheroidal to

https://doi.org/10.1017/jpa.2016.49 Published online by Cambridge University Press

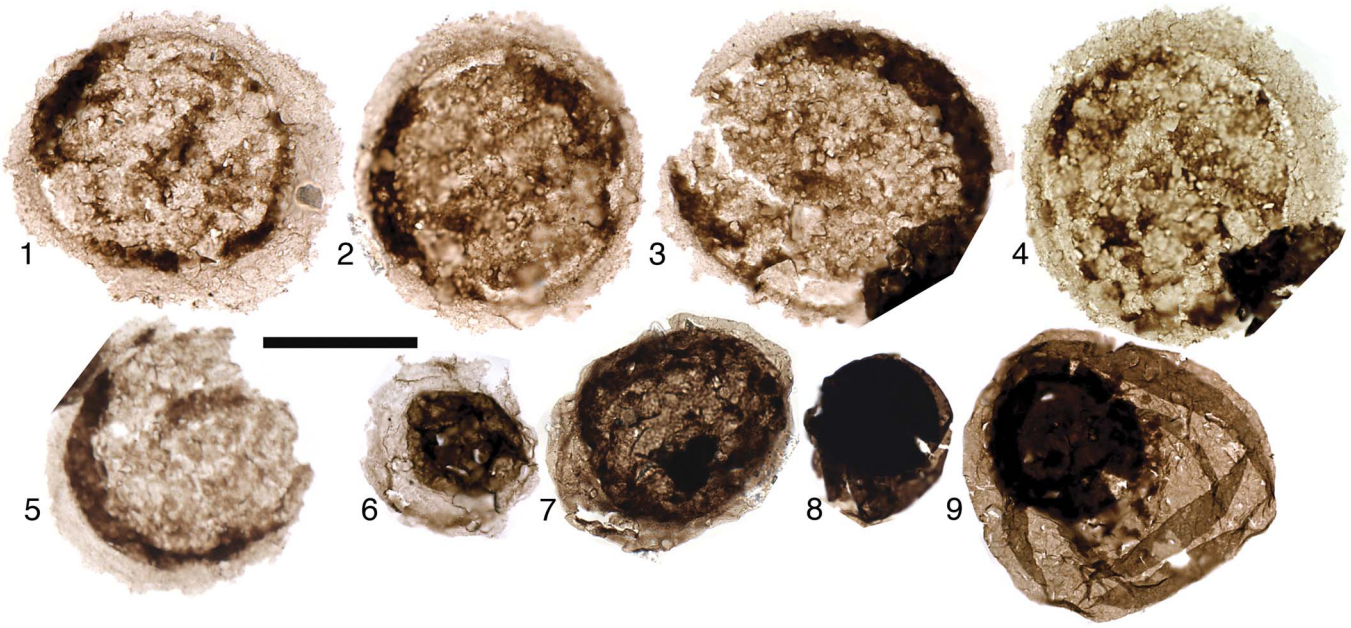

Figure 12. (**1–5**) *Simia annulare*: (**3, 5**) note tears extending from equatorial flap into central portion. (**6–9**) *Pterospermopsimorpha insolita*: (**6, 9**) note wrinkles and folds in outer vesicle; (**7–9**) note tears in outer vesicle. Scale bar = 50 μm. Slide and coordinates: (**1**) 1244.17-14B/F16-1 (P49471); (**2**) 1244.17-14B/N36-2 (P49472); (**3**) 1244.17-14B/O34-0 (P49473); (**4**) 1244.17-14B/E31-0 (P49474); (**5**) 1244.17-14A/H22-0 (P49468); (**6**) 1244.17-14B/N36-2 (P49475); (**7**) 1237.74-12/O25-3 (P49466); (**8**) 1265.71-105A/Q38-3 (P49554); (**9**) 1265.71-105A/P11-2 (P49555).

discoidal body bearing an equatorial flange, not unlike a ballerina's tutu, whereas *Pterospermopsimorpha* is a dispheromorph, an acritarch composed of sphere-within-a-sphere construction. However, accurate fossil identification is problematic because *Simia* fossils are preserved as flattened bodies viewed from the poles, not the equator (as the 'equator' is represented by the great circle of the flange or 'tutu'). Part of this confusion may likely be attributed to the unfortunate choice of the name *Pterospermopsimorpha*, a name misleadingly suggestive of the pteromorph (wing or flap-bearing) acritarchs (Downie et al., 1963).

In practical terms, certain characters aid in distinguishing these two forms. Convenient wrinkles, folds, and tears (e.g., radial cracking of the internal body independently of the external envelope; Fig. 12.8, 12.9) can often suggest the presence of two nested vesicles. In addition, if the fossil's opacity remains more or less consistent from the center to the edge, one would expect this to be indicative of *Simia*. In a dispheromorph such a *Pterospermopsimorpha*, one would expect the central region to be darker in transmitted light; in this area the light must pass through four vesicle layers, as opposed to only two nearer its edges. This is in contrast to the two layers in the central body of a pteromorph such as *Simia* and the one or two layers at its edges.

Simia annulare (Timofeev, 1969) Mikhailova
(in Jankauskas et al., 1989)
Figure 12.1–12.5

1969 *Pterospermopsimorpha annulare* Timofeev, p. 17, pl. 3, fig. 9.

1989 *Simia annulare*; Mikhailova in Jankauskas, Mikhailova, and Hermann, p. 66, pl. 6, figs. 5–8.

?1992 *Simia annulare*; Zang and Walter, p. 307, pl. 7, figs. A–B.

1995 *Simia annulare*; Zang, fig. 28E.

1999 *Simia annulare*; Cotter, 1999, p. 77, fig. 7H.

1999 *Simia annulare*; Samuelsson, Dawes, and Vidal (in part), figs. 7B–E, non 7A.

?2005 *Simia annulare*; Prasad, Uniyal, and Asher, p. 46, pl. 3, fig. 8, pl. 5, fig. 9.

2009 *Ostiumsphaeridium complitum* Vorob'eva, Sergeev, and Knoll, p. 186, fig. 14.1–14.5.

2013 *Simia annulare*; Tang et al., fig. 4F–G.

Holotype.—(Timofeev, 1969; pl. 3, fig. 9), preparation number 147/4 of Biostratigraphy Laboratory ИГТД АН СССР, Riphean Kildinskaya Suite.

Occurrence.—Occurrences are difficult to establish from published reports due to confusion between *Simia* and *Pterospermopsimorpha* species. *S. annulare* appears to range from the late Mesoproterozoic into at least the middle Ediacaran Period. This form has been reported from the Thule Supergroup of Greenland (Samuelsson et al., 1999), Vychegda Formation of eastern Russia (Vorob'eva et al., 2009), and Liulaobei Formation of North China (Tang et al., 2013).

Description.—Organic-walled microfossils 20.4 to 209.5 μm in diameter ($\bar{x}$ = 81.4 μm, s = 37.5 μm, N = 44), spheroidal to discoidal central bodies bearing an equatorial flange of width 3.3 to 32.4 μm ($\bar{x}$ = 9.4 μm, s = 5.6 μm) that is 5% to 20% the diameter of the central body.

Material examined.—Forty-four specimens from Alinya Formation, Giles1 drill core depths 1,237.74, 1,242.84, 1,244.17, 1,248.91, and 1,265.57 m.

https://doi.org/10.1017/jpa.2016.49 Published online by Cambridge University Press

Remarks.—Specimens of *Simia annulare* described in this study are closely comparable to those identified as *Ostiumsphaeridium complitum* (Vorob'eva et al., 2009), which is considered here to be a junior synonym of *S. annulare*. *O. complitum* was described as a spheroidal to subspheroidal vesicle with a distinctive slit-like opening that causes the vesicle to pop open and "forms a flap that surrounds [the] vesicle like a halo 10–30 μm wide with a fringed margin" (Vorob'eva et al., 2009; p. 186). The formation of this halo or flange is problematic as even a flexible spheroidal membrane, when everted, will exhibit radial splits, not form a continuous border. In addition, if the equatorial flange is formed by the opened vesicle, the split itself should no longer be visible on the specimen; instead there should be only a roughly circular sheet of vesicle with radial splitting that occurred during eversion. Instead, specimens of *O. complitum* exhibit a spheroidal central body surrounded by a fringed border; this accords well with the diagnosis of *S. annulare*, although requiring an increase in diameter for the species description. The identification of these forms with the larger *Simia* species, *S. nerjenica* Veis, 1989 in Jankauskas et al., 1989, was rejected due to their lack of the characteristic 4 to 6 concentric folds surrounding the central body and a general dissimilarity with the *S. nerjenica* holotype (Jankauskas et al., 1989, pl. 9, fig. 10). Specimens from the Alinya Formation lack the slit-like opening that Vorob'eva and colleagues considered diagnostic of *O. complitum*, but these forms are similar in dimension and presence of a fringed equatorial border.

Genus *Valeria* Jankauskas, 1982

Type Species.—*Valeria lophostriata* Jankauskas (1979) 1982.

Valeria lophostriata Jankauskas (1979) 1982
Figure 4.1

1979 *Kildinella lophostriata* Jankauskas, p. 53, fig. 1.13–1.15.
1982 *Valeria lophostriata*; Jankauskas, p. 109, pl. 39, fig. 2.
1989 *Valeria lophostriata*; Jankauskas in Jankauskas, Mikhailova, and Hermann, p. 86, pl. 16, figs. 1–5 (see for additional synonymy).
1995 *Valeria lophostriata*; Zang, p. 170, fig. 28I.
1999 *Valeria lophostriata*; Samuelsson, Dawes, and Vidal, fig. 8E.
2001 *Valeria lophostriata*; Javaux, Knoll, and Walter, fig 1D.
2009 *Valeria lophostriata*; Nagy, Porter, Dehler, and Shen, fig. 1a, b.
2009 *Valeria lophostriata*; Nagovitsin, p. 144, fig. 4E.
?2011 *Valeria lophostriata*; Couëffé and Vecoli, fig. 6.4.
?2012 dark-walled megaspheric coccoid; Battison and Brasier, fig. 8B.
2016 *Valeria lophostriata*; Porter and Riedman, p. 842, figs. 19.1–19.3

(For additional synonymy, see also Hofmann, 1999, table 1)

Holotype.—(Jankauskas, 1979; fig. 1.14), Lithuanian Geological Prospecting Research Institute, number 16-62-4762/16, sp. 1, DH Kabakovo 62 drill core, depth 4,762 to 4,765 m, Zigazino-Komarovo suite, middle Riphean.

Occurrence.—Widely distributed in late Paleoproterozoic through early (pre-Sturtian glacial) Neoproterozoic rocks.

Description.—Spheroidal organic-walled microfossils bearing distinctive sculpture of parallel ridges, similar to corduroy fabric. Vesicle diameters range from 50.4 to 119.0 μm ($\overline{x} = 79.3\,\mu$m, s = 26.2 μm, N = 13); ridges are ~0.5 μm apart.

Material examined.—Fourteen specimens from Alinya Formation, Giles1 drill core depths 1,265.46, 1,265.57, and 1,265.71 m.

Genus *Vidalopalla* new genus

Type species.—*Vidalopalla verrucata* (Vidal in Vidal and Siedlecka, 1983) n. comb., by monotypy.

Diagnosis.—Spheroidal organic-walled microfossil bearing more or less regularly arranged, solid, small (typically 1 to 2 μm in diameter), hemispherical verrucate external ornament.

Etymology.—Named in honor of the Precambrian paleontologist Gonzalo Vidal with the addition of the Greek, *palla*, describing the spherical form of the fossils.

Remarks.—The genus *Vidalopalla* is erected here to accommodate the species *V. verrucata* (= *Kildinosphaera verrucata*). Originally erected in 1983 by Vidal (in Vidal and Siedlecka, 1983) as a species of the new genus *Kildinosphaera*, *K. verrucata* was born into limbo. In erecting *Kildinosphaera* and naming one of its constituent species as *Kildinosphaera lophostriata* (transferring it from *Kildinella*), Vidal and Siedlecka unknowingly transferred the newly minted type species of the genus *Valeria* that Jankauskas (1982) had created less than a year previous. This caused the genus *Kildinosphaera* to instantaneously become a junior (homotypic) synonym of *Valeria*. The other species Vidal and Siedlecka named to *Kildinosphaera* (*K. chagrinata*, *K. granulata*, and *K. verrucata*) were left homeless—validly published but belonging to an illegitimate genus. In 1990, Fensome and colleagues suggested a new combination, placing '*K.*' *verrucata* into the genus *Valeria* as *V. tschapomica*. This specific epithet was chosen in light of implications in the species remarks by Vidal and Siedlecka (1983) and the more formal recommendation by Amard (1984) that *Kildinosphaera verrucata* was synonymous with the earlier named form *Kildinella tschapomica* Timofeev 1966 (Amard also suggested synonymy with *Kildinella exsculpta* Timofeev, 1969, but *K. tschapomica* would have priority if these forms were truly synonymous). The recommendation of Fensome and colleagues (1990), and suggested synonymies of Amard (1984), are rejected here, as done tacitly by others such as Knoll (1994) and Butterfield and Rainbird (1998). The ornaments of *K. tschapomica* and *K. exsculpta* appear to be diagenetically introduced features on a smooth-walled acritarch belonging to the form genus, *Leiosphaeridia* (Knoll, 1996, p.70).

Samuelsson and colleagues (1999) informally suggested the transfer of 'K.' *verrucata* to the genus *Lophosphaeridium.*

https://doi.org/10.1017/jpa.2016.49 Published online by Cambridge University Press

This suggestion is not taken here because the descriptions of the genus and type species, although broadly permissive ("thick, knobby envelope," Timofeev, 1969, p. 29), are so broad as to include a number of other genera, and the illustration of the holotype material, a hand-drawn figure (plate 2, fig. 5, Timofeev, 1959), appears to show the tubercles as hollow protuberances of the vesicle rather than solid verrucae as diagnostic of the new genus *Vidalopalla*.

Vidalopalla verrucata (Vidal and Siedlecka, 1983)
new combination
Figure 11.3, 11.4, 11.8

1981 *Kildinella* sp. B; Vidal, p. 26, fig. 13 A–D.

1983 *Kildinosphaera verrucata* Vidal and Siedlecka, p. 62, fig. 5C.

?1984 *Kildinosphaera verrucata*; Amard, p. 1406, fig. 3C.

1985 *Kildinosphaera verrucata*; Vidal and Ford, p. 363, fig. 4A.

?1990 *Leiosphaeridia exculpta* (sic); Hermann, pl. 1, fig. 3.

?1992 *Leiosphaeridia verrucata*; Zang and Walter, p. 68, fig. 52I, *non* 50I.

Non 1994 *Kildinosphaera verrucata*; Yin and Sun, p. 100, figs. 5I, 5J, 7A.

1996 *Kildinosphaera verrucata*; Knoll, p. 70, pl. 4, fig. 5.

?1999 *Lophosphaeridium* sp. A; Samuelsson, Dawes, and Vidal, figs. 4E and 4H.

?2005 *Kildinosphaera verrucata*; Prasad, Uniyal, and Asher, figs. 7.19, 8.12, 11.15.

non 2009 *?Kildinosphaera verrucata*; Nagy, Porter, Dehler, and Shen, fig.1F.

?2011 *Lophosphaeridium* sp.; Strother, Battison, Brasier, and Wellman , fig. 1C–D.

?2016 *Vidalopalla* cf. *verrucata*; Porter and Riedman, p. 842, fig. 20.1.

Holotype.—(Vidal 1981; p. 26, fig. 13A–D), specimen E74–02: V/47 from the Neoproterozoic Ekkerøy Formation. Designated by Vidal and Siedlecka (1983).

Occurrence.—Occurs as an occasional component of early Neoproterozoic organic-walled microfossil assemblages. Distribution includes Vadsø and Barents Sea groups of East Finnmark (Vidal and Siedlecka, 1983) and Baffin Bay Group of Greenland (Samuelsson et al., 1999). Occurrence of this species was reported from the Wynniatt Formation of Arctic Canada (Butterfield and Rainbird, 1998), but no fossils were figured.

Description.—Spheroidal organic-walled microfossil with vesicle of moderate opacity, ~50 μm in diameter (range 25.8 μm to 68.6 μm, $\bar{x} = 50.4\ \mu m$, s = 17.8 μm, N = 4) with circular to ellipsoidal solid verrucae ~1 μm in diameter (range 0.7 to 1.3 μm, $\bar{x} = 0.9\ \mu m$, s = 0.3 μm, N = 4) on the exterior of vesicle.

Material examined.—Four specimens from the Alinya Formation, Giles 1 drill core depths 1,244.17, 1,265.46, and 1,265.57 m.

Basionym.—*Kildinosphaera verrucata* Vidal (in Vidal and Siedlecka, 1983, p. 62).

Remarks.—The Alinya specimens are somewhat smaller than those of the Ekkerøy Formation (Vidal, 1981; 40–132 μm) and somewhat larger than those of the Atar Formation (Amard, 1984; 24–40 μm) but are generally in accordance with both.

Vidal (1976) reports *Stictosphaeridium verrucatum* from the upper Visingsö beds of southern Sweden, but the specimen figured does not conform to the concept of *V. verrucata* (= *K. verrucata*) that he and Anna Siedlecka described from the Båtsfjord Formation of the Barents Sea Group, Norway. Instead, the specimen appears to be a leiosphaerid that may bear sparse, possibly taphonomically induced spots or bumps. Vidal (1979) also reports *S. verrucatum* from the Eleonore Bay Group of East Greenland, but no specimens were figured.

Vidalopalla verrucata can be distinguished from *Coneosphaera arctica* because the former bears ~1 to 2 μm solid, hemispherical vesicular ornament, whereas the latter is distinguished by bearing loosely aggregated, irregularly distributed, hollow spheroids about one-eight to one-tenth the diameter of the main vesicle.

Genus *Volleyballia* Porter and Riedman, 2016

Type species.—*Volleyballia dehlerae* Porter and Riedman 2016, by monotypy.

Remarks.—The striae of *Volleyballia dehlerae* are dissimilar from those of *Karenagare alinyaensis* n. gen, n. sp. in that *K. alinyaensis* bears wide, parallel, undulating ripple-like striations (Fig. 5.1–5.5) rather than ruts or gouges that incise the vesicle of *V. dehlerae* (Fig. 5.9–5.14).

Volleyballia dehlerae Porter and Riedman 2016
Figure 3.9–3.14

?1995 *Striasphaera radiata* Gao, Xing, and Liu, p. 14, 20, fig. 2.10, 2.11.

1999 ? *Leiosphaeridia* sp.; Cotter, fig. 8H.

?2000 Form 1; Simonetti and Fairchild, p. 25, fig. 8S.

?2009 Unnamed form A; Nagy, Porter, Dehler, and Shen, fig. 4D.

2016 *Volleyballia dehlerae* Porter and Riedman, p. 844, fig. 21.1–21.7.

Holotype.—(Porter and Riedman, 2016; fig. 16.1–16.3), UCMP 36080d, sample SP14-63-11, SEM slide = ker-2, EF = Q49. Neoproterozoic Tanner Member, Chuar Group, Grand Canyon, USA.

Occurrence.—This form is comparable to those reported from early Neoproterozoic units in the Chuar Group, USA (Nagy et al., 2009; Porter and Riedman, 2016), Officer Basin, Australia (Cotter, 1999), a Mesoproterozoic unit of northeastern China (Gao et al., 1995) and a poorly constrained unit considered an equivalent of the Mesoproterozoic Conselheiro Mata Group of Brazil (Simonetti and Fairchild, 2000).

https://doi.org/10.1017/jpa.2016.49 Published online by Cambridge University Press

Description.—Spheroidal organic-walled microfossils 20.1 to 35.4 μm in diameter ($\bar{x} = 26.2\,\mu$m, s = 3.8 μm, N = 15) bearing linear striations 0.9 to 1.8 μm wide ($\bar{x} = 1.2\,\mu$m, s = 0.2 μm, N = 15) as measured from crest to crest on vesicle surface. Vesicle optically dense. Groups of two to four striae frequently oriented at opposing angles to each other. Individual striae are typically visible for less than half the diameter of the vesicle surface. SEM specimens indicate the presence of unornamented outer envelope that may obscure the identity of this fossil, the additional layers serving to make some specimens opaque in transmitted light microscopy.

Material examined.—Fifteen specimens from the Alinya Formation, Giles1 drill core depths 1,255.43, 1,265.46, 1,265.57 m.

Unnamed Acritarch species A
Figure 11.1, 11.2

?1978 cells and endospores; Peat, Muir, Plumb, McKirdy, and Norvick, fig. 5B, D.

?1999 *Coneosphaera* sp. cf. *C. arctica*; Cotter, p. 72, fig. 7E.

Description.—Spheroidal organic-walled microfossils 32.8 to 47.5 μm in diameter ($\bar{x} = 36.9\,\mu$m, s = 7.1 μm, N = 4), bearing dark spots 2.1 to 3.7 μm in diameter ($\bar{x} = 2.9\,\mu$m, s = 0.7 μm, N = 4) on vesicle.

Material examined.—Four specimens from the Alinya Formation, Giles 1 drill core depths 1,242.84, 1,255.43, and 1,265.71 m.

Remarks.—These specimens possess dark spots on the vesicle, but since none of these occur along the periphery, it cannot be confirmed that these project from the vesicle surface as would processes or verrucae. It is possible these spots indicate variations in composition or density of the vesicle.

These specimens were not placed into the genus *Lophosphaeridium* Timofeev, 1959 ex Downie 1963 because that genus appears to have hollow protuberances from the vesicle, a feature inconsistent with these Alinya specimens.

Unnamed Acritarch species B
Figure 4.5

Description.—A single specimen of an optically dense, spheroidal, organic-walled acritarch bearing frequent (2 to 3 per 10 μm of vesicle periphery) tubular processes. Vesicle is 26.9 μm in diameter and processes are 2 μm in width and up to 3 μm in length, although they have probably been shortened by breakage.

Material examined.—Single specimen from the Alinya Formation, Giles 1 drill core depth 1,242.84 m.

Remarks.—This specimen is somewhat similar to two recovered from the upper Svanbergfjellet Formation (Butterfield et al., 1994, fig. 14F, G) and left in open nomenclature as *Goniosphaeridium* sp. With only one specimen recovered from the Alinya material, we hesitate to formally assign a taxonomic home.

Unnamed Acritarch species C
Figure 4.6

Description.—A single specimen of an optically dense, ellipsoidal, organic-walled acritarch measuring 24.9 μm by 34.6 μm and bearing a single neck-like structure that extends from the main vesicle; structure is 7.0 μm wide at base and extends 3.0 μm, tapering to 3.8 μm at what may be a broken tip.

Material examined.—Single specimen from the Alinya Formation, Giles 1 drill core depth 1,255.43 m.

Unnamed Acritarch species D
Figure 4.7–4.11

Description.—Three specimens of spheroidal, organic-walled acritarchs 30.6 to 47.9 μm diameter that bear frequent but variable processes that are up to 3.0 μm in length and less than 0.5 μm in width and that show occasional bifurcation (Fig. 4.7 [left-hand black arrow], 4.8). In transmitted light microscopy, bifurcation of the processes can be difficult to distinguish from overlap of adjacent processes (Fig. 4.7, right-hand black arrow).

Material examined.—Three specimens from the Alinya Formation, Giles 1 drill core depth 1,255.76, 1,265.46, and 1,265.57 m.

Remarks.—These specimens share some resemblance with forms from the 750–850 Ma Wynniatt Formation of northwestern Canada. Butterfield (2005) identified those forms as *Tappania* sp., a fossil genus previously known only from Paleo- and Mesoproterozoic units. Javaux (2011) has cited uncertainty about the assignment of the Wynniatt fossils to *Tappania* as the Wynniatt fossils lack the diagnostic neck-like extension and possess distinctive distal fusion not seen in the type material (a feature Butterfield, 2005, suggested may have been destroyed by laboratory processing of the older materials). The occurrence of occasional septae in the processes is a feature shared by the Mesoproterozoic and Wynniatt forms (not seen in the Alinya specimens).

The fossils recovered from the Alinya Formation do not conform well to the description of *Tappania* species from the Paleoproterozoic (He et al., 2009; Su et al., 2012) Ruyang Group type material (Yin, 1997) or from the somewhat younger Roper Group (1.5 Ga; Javaux et al., 2001). Although the vesicles of the Alinya fossils are only slightly smaller, the processes of the Alinya forms are significantly narrower than those described for these Mesoproterozoic *Tappania* species. In addition, the fossils described here do not possess the diagnostic neck-like protrusion.

The fossils described here are smaller but in keeping with the vesicle and process diameters of the Wynniatt material and demonstrate the irregularly furcating processes of both the Wynniatt '*Tappania*' and *Tappania* spp. of Yin (1997) and Javaux and colleagues (2001). In addition, the broad extension of the vesicle into a conical base of a process as seen in the

https://doi.org/10.1017/jpa.2016.49 Published online by Cambridge University Press

Wynniatt fossils is seen in one of the Alinya specimens (Fig. 4.7, white arrow). No fusion of the processes is seen in the Alinya material. The ends of the processes of the SEM specimens are unbroken and lobe-shaped; a similar feature is seen in some specimens of '*Tappania*' (Butterfield, 2005; figs. 3A, B, 7B).

Unnamed Acritarch species E
Figure 4.12, 4.13

Description.—A single specimen of an organic-walled, probably originally spheroidal acritarch measuring 31.6 µm across and bearing frequent, irregularly distributed hemispherical bodies (0.6 to 1.0 µm in diameter) as well as processes up to 1.5 µm in length and 0.6 to 0.8 µm in width. Processes may originate as hemispherical bodies. In addition to these features, this specimen bears a number of what appear to be ruptured blisters; these have centers of about 0.7 µm diameter and a flaring collar that extends 1.5 to 3.0 µm away from the center (Fig. 4.13). It is currently unclear whether this feature is primary or is a result of heterotrophic degradation.

Material examined.—Single specimen from the Alinya Formation, Giles 1 drill core depth 1,265.57 m.

Unnamed Acritarch species F
Figures 13.1–13.3, 13.11, 14

Description.—Spheroidal organic-walled microfossils bearing typically one, occasionally more than one, optically dense spot as a part of the vesicle. This is distinct from reports of dark bodies within vesicles that are interpreted to represent condensed cytoplasm (e.g., Knoll and Barghoorn, 1975). Vesicles range in diameter from 19.7 to 285.0 µm ($\overline{x}$ = 54.6 µm, s = 43.3 µm, N = 52), and dark spots range from 3.1 to 142.7 µm ($\overline{x}$ = 21.9 µm, s = 23.3 µm, N = 52). In one case, two spots are seen upon a vesicle; it appears to be in the process of fission (Fig. 13.1).

Material examined.—Sixty-two specimens from the Alinya Formation, Giles 1 drill core depths 1,237.74, 1,242.84, 1,244.17, 1,248.91, 1,255.43, 1,255.76, 1,257.73, 1,265.36, 1,265.46, 1,265.71, and 1,266.31 m.

Remarks.—The spots appear to be a (probably thickened) part of the vesicle, rather than a separate body within the vesicle as with the vesicle-within-a-vesicle construction of *Pterospermopsimorpha* sp. or in cases of shrunken cell contents of forms such as *Caryosphaeroides* sp. and *Glenobotrydion* sp. (e.g., Knoll and Barghoorn, 1975). The surficial nature is indicated in observation by light microscopy that the spots are in the same focal plane as the rest of the vesicle (often with somewhat diffuse edges as opposed to the distinct edges of internal bodies) as well as by the fact that occasional torn specimens show tearing across the spots (Fig. 13.3), and in some instances, degradation of the spot allows the viewer to see through the fossil to the back wall of the vesicle (Fig. 13.2, 13.11). This said, it is clear both from work by Pang and colleagues (2013) and from FIB-EM analyses of *Culcitulisphaera revelata* in this paper that acritarch vesicle walls do fuse during diagenesis, sandwiching any internal bodies between the walls and complicating interpretations of life positions. Cross sectioning of specimens and study by SEM and transmission electron microscopy (TEM) would aid in resolution of this matter.

This group appears to comprise one taxon; the distribution of vesicle diameters (Fig. 14) is weakly bimodal with a major mode at 20 to 30 µm and a minor mode from 60 to 80 µm. There is a linear relationship between vesicle diameters and spot diameters (m = 0.51, R^2 = 0.90658; Fig. 14). This linear relationship in spot and vesicle diameters is also seen in *Leiosphaeridia* species A of Nagy et al. (2009) (S.M.P., unpublished observations). In that form, the body or 'spot' upon the vesicle is clearly an operculum. It is unclear whether variability reflects an ontogenetic sequence or simply variation within a population.

The function of the spots in the Alinya specimens is unclear; were they opercula, one would reasonably expect to find a number of specimens opened, with opercula either attached or detached and showing distinctive holes, or even loose opercula within the strewn mount. None of these has been observed.

It is worth noting that similar features are seen in some specimens of *Synsphaeridium* spp. reported here (Fig. 13.6, 13.7, 13.13, 13.14). It is conceivable that this unnamed group and *Synsphaeridium* spp. are conspecific, their differences perhaps indicative of ontogenetic or ecophenotypic variation.

Unnamed Acritarch species G
Figure 13.4, 13.5, 13.9

Description.—Small (~36 µm), spheroidal, organic-walled microfossils bearing a ring (~3 µm wide) about the perimeter. Vesicle diameters range from 28.6 to 48.0 µm including the ring ($\overline{x}$ = 35.8 µm, s = 6.7 µm, N = 7), and ring widths range from 2.6 to 3.8 µm ($\overline{x}$ = 3.1, s = 0.4 µm, N = 7). This ring is not considered a happenstance of concentric folding as there is no evidence of radial cracking, and in one fossil (Fig. 13.9) the ring is no darker than the interior, arguing against the presence of more layers of vesicle in the periphery. This group may be another example of a winged, or pteromorphic, morphotype.

Material examined.—Seven specimens from the Alinya Formation, Giles1 drill core depths 1,265.46 and 1,265.57 m.

Cellular aggregates

Genus *Synsphaeridium* Eisenack, 1965

Type species.—*Synsphaeridium gotlandicum* Eisenack 1965.

Synsphaeridium spp.
Figure 13.6–13.8, 13.10, 13.12–13.16

Occurrence.—Ubiquitous in Precambrian and Phanerozoic organic-walled microfossil assemblages.

https://doi.org/10.1017/jpa.2016.49 Published online by Cambridge University Press

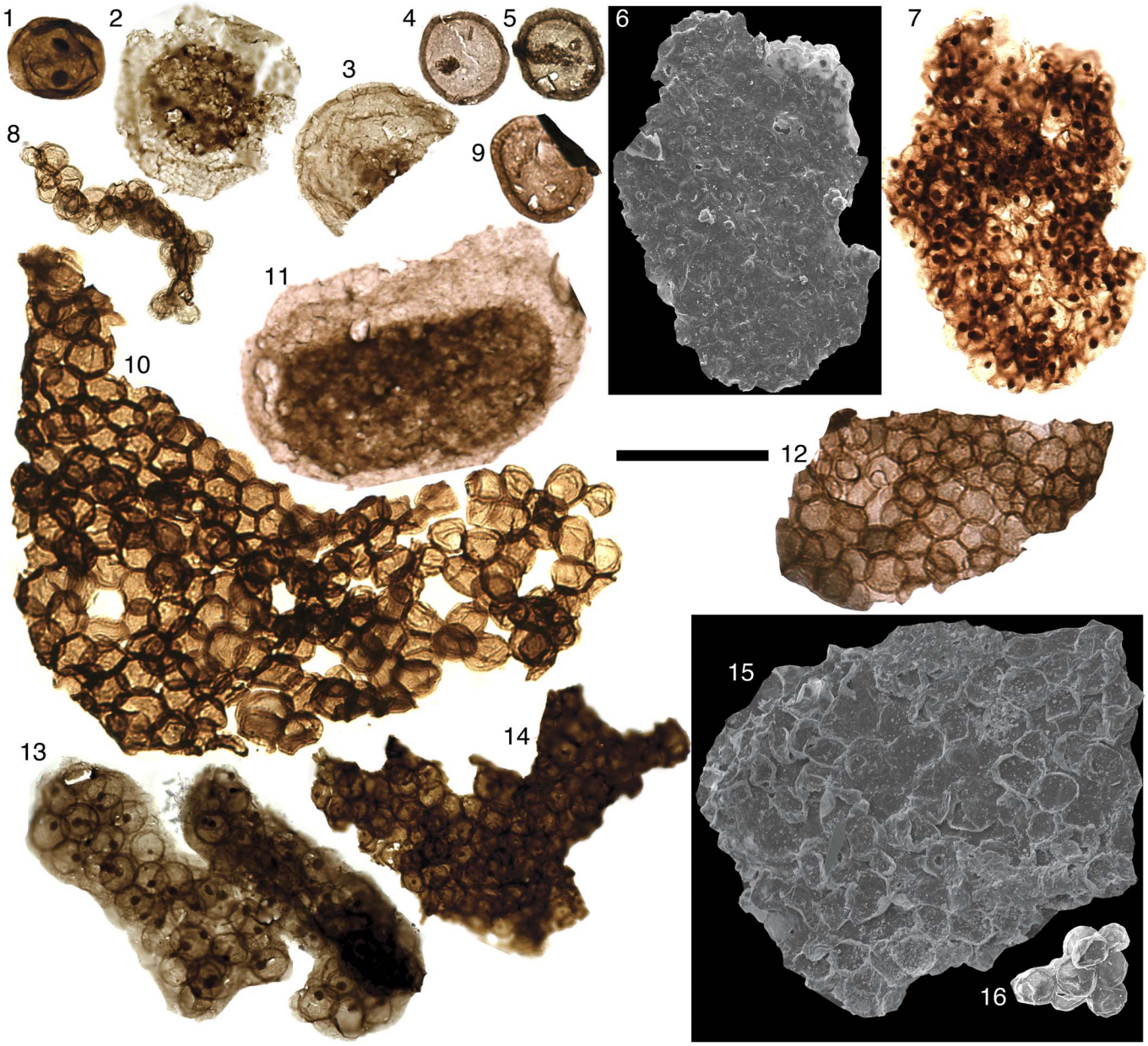

Figure 13. (**1–3, 11**) Unnamed Acritarch sp. F. (**2**) Note the darkened spot has a tear in the lower left quadrant through which the back side of the sphaerical vesicle is visible; in (**3**) the cell has torn across the darkened spot. (**4, 5, 9**) Unnamed Acritarch sp. G. (**6–8, 10, 12–16**) *Synsphaeridium* spp.; (**6, 7**) the same specimen imaged by SEM and transmitted light microscopy, respectively; note opaque spots in (**7**) are visible as raised knobs in (**6**); (**10**) illustrates variation of cell packing, ranging from a polygonal close-packing habit at the top left to loose-pack habit at the right. Scale bar = 50 µm. Slide/Stub and coordinates: (**1**) 1265.71-105A/R16-3 (P49551); (**2**) 1244.17-14B/S30-3 (P49469); (**3**) 1237.74-12/E27-2 (P49465); (**4**) 1265.57-19A/M21-3 (P49522); (**5**) 1265.57-19A/L17-3 (P49523); (**6, 7**) 1265.46-2_28B/W53-0 (P49505); (**8**) 1266.31-20/U35-0(P49557); (**9**) 1265.57-19A/R23-1 (P49524); (**10**) 1265.57-19A/O19-4 (P49525); (**11**) 1244.17-14B/P17-3 (P49470); (**12**) 1255.43-15B/J19-4 (P49480); (**13**) 1265.71-105A/J26-2 (P49552); (**14**) 1265.71-105A/S34-2 (P49553); (**15**) 1265.57-March20_epoxyA (P49548); (**16**) 1265.57- LittleStubB (P49544).

Description.—Aggregates of organic-walled, spheroidal cells; tight-packing habit may lead to compression and polygonal cell outline. Cell diameters range from 7.5 to 33.7 µm ($\overline{x} = 14.8\,\mu$m, s = 4.6 µm, N = 450 measured cells from 221 colonies) across forms showing loose association, tight-packing, optically dense and not dense vesicles and forms with dark spots upon the vesicle surface (those with dark bodies within the interior of the vesicle rather than a part of the vesicle were not counted separately).

Material examined.—Two hundred seventy-six colonies from the Alinya Formation, Giles 1 drill core depths 1,237.74, 1,242.84, 1,244, 1,244.17, 1,248.91, 1,255.43, 1,255.76, 1,257.73, 1,265.36, 1,265.46, 1,265.57, 1,265.71, 1,266.03, and 1,266.31 m.

Remarks.—Initially, variations in cell packing, vesicle opacity, and presence of dark spots were thought to indicate separate taxa, but over the course of the study, these characters were seen

https://doi.org/10.1017/jpa.2016.49 Published online by Cambridge University Press

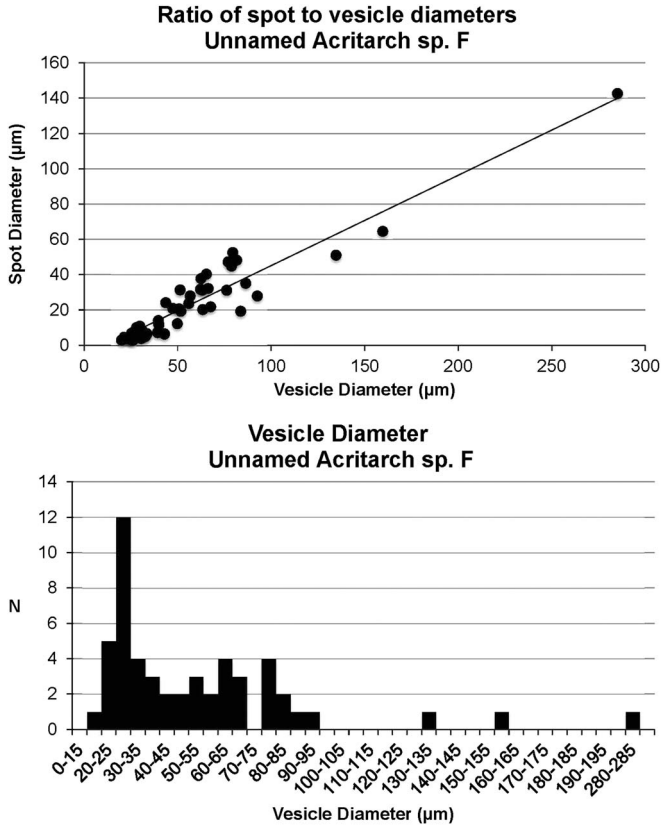

Figure 14. Unnamed Acritarch sp. F vesicle diameter as compared with diameter of spot and histogram of vesicle diameters. Upper panel illustrates the linear relationship between diameters of vesicle and of spot upon vesicle.

to grade into each other—even within single colonies (Fig. 13.10).

A number of genera have been erected for smooth-walled colonial aggregates of cells (e.g., *Synsphaeridium* Eisenack, 1965; *Myxococcoides* Schopf, 1968; *Symplassosphaeridium* Timofeev, 1959 ex Timofeev, 1969; *Ostiana* Hermann, 1976 in Timofeev et al., 1976). Descriptions vary slightly but all generally describe aggregations of cells 3 to ~90 µm in diameter that may show tight- or loose-packing habit, may or may not have optically dense vesicles, and occasionally display optically dense or opaque spots upon or within the vesicle. Specimens recovered from the Alinya Formation have been placed in open nomenclature with attribution to *Synsphaeridium*, the first erected of these genera.

This morphologically simple group is almost certainly polyphyletic, but there is also no indication that the preponderance of available generic designations addresses this issue in a biologically relevant way. A major revision of fossil colonial aggregates is warranted and should be guided by neontology, including consideration of phenotypic plasticity as well as actualistic studies of taphonomic variation.

Filamentous microfossils

Genus *Cyanonema* Schopf 1968 emend. Butterfield, Knoll, and Swett, 1994

Type Species.—*Cyanonema attenuata* Schopf, 1968.

Remarks.—Members of the genus *Cyanonema* are unbranched, uniseriate cellular trichomes that are distinguished from those of *Oscillatoriopsis* on the basis of length-to-width ratios of the cells. Members of *Cyanonema* have cell lengths greater than cell widths, and members of *Oscillatoriopsis* have cell lengths less than, or equal to, cell widths.

Cyanonema sp.
Figure 15.4

Description.—The single specimen recovered in the present study has cells of length ~6 µm and width ~5 µm, thus falling into the genus *Cyanonema*. However, these dimensions are greater than those indicated for the type species, *C. attenutata*, and the length-to-width ratio of 1.1 is less than the diagnosed 1.5 to 2.5 for the type.

Material examined.—One specimen from the Alinya Formation, Giles 1 drill core depth 1,244.17 m.

Genus *Obruchevella* Reitlinger, 1948, emend. Yakshchin and Luchinina, 1981

Type species.—*Obruchevella delicata* Reitlinger, 1948

Obruchevella parva Reitlinger, 1959
Figure 15.1, 15.2

1959 *Obruchevella parva* Reitlinger, p. 21, pl. 6, figs. 1, 2.
1992 *Obruchevella parva*; Knoll, p. 756, pl. 1, figs. 2, 5.

Holotype.—(Reitlinger, 1959; p. 21, pl. 6, fig. 2) Tinov Formation, Nohtuyska region, Siberia.

Occurrence.—Widely distributed in Proterozoic through Paleozoic units.

Description.—Helically coiled, organic-walled filaments measuring ~5 µm in filament diameter (range 3.4 to 6.0 µm, $\bar{x} = 4.7\ \mu m$, s = 1.2 µm, N = 5). These fossils have the appearance of concentric circles due to the long-axis view provided by macerates.

Material examined.—Five specimens from the Alinya Formation, Giles 1 drill core depth 1,265.57 m.

Remarks.—Reitlinger erected three species of *Obruchevella,* differentiated chiefly by filament width: *O. delicata* (12–18 µm; Reitlinger, 1948), *O. parva* (6.8–8.5 µm; Reitlinger, 1959), and *O. sibirica* (14–17 µm; Reitlinger, 1959). The difference between *O. delicata* and *O. sibirica* is the total width of the specimen, effectively the number of whorls preserved of the filament. This character is taphonomically controlled, thus *O. sibirica* is a junior synonym of *O. delicata*.

The Alinya Formation specimens are somewhat smaller in diameter than the dimensions of 6.8 to 8.5 µm given in the original description of *O. parva* (Reitlinger, 1959; p. 20–21). However, the size of the Alinya forms is in keeping with those

https://doi.org/10.1017/jpa.2016.49 Published online by Cambridge University Press

from the Baklia Formation of the Scotia Group (Knoll, 1992), which measured 4 to 5 μm in diameter. This is also consistent with specimens of the Bylot Group (3 to 10 μm in filament diameter); however, those specimens were assigned to *O. valdaica* rather than *O. parva* without mention of the latter. We place the Alinya specimens into *O. parva* rather than the also comparable *O. valdaica* (erected as *Volyniella valdaica* by Shepeleva in an unpublished dissertation, validly published by Aseeva, 1974, and then moved to *Obruchevella* by Jankauskas et al., 1989) due to the nomenclatural priority of *O. parva*.

Mankiewicz (1992) gives a careful analysis of the genus and lists seventeen validly named species of *Obruchevella*, suggesting many may be synonyms, but stops short of a major revision.

Genus *Polythrichoides* Hermann, 1974 emend.
Timofeev et al., 1976

Type species.—*Polythrichoides lineatus* Hermann, 1974 emend. Knoll et al., 1991

Polythrichoides lineatus Hermann, 1974 emend.
Knoll et al., 1991
Figure 15.5, 15.9, 15.15

1974 *Polythrichoides lineatus* Hermann, p. 8, pl. 6, figs. 3, 4.
1976 *Polythrichoides lineatus*; Timofeev and Hermann in Timofeev, Hermann, and Mikhailova, p. 37, pl. 14, fig. 7.
1989 *Polytrichoides* (*sic*) *lineatus*; Jankauskas, Mikhailova, and Hermann, p. 119, pl. 30, figs. 5A, B, 6, 7.
1991 *Polytrichoides* (*sic*) *lineatus*; Knoll, Swett, and Mark, p. 563, fig. 4.3, 4.5.
1992 *Polytrichoides* (*sic*) *lineatus*; Knoll, p. 760, pl. 2, fig. 6.
1994 *Polythrichoides lineatus*; Hofmann and Jackson, p. 12, fig. 11.13–11.17.
1995 *Quaestiosignum filum*; Zang, p. 171, figs. 32A–C.
2008 *Polythrichoides lineatus*; Moczydłowska, p. 81, fig. 7E.
2009 *Polytrichoides* (*sic*) *lineatus*; Vorob'eva, Sergeev, and Knoll, p. 188, figs. 15.13, 15.14.

Holotype.—(Hermann in Timofeev et al., 1974, p. 8, pl. 6, fig. 3), preparation number 49/11 from Krasnoyarsk Krai in Turukhansk region, near Maya River, Neoproterozoic Miroyedikha Formation, Russia.

Occurrence.—Widely distributed in Proterozoic organic-walled microfossil assemblages.

Description.—Tightly grouped bundles of parallel, smooth-walled, apparently aseptate trichomes ranging in width from 0.9 to 2.5 μm ($\bar{x} = 1.4\,\mu$m, s = 0.5 μm, N = 10). Filament bundles range in width from 8 to 24 μm ($\bar{x} = 14.1\,\mu$m, s = 5.6 μm, N = 11).

Material examined.—Eleven specimens from the Alinya Formation, Giles 1 drill core depths 1,265.46, 1,265.57, 1,265.71, and 1,266.31 m.

Remarks.—The *P. lineatus* specimens recovered from the Alinya Formation are slightly smaller than the 3.9 μm indicated in the diagnosis by Hermann (1974) and the range of 3 to 5 μm given in her later emendation (in Timofeev et al., 1976) but are very similar in range to those described from the Bylot Supergroup (1 to 3 μm) by Hofmann and Jackson (1994). Similarly, the widths of the bundles of filaments found in the Alinya Formation (8 to 24 μm) are somewhat smaller than those

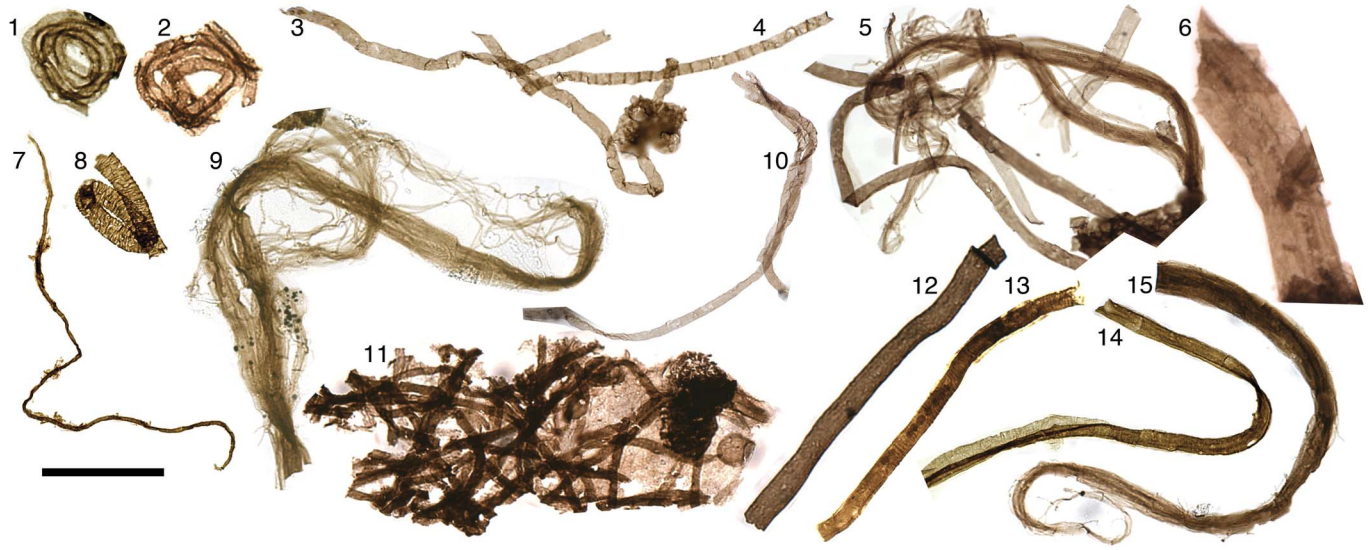

Figure 15. Filamentous microfossils: (**1, 2**) *Obruchevella parva*; (**3, 10**) *Siphonophycus typicum*; (**4**) *Cyanonema* sp.; (**5**) *S. typicum* and *Polythricoides lineatus*; (**6**) *S. solidum*; (**7**) *S. septatum*; (**8, 14**) *R. tenuis*; (**9**) *P. lineatus*; (**11**) *S. robustum*; (**12**) *S. kestron*; (**13**) *Rugosoopsis tenuis*; (**15**) *P. lineatus*. Scale bar = 50μm. Slide and coordinates: (**1**) 1265.57-19A/O30-2 (P49526); (**2**) 1265.57-19A/L24-3 (P49527); (**3, 4**) 1244.17-14B/T35-3 (P49476); (**5**) 1265.57-19A/O35-3 (P49528); (**6**) 1265.46-18A/Q38-1 (P49490); (**7**) 1265.57-19A/M41-2 (P49529); (**8**) 1265.57-19A/J37-2 (P49532); (**9**) 1266.31-20/V33-0 (P49558); (**10**) 1255.76-16A/J35-3 (P49483); (**11**) 1255.43-15B/S18-0 (P49481); (**12**) 1265.46-18A/M38-0 (P49489); (**13**) 1265.57-19A/O20-2 (P49531); (**14**) 1265.57-19A/L42-3 (P49533); (**15**) 1265.57-19A/H22-3 (P49530).

https://doi.org/10.1017/jpa.2016.49 Published online by Cambridge University Press

of the type material (19.5 to 39 μm), but are consistent with findings from Bylot Supergroup specimens (5 to 30 μm). This form is often compared with members of the extant cyanobacterial genus *Microcoleus* in which the width of filaments is typically 2 to 10 μm and the number of filaments within a sheath varies from 2 or 3 to more than 100, resulting in a wide range of bundle widths.

Genus *Rugosoopis* (Timofeev and Hermann, 1979), emend. Butterfield, Knoll, and Swett, 1994

Type species.—*Rugosoopsis tenuis* Timofeev and Hermann, 1979.

Remarks.—In the emended diagnosis of Butterfield et al., 1994 (followed here), this genus is indicated to be bilayered, consisting of a smooth-walled or pseudoseptate inner sheath surrounded by a diagnostic outer sheath bearing a transverse fabric. In the material recovered from the Alinya Formation, this form is most frequently found to be missing the inner smooth-walled filament.

Butterfield and colleagues (1994) suggest a cyanobacterial affinity for *Rugosoopsis* based on observations of *Rugosoopsis*-like transverse fabric developed during cyanobacterial response to desiccation in modern lagoonal systems (Horodyski et al., 1977).

Rugosoopsis tenuis Timofeev and Hermann, 1979 emend. Butterfield, Knoll, and Swett, 1994
Figure 15.8, 15.13, 15.14

1979 *Rugosoopsis tenuis* Timofeev and Hermann, p. 139, pl. 29, figs. 5, 7.
1994 *Rugosoopsis tenuis*; Butterfield, Knoll and Swett, p. 62, figs. 25A-D, 27B (see for additional synonymy).
2001 *Rugosoopsis tenuis*; Samuelsson and Butterfield, fig. 3.
2016 *Rugosoopsis tenuis*; Porter and Riedman, p. 830, fig. 11.12.

(For additional synonymy see also Moczydłowska, 2008.)

Holotype.—(Timofeev and Hermann, 1979; p. 139, pl. 29, fig. 7), preparation number 1-22/1-77/1, Mesoproterozoic to Neoproterozoic Lakhanda Group, Maya River, Khabarovsk Krai, Russia.

Occurrence.—This form has been reported from early Neoproterozoic units such as the Lakhanda Group (Timofeev and Hermann, 1979), Svanbergfjellet Formation (Butterfield et al., 1994), and Lone Land (Samuelsson et al., 1999) Formation.

Description.—Rugose filaments 6.2 to 29.5 μm in diameter ($\overline{x} = 11.7\,\mu$m, s = 4.9 μm, N = 23), consistent with the forms described from the Svanbergfjellet Formation (7 to 57 μm in diameter) described by Butterfield and colleagues (1994) and from which the emended diagnosis was made. In two specimens, cellular contents are retained (Fig. 15.13).

Material examined.—Twenty-three specimens from the Alinya Formation, Giles 1 drill core depths 1,265.46, 1,265.57, 1,265.71, and 1,266.31 m.

Genus *Siphonophycus* Schopf, 1968 emend. Knoll, Swett, and Mark, 1991

Type species.—*Siphonophycus kestron* Schopf, 1968.

Remarks.—*Siphonophycus* is a form genus of unbranched, smooth-walled, originally tubular filamentous sheaths that are differentiated into form species based on width.

Siphonophycus septatum (Schopf, 1968) Knoll, Swett, and Mark, 1991
Figure 15.7

1968 *Tenuofilum septatum* Schopf, p. 679, pl. 86, figs. 10–12.
1991 *Siphonophycus septatum*; Knoll, Swett, and Mark, p. 565, fig. 10.2.
1994 *Siphonophycus* septatum; Butterfield, Knoll, and Swett, p. 64, figs. 10H, 22G–H (see for additional synonymy).
1994 *Siphonophycus septatum*; Hofmann and Jackson, p. 10, fig. 11.1–11.4.
2016 *Siphonophycus septatum*; Porter and Riedman, p. 830, fig. 11.10.

Holotype.—(Schopf, 1968; p. 679, pl. 86, fig. 11), thin section Bit/Spr 6–3, Paleobotanical collections, Harvard University, number 58527 from Neoproterozoic Bitter Springs Formation, Amadeus Basin, Australia.

Diagnosis.—Unbranched, nonseptate, smooth-walled filamentous microfossil 1 to 2 μm in diameter.

Occurrence.—Widely distributed; found in Mesoproterozoic through Paleozoic units.

Description.—Unbranched, nonseptate, smooth-walled filamentous microfossils, both specimens 1.6 μm in diameter. One specimen ~235 μm in length.

Material examined.—Two specimens recovered from the Neoproterozoic Alinya Formation, 1,265.57 and 1,265.71 meters depth in Giles 1 drill core, Officer Basin, South Australia.

Siphonophycus robustum (Schopf, 1968) Knoll, Swett, and Mark, 1991
Figure 15.11

1968 *Eomycetopsis robusta* Schopf, p. 685, pl. 82, figs. 2, 3, pl. 83, figs. 1–4.
1991 *Siphonophycus robustum*; Knoll, Swett, and Mark, p. 565, fig. 10.3, 10.5.
1994 *Siphonophycus robustum*; Butterfield, Knoll, and Swett, p. 64, fig. 26A, G (see for additional synonymy).
1994 *Siphonophycus robustum*; Hofmann and Jackson, p. 10, fig. 11.5.

https://doi.org/10.1017/jpa.2016.49 Published online by Cambridge University Press

1998 *Siphonophycus robustum*; Yuan and Hofmann, p. 209, fig. 13I.
2001 *Siphonophycus robustum*; Samuelsson and Butterfield, figs. 2B, 9F–H.
2009 *Siphonophycus robustum*; Dong et al., p. 39, fig. 6.12.
2010 *Siphonophycus robustum*; Sergeev and Schopf, p. 387, fig. 6.4.
2016 *Siphonophycus robustum*; Porter and Riedman, p. 837, fig. 16.4.

Holotype.—(Schopf, 1968; p. 685, pl. 83, fig. 1), thin section Bit. Spr. 10-1, Paleobotanical collections, Harvard University number 58491 from Neoproterozoic Bitter Springs Formation, Amadeus Basin, Australia.

Diagnosis.—Unbranched, nonseptate, smooth-walled filamentous microfossil 2 to 4 μm in diameter.

Occurrence.—Widely distributed; found in Mesoproterozoic through Paleozoic units.

Description.—The Alinya specimens range in diameter from 2.1 to 3.8 μm ($\bar{x} = 3.2\,\mu$m, s = 0.6 μm, N = 7).

Material examined.—Twelve specimens from the Alinya Formation, Giles 1 drill core depths 1,244.17, 1,255.43, 1,265.36, 1,265.57, and 1,266.21 m.

Siphonophycus typicum (Hermann, 1974) Butterfield (in Butterfield et al., 1994)
Figure 15.5, 15.10

1974 *Leiothrichoides tipicus* Hermann, p. 7, pl. 6, figs. 1–2.
1994 *Siphonophycus typicum*; Butterfield in Butterfield et al., p. 66, figs. 23B–D, 26B, H, I (see for additional synonymy).
1995 *Siphonophycus robustum*; Zang, fig. 32L, M.
2001 *Siphonophycus typicum*; Samuelsson and Butterfield, figs. 2A, 8F.
2008 *Siphonophycus typicum*; Moczydłowska, p. 83, fig. 5E.
2010 *Siphonophycus typicum*; Sergeev and Schopf, p. 387, fig. 6.4.
2016 *Siphonophycus typicum*; Porter and Riedman, p. 837, fig. 16.3.

Holotype.—(Hermann, 1974; p. 7, pl. 6, figs. 1, 2), preparation number 49/2T from Krasnoyarsk Krai in Turukhansk region, near Maya River, Neoproterozoic Miroyedikha Formation, Russia.

Diagnosis.—Unbranched, nonseptate, smooth-walled filamentous microfossil 4 to 8 μm in diameter.

Occurrence.—Widely distributed; found in Mesoproterozoic through late Ediacaran units.

Description.—The Alinya specimens range in diameter from 4.0 to 8.0 μm ($\bar{x} = 5.8\,\mu$m, s = 1.2 μm, N = 35).

Material examined.—Forty-seven specimens from the Alinya Formation, Giles 1 drill core depths 1,244.17, 1,255.43, 1,255.76, 1,265.36, 1,265.46, 1,265.57, 1,265.71, and 1,266.31 m.

Siphonophycus kestron Schopf, 1968
Figure 15.12

1968 *Siphonophycus kestron* Schopf, p. 671, pl. 80, figs. 1–3.
1994 *Siphonophycus kestron*; Butterfield, Knoll, and Swett, p. 67, fig. 21D (see for additional synonymy).
1994 *Siphonophycus kestron*; Hofmann and Jackson, p. 12, fig. 11.8, 11.9.
1995 *Siphonophycus* sp. cf. *S. kestron*; Zang, p. 171, fig. 32G non 32F.
1998 *Siphonophycus rugosum*; Yuan and Hofmann, fig. 13H.
2001 *Siphonophycus kestron*; Samuelsson and Butterfield, fig. 8F.
2008 *Siphonophycus kestron*; Moczydłowska, p. 82, fig. ?4G, 5F, 7F.
2010 *Siphonophycus kestron*; Sergeev and Schopf, p. 385, fig. 8.5.

Holotype.—(Schopf, 1968; p. 671, pl. 80, fig. 1) thin section Bit/Spr 6-3, Paleobotanical collections, Harvard University, number 58469 from the Neoproterozoic Bitter Springs Formation, Amadeus Basin, Australia.

Diagnosis.—Unbranched, nonseptate, smooth-walled filamentous microfossil 8 to 16 μm in diameter.

Occurrence.—Widely distributed; found in Mesoproterozoic through early Cambrian units.

Description.—The Alinya specimens range in diameter from 8.3 to 15.2 μm ($\bar{x} = 10.9\,\mu$m, s = 2.1 μm, N = 22).

Material examined.—Twenty-six specimens from the Alinya Formation, Giles 1 drill core depths 1,255.43, 1,265.36, 1,265.46, 1,265.57, and 1,266.31 m.

Siphonophycus solidum (Golub, 1979) Butterfield (in Butterfield et al., 1994)
Figure 15.6

1979 *Omalophyma solida* Golub, p. 151, pl. 31, figs. 1–4, 7.
1994 *Siphonophycus solidum*; Butterfield, Knoll, and Swett, p. 67, fig. 25H–I, 27D (see for additional synonymy).
?1995 *Siphonphycus* sp. cf. *S. kestron*; Zang, p. 171, fig. 32F.
2001 *Siphonophycus solidum*; Samuelsson and Butterfield, fig. 8A, C, ?D, E.
2002 *Siphonophycus solidum*; Xiao, Yuan, Steiner, and Knoll, p. 371, fig. 10.1–10.3.
2010 *Siphonophycus solidum*; Sergeev and Schopf, p. 387, figs. 7.6–7.8, 8.1, 8.2.

https://doi.org/10.1017/jpa.2016.49 Published online by Cambridge University Press

Holotype.—(Golub, 1979; p. 151, pl. 31, fig. 1) ВСЕГЕИ, preparation P-163/3, Rudnyanskaya collection, upper Smolensk Suite, Neoproterozoic, Russia.

Diagnosis.—Unbranched, nonseptate, smooth-walled filamentous microfossil 16 to 32 μm in diameter.

Occurrence.—Widely distributed in Proterozoic and Paleozoic organic-walled microfossil assemblages.

Description.—The Alinya specimens range in diameter from 16.9 to 32.6 μm ($\bar{x} = 24.3\ \mu m$, s = 6.4 μm, N = 6).

Material examined.—Seven specimens from the Alinya Formation, Giles 1 drill core depths 1,265.36, 1,265.46, and 1,266.31 m.

Conclusions

The high taxonomic richness of the middle Neoproterozoic Alinya Formation is consistent with the elevated levels of eukaryotic diversity seen from other Tonian units. However, the Alinya assemblage is more similar to that of the 770–742 Ma Chuar Group than to the somewhat older Svanbergfjellet and Wynniatt formations. Indeed, the Alinya and Chuar assemblages may be two of the youngest records of high organic-walled microfossil diversity before the diversity downturn that preceded the Cryogenian snowball earth glaciations.

Study of micro- and nano-scale morphology by SEM has proven to be of great use in the description of the Alinya assemblage. It appears that the apparent lack of morphological detail in early to middle Neoproterozoic acritarchs is partly a methodological limitation; the traditional use of transmitted light microscopy does not permit appreciation of the very subtle diagnostic detail found in some of these taxa. More widespread use of SEM in study of middle Neoproterozoic taxa may illustrate that fine detail is common in acritarchs of this age. Such a finding could have a significant effect on Neoproterozoic biostratigraphy and, in turn, our understanding of early eukaryotic diversity trends. Routine use of SEM in acritarch studies would also reduce taxonomic inflation and depression caused by taphonomic variation—results not only valuable for within-assemblage diversity assessment, but also important for identification of taxa from units of poor preservational quality.

Acknowledgments

This work was supported by National Science Foundation grant EAR-0922305 to S.M.P. Authors thank managers and staff of core facilities at Glenside Core Library, Adelaide, SA, for aid in sampling, G. Waanders for sample preparations, and J.L. Moore for manuscript feedback and a generally insightful nature. Thank you to M. Moczydłowska, S. Xiao, and A.H. Knoll for insightful and thorough reviews.

Accessibility of supplemental data

Data available from the Dryad digital repository: http://dx.doi.org/10.5061/dryad.7vv37.

References

Agić, H., Moczydłowska, M., and Yin, L-M., 2015, Affinity, life cycle, and intracellular complexity of organic-walled microfossils from the Mesoproterozoic of Shanxi, China: Journal of Paleontology, v. 89, p. 28–50.

Allison, C.W., and Awramik, S.M., 1989, Organic-walled microfossils form the earliest Cambrian or latest Proterozoic Tindir Group Rocks, northwest Canada: Precambrian Research, v. 43, p. 253–294.

Amard, B., 1984, Nouveaux éléments de datation de la couverture Protérozoïque du craton ouest-africain: un assemblage de microfossiles (Acritarches) caractéristique du Riphéen supérieur dans la formation d'Atar (Mauritanie): Comptes rendus des séances de l'Academie des sciences. Série 2, Mécanique-physique, Chimie, Sciences de l'univers, Sciences de la Terre, v. 299, p. 1405–1410.

Arouri, K., Greenwood, P.F., and Walter, M.R., 1999, A possible chlorophycean affinity of some Neoproterozoic acritarchs: Organic Geochemistry, v. 30, p. 1323–1337.

Aseeva, E.A., 1974, O spirale-i kol'tsevidnykh obrazovaniiakh v verkhnedokembriiskikh otlozheniiakh Podolii [On spiral and ringformed structures in the upper Precambrian deposits of Podolia]: Paleontologicheskii Sbornik, v. 11, p. 95–98, 1 plate [in Russian].

Battison, L., and Brasier, M.D., 2012, Remarkably preserved prokaryote and eukaryote microfossils within 1 Ga-old lake phosphates of the Torridon Group, NW Scotland: Precambrian Research, v. 196–197, p. 204–217.

Berney, C., and Pawlowski, J., 2006, A molecular time-scale for eukaryote evolution recalibrated with the continuous microfossil record: Proceedings of the Royal Society, B, v. 273, p. 1867–1872.

Buick, R., and Knoll, A.H., 1999, Acritarchs and microfossils from the Mesoproterozoic Bangemall Group, northwestern Australia: Journal of Paleontology, v. 73, p. 744–764.

Butterfield, N.J., 2005, Probable Proterozoic fungi: Paleobiology, v. 31, p. 165–182.

Butterfield, N.J., and Rainbird, R.H., 1998, Diverse organic-walled fossils, including "possible dinoflagellates" from the early Neoproterozoic of arctic Canada: Geology, v. 26, p. 963–966.

Butterfield, N.J., Knoll, A.H., and Swett, K., 1994, Paleobiology of the Neoproterozoic Svanbergfjellet Formation, Spitsbergen: Fossils and Strata, v. 34, p. 1–84.

Canfield, D.E., 2014, Oxygen: A Four Billion Year History: Princeton, Princeton University Press, 224 p.

Cohen, P.A., and Macdonald, F.A., 2015, The Proterozoic record of eukaryotes: Paleobiology, first look view, 23 p. doi: 10.1017/pab.2015.25.

Combaz, A., Lang, F.W., and Pansart, J., 1967, Les "Leiofusidae" Eisenack, 1938: Review of Palaeobotany and Palynology, v. 1, p. 291–307.

Cotter, K.L., 1997, Neoproterozoic microfossils from the Officer Basin, Western Australia: Alcheringa, v. 21, p. 247–270.

Cotter, K.L., 1999, Microfossils from Neoproterozoic Supersequence 1 of the Officer Basin, Western Australia: Alcheringa, v. 23, p. 63–86.

Couëffé, R., and Vecoli, M., 2011, New sedimentological and biostratigraphic data in the Kwahu Group (Meso- to Neo-Proterozoic), southern margin of the Volta Basin, Ghana: stratigraphic constraints and implications on regional lithostratigraphic correlations: Precambrian Research, v. 189, p. 155–175.

Dong, L., Xiao, S., Shen, B., Zhou, C., Li, G., and Yao, J., 2009, Basal Cambrian microfossils from the Yangtze Gorges area (South China) and the Aksu area (Tarim Block, northwestern China): Journal of Paleontology, v. 83, p. 30–44.

Downie, C., 1963, 'Hystrichospheres' (acritarchs) and spores of the Wenlock Shales (Silurian) of Wenlock, England: Palaeontology, v. 6, p. 625–652.

Downie, C., and Sarjeant, W.A.S., 1963, On the interpretation and status of some hystrichosphere genera: Palaeontology, v. 6, p. 83–96.

Downie, C., Evitt, W.R., and Sarjeant, W.A.S., 1963, Dinoflagellates, Hystrichospheres, and the Classification of the Acritarchs: Stanford, School of Earth Sciences, Stanford University, 16 p.

Eisenack, A, 1938, Neue Mikrofossilien des baltischen Silurs. IV: Palaeontologisch Zeitschrift, v. 19, no. 3–4, p. 217–243, pl. 15, 16 [in German].

Eisenack, A., 1958a, Mikrofossilien aus dem Ordovizium des Baltikums. 1. Markasitschicht, *Dictyonema*-Schiefer, Glaukonitsand, Glaukonitkalk: Senckenbergiana Lethaea. v. 39, no. 5/6, p. 389–405 [in German].

Eisenack, A., 1958b, *Tasmanites* Newton 1875 und *Leiosphaeridia* n. g. als Gattungen der Hystrichosphaeridea: Palaeontographica, Abteilung A., v. 110, no. 1–3, p. 1–19, pl. 1, 2 [in German].

Eisenack, A., 1965, Mikrofossilien aus dem Silur Gotlands Hystrichosphären, Problematika: Neues Jarbuch für Geologie und Paläontologie Abhandlungen, v. 122, p. 257–274 [in German].

Eisenack, A., 1976, Mikrofossilien aus dem Vaginatenkalk von Hälludden, Öland: Palaeontographica, Abteilung A., v. 154, no. 4–6, p. 181–203, pl. 1–7 [in German].

Evitt, W.R., 1963, A discussion and proposals concerning fossil dinoflagellates, hystrichospheres, and acritarchs, II: Proceedings of the National Academy of Sciences, v. 49, p. 298–302.
Fensome, R.A., Williams, G.L., Barss, M.S., Freeman, J.M., and Hill, J.M., 1990, Acritarchs and fossil prasinophytes: and index to genera, species and infraspecific taxa: American Association of Stratigraphic Palynologists Foundation, AASP Contributions Series Number 25, 771 p.
Gao, L., Xing, Y., and Liu, G., 1995, Neoproterozoic micropalaeoflora from Hunjiang area, Jilin province and its sedimentary environment: Professional Papers of Stratigraphy and Palaeontology, v. 26, p. 1–23, and 4 plates.
Golub, I.N., 1979, Novaia gruppa problematichnykh mikroobrazovanii v vendskikh otlozheniiakh orshanskoi vpadiny (Russkaia platforma) [A new group of problematic microforms in the Vendian Orsha depressions (Russian Platform)], *in* Sokolov, B.S., ed., Paleontologiia Dokembriia i Rannego Kembriia [Precambrian and Early Cambrian Paleontology]: Leningrad, Nauka, p. 147–155 [in Russian].
Gravestock, D.I., 1997, Geological setting and structural history, *in* Morton, J.G.G., and Drexel, J.F., eds., The Petroleum Geology of South Australia. Vol 3: Officer Basin. South Australia: Department of Mines and Energy Resources, Report Book, 97/19, p. 35–45.
Gray, J., and Boucot, A.J., 1989, Is *Moyeria* a euglenoid?: Lethaia, v. 22, p. 447–456.
Grey, K., 1999, A modified palynological preparation technique for the extraction of large Neoproterozoic acanthomorph acritarchs and other acid-insoluble microfossils: Western Australia Geological Survey, Record 1999/10, 23 p.
Grey, K., 2005, Ediacaran palynology of Australia: Memoirs of The Association of Australiasian Palaeontologists, v. 31, 439 p.
Grey, K., and Willman, S., 2009, Taphonomy of Ediacaran acritarchs from Australia: significance for taxonomy and biostratigraphy: Palaios, v. 24, p. 239–256.
Grey, K., Hill, A.C., and Calver, C., 2011, Biostratigraphy and stratigraphic subdivision of Cryogenian successions of Australia in global context, *in* Arnaud, E., Halverson, G.P., and Shields-Zhou, G., eds., The Geological Record of Neoproterozoic Glaciations: London, Geological Society, Memoirs, v. 36, p. 113–134.
Guan, B., Geng, W., Rong, Z., and Du, H., 1988, The middle and upper Proterozoic in the northern slope of the eastern Qinling Ranges, Henan, China, ZhengZhou, China: Henan Science and Technology Press, 210 p.
Halverson, G.P., Hoffman, P.F., Schrag, D.P., Maloof, A.C., and Rice, A.H.N., 2005, Toward a Neoproterozoic composite carbon-isotope record: Geological Society of America Bulletin, v. 117, p. 1181–1207.
He, Y., Zhao, G., Sun, M., and Xia, X., 2009, SHRIMP and LA-ICP-MS zircon geochronology of the Xiong'er volcanic rocks: implications for the Paleo-Mesoproterozoic evolution of the southern margin of the North China Craton: Precambrian Research, v. 168, p. 213–222.
Hermann, T.N., 1974, Nakhodki massovykh skoplenii trikhomov v rifee [Discovery of Massive Clusters of Trichomes in the Riphean], *in* Timofeev, B.V., ed., Mikrofitofossilii Proterozoia i rannego Paleozoia SSSR [Microfossils of the Proterozoic and early Paleozoic, USSR], Leningrad, Nauka, p. 6–10 [in Russian].
Hermann, T.N., 1990, Organic World One Billion Years Ago: Leningrad, Nauka, 51 p.
Hill, A.C., 2005, Stable isotope stratigraphy, GSWA Lancer 1, Officer Basin, western Australia, *in* Mory, A.J., and Haines, P.W., eds., GSWA Lancer 1 Well Completion Report (Interpretive Papers), Officer and Gunbarrel Basins, Western Australia: Western Australia Geological Survey, Record 2005/4, p. 1–11.
Hill, A.C., and Walter, M.R., 2000, Mid-Neoproterozoic (~830–750 Ma) isotope stratigraphy of Australia and global correlation: Precambrian Research, v. 100, p. 181–211.
Hill, A.C., Cotter, K.L., and Grey, K., 2000, Mid-Neoproterozoic biostratigraphy and isotope stratigraphy in Australia: Precambrian Research, v. 100, p. 281–298.
Hill, A.C., Grey, K., Gostin, V.A., and Webster, L.J., 2004, New records of Late Neoproterozoic Acraman ejecta in the Officer Basin: Australian Journal of Earth Sciences, v. 51, p. 47–51.
Hofmann, H.J., 1999, Global distribution of the Proterozoic sphaeromorph acritarch *Valeria lophostriata* (Jankauskas): Acta Micropalaeontologica Sinica, v. 16, p. 215–224.
Hofmann, H.J., and Jackson, G.D., 1994, Shale-facies microfossils from the Proterozoic Bylot Supergroup, Baffin Island, Canada: Memoir, The Paleontological Society, v. 37, p. 1–39.
Horodyski, R.J., Bloeser, B., and Vonder Haar, S., 1977, Laminated algal mats from a coastal lagoon, Laguna Mormona, Baja California, Mexico: Journal of Sedimentary Petrology, v. 47, p. 680–696.
Huntley, J.W., Xiao, S., and Kowalewski, M., 2006, 1.3 Billion years of acritarch history: An empirical morphospace approach: Precambrian Research, v. 144, p. 52–68.
Jankauskas, T.V., 1979, Srednerifeyski microbiota Yuzhnogo Urala i Bashkirskogo Priural'ya [Middle Riphean microbiota of the southern Urals and the Ural region in Bashkiria]: Akademii Nauk SSSR, Doklady, v. 248, p. 190–193 [1981, v. 248, p. 51–54 for English version].
Jankauskas, T. V., 1980, Shishenyakskaya mikrobiota verkhnego rifeya yuzhnogo Urala [Shisheniak microbiota of the upper Riphean of the southern Urals]: Doklady Akademii Nauk SSSR, v. 251, no. 1, p. 190–192.
Jankauskas, T.V., 1982, Mikrofossilii rifeiia Iuzhnogo Urala [Riphean microfossils of the Southern Urals], *in* Keller, B.M., ed., Stratotip Rifeya-Paleontologiya paleomagnetizm [Riphean Stratotype: Paleontology and Paleomagnetism]: Akademiya Nauk SSSR Transactions, v. 368, p. 84–120, plates, p. 31–48 [in Russian].
Jankauskas, T.V., Mikhailova, N.S., and Hermann, T.N., eds., 1989, Mikrofossilii Dokembriia SSSR [Precambrian Microfossils of the USSR], Leningrad, Nauka, 191 p. [in German].
Javaux, E.J., 2011, Early Eukaryotes in Precambrian oceans, *in* Gargaud, M., Lopez-Garcia, P., and Martin, H., eds., Origins and Evolution of Life: An Astrobiological Perspective, New York, Cambridge University Press, p. 414–449.
Javaux, E.J., Knoll, A.H., and Walter, M.R., 2001, Morphological and ecological complexity in early eukaryotic ecosystems: Nature, v. 412, p. 66–69.
Javaux, E.J., Knoll, A.H., and Walter, M. R., 2003, Recognizing and interpreting the fossils of early eukaryotes: Origins of Life and evolution of the Biosphere, v. 33, p. 75–94.
Javaux, E.J., Knoll, A.H., and Walter, M.R., 2004, TEM evidence for eukaryotic diversity in mid-Proterozoic oceans: Geobiology, v. 2, p. 121–132.
Kaufman, A.J., Knoll, A.H., and Awramik, S.M., 1992, Biostratigraphic and chemostratigraphic correlation of Neoproterozoic sedimentary successions: Upper Tindir Group, northwestern Canada, as a test case: Geology, v. 20, p. 181–185.
Knoll, A. H., 1984, Microbiotas of the late Precambrian Hunnberg Formation, Nordaustlandet, Svalbard: Journal of Paleontology, v. 58, p. 131–162.
Knoll, A.H., 1992, Vendian microfossils in metasedimentary cherts of the Scotia Group, Prins Karls Forland, Svalbard: Palaeontology, v. 35, p. 715–774.
Knoll, A.H., 1994, Proterozoic and early Cambrian protists: evidence for accelerating evolutionary tempo: Proceedings of the National Academy of Sciences, v. 91, p. 6743–6750.
Knoll, A.H., 1996, Archean and Proterozoic paleontology, *in* Jansonius, J., and McGregor, D.C., eds., Palynology: Principles and Applications, Volume 1: American Association of Stratigraphic Palynologists Foundation, p. 51–80.
Knoll, A.H., 2011, The multiple origins of complex multicellularity: Annual Reviews in Earth and Planetary Sciences, v. 39, p. 217–239.
Knoll, A.H., and Barghoorn, E.S., 1975, Precambrian eukaryotic organisms: a reassessment of the evidence: Science, v. 190, p. 52–54.
Knoll, A.H., Swett, K., and Mark, J., 1991, Paleobiology of a Neoproterozoic tidal flat/lagoonal complex: the Draken Conglomerate: Journal of Paleontology, v. 65, p. 531–570.
Knoll, A.H., Javaux, E.J., Hewitt, D., and Cohen, P., 2006, Eukaryotic organisms in Proterozoic oceans: Philosophical Transactions of the Royal Society, B, v. 361, p. 1023–1038.
Li, Z.X., *et al*, 2008, Assembly, configuration, and break-up history of Rodinia: a synthesis: Precambrian Research, v. 160, p. 179–210.
Lindsay, J.F., and Leven, J.H., 1996, Evolution of a Neoproterozoic to Palaeozoic intracratonic setting, Officer Basin, South Australia: Basin Research, v. 8, p. 403–424.
Lücking, R., Huhndorf, S., Pfister, D.H., Plata, E.R., and Lumbsch, H.T., 2009, Fungi evolved on the right track: Mycologica, v. 101, p. 810–822.
Macdonald, F.A., Schmitz, M.D., Crowley, J.L., Roots, C.F., Jones, D.S., Maloof, A.C., Strauss, J.V., Cohen, P.A., Johnston, D.T., and Schrag, D.P., 2010a, Calibrating the Cryogenian: Science, v. 327, p. 1241–1243.
Macdonald, F.A., Cohen, P.A., Dudás, F.Ö., and Schrag, D.P., 2010b, Early Neoproterozoic scale microfossils in the Lower Tindir Group of Alaska and the Yukon Territory: Geology, v. 38, p. 143–146.
Mankiewicz, C., 1992, *Obruchevella* and other microfossils in the Burgess Shale: preservation and affinity: Journal of Paleontology, v. 66, p. 717–729.
Meyer, K.M., and Kump, L.R., 2008, Oceanic euxinia in Earth history: Causes and Consequences: Annual Review of Earth and Planetary Sciences, v. 36, p. 251–288.
Moczydłowska, M., 2008, New records of late Ediacaran microbiota from Poland: Precambrian Research, v. 167, p. 71–92.
Moczydłowska, M., and Willman, S., 2009, Ultrastructure of cell walls in ancient microfossils as a proxy to their biological affinities: Precambrian Research, v. 173, p. 27–38.
Morton, J.G.G., 1997, Lithology and environments of deposition, *in* Morton, J.G.G., and Drexel, J.F., eds., The Petroleum Geology of South Australia. Volume 3: Officer Basin. South Australia: Department of Mines and Energy Resources, Report Book, 97/19. p. 47–86.

https://doi.org/10.1017/jpa.2016.49 Published online by Cambridge University Press

Nagovitsin, K., 2009, *Tappania*-bearing association of the Siberian platform: biodiversity, stratigraphic position and geochronological constraints: Precambrian Research, v. 173, p. 137–145.
Nagy, R.M., Porter, S.M., Dehler, C.M., and Shen, Y., 2009, Biotic turnover driven by eutrophication before the Sturtian low-latitude glaciation: Nature Geoscience, v. 2, p. 415–418.
Naumova, S.N., 1949, Spory nizhnego Kembriia [Spores of the lower Cambrian]: Izvestiia Akademii Nauka, Seriia Geologicheskaia, v. 4, p. 49–56 [in Russian].
Pang, K., Tang, Q., Schiffbauer, J.D., Yao, J., Yuan, X., Wan, B., Chen, L., Ou, Z., and Xiao, S., 2013, The nature and origin of nucleus-like intracellular inclusions in Paleoproterozoic eukaryote microfossils: Geobiology, v. 11, p. 499–510.
Parfrey, L.W., Lahr, D.J.G., Knoll, A.H., and Katz, L.A., 2011, Estimating the timing of early eukaryotic diversification with multigene molecular clocks: Proceedings of the National Academy of Sciences, v. 108, p. 13624–13629.
Peat, C.J., Muir, M.D., Plumb, K.A., McKirdy, D.M., and Norvick, M.S., 1978, Proterozoic microfossils from the Roper Group, Northern Territory, Australia: BMR Journal of Australian Geology and Geophysics, v. 3, p. 1–17.
Peng, Y., Bao, H., and Yuan, X., 2009, New morphological observations for Paleoproterozoic acritarchs from the Chuanlinggou Formation, North China: Precambrian Research, v. 168, p. 223–232.
Pierrehumbert, R.T., Abbot, D.S., Voigt, A., and Koll, D., 2011, Climate of the Neoproterozoic: Annual Review of Earth and Planetary Sciences, v. 39, p. 417–460.
Pisarevsky, S.A., Li, Z.X., Grey, K., and Stevens, M.K., 2001, A paleomagnetic study of Empress 1A, a stratigraphic drillhole in the Officer Basin: evidence for a low-latitude position of Australia in the Neoproterozoic: Precambrian Research, v. 110, p. 93–108.
Pisarevsky, S.A., Wingate, M.T.D., Stevens, M.K., and Haines, P.W., 2007, Palaeomagnetic results from the Lancer 1 stratigraphic drillhole, Officer Basin, Western Australia, and implications for Rodinia reconstructions: Australian Journal of Earth Sciences, v. 54, p. 561–572.
Porter, S.M., and Knoll, A.H., 2000, Testate amoebae in the Neoproterozoic Era: evidence from vase-shaped microfossils in the Chuar Group, Grand Canyon: Paleobiology, v. 26, p. 360–385.
Porter, S.M., and Riedman, L.A., 2016, Systematics of organic-walled microfossils from the mid-Neoproterozoic Chuar Group, Grand Canyon, Arizona: Journal of Paleontology, v. 90, p. 815–853.
Porter, S.M., Meisterfeld, R., and Knoll, A.H., 2003, Vase-shaped microfossils from the Neoproterozoic Chuar Group, Grand Canyon: a classification guided by modern testate amoebae: Journal of Paleontology, v. 77, p. 409–429.
Prasad, B., Uniyal, S.N., and Asher, R., 2005, Organic-walled microfossils from the Proterozoic Vindhyan Supergroup of Son Valley, Madhya Pradesh, India: The Palaeobotanist, v. 54, p. 13–60.
Pyatiletov, G., 1980, O nakhodkakh mikrofossilii roda *Navifusa* v Lakhandinskoi Svite [On finds of microfossils of the genus *Navifusa* in the Lakhanda Suite]: Palaeontological Journal, v. 3, p. 143–145 [in Russian].
Rainbird, R. H., Stern, R. A., Khudoley, A. K., Kropachev, A. P., Heaman, L. M., and Sukhorukov, V. I., 1998, U-Pb geochronology of Riphean sandstone and gabbro from southeast Siberia and its bearing on the Laurentia-Siberia connection: Earth and Planetary Science Letters, v. 164, p. 409–420.
Reitlinger, E.A., 1948, Kembriiskie foraminifery Iakutii [Cambrian foraminifera of Yakutia]: Biulleten Moskovskogo Obshchestva Ispytalelej Prirody: Otdlenie Geologii [Bulletin of Moscow Nature Investigators Society, Geological Section], v. 23, p. 77–81 [in Russian].
Reitlinger, E.A., 1959, Atlas mikroskopicheskikh organicheskikh ostatkov i problematiki drevnikh tolshch Sibiri [Atlas of miscroscopic organic matter and problems of the ancient strata of Siberia]. Trudy Geologicheskogo Instituta. Akademiia Nauka SSSR, Moscow. 63 p., 22 plates [in Russian].
Riedman, L.A., Porter, S.M, Halverson, G.P., Hurtgen, M.T., and Junium, C.K., 2014, Organic-walled microfossil assemblages from glacial and interglacial Neoproterozoic units of Australia and Svalbard: Geology, v. 42, p. 1011–1014.
Rothman, D.H., Hayes, J.M., and Summons, R.E., 2003, Dynamics of the Neoproterozoic carbon cycle: Proceedings of the National Academy of Sciences, USA, v. 100, p. 8124–8129.
Samuelsson, J., 1997, Biostratigraphy and palaeobiology of early Neoproterozoic strata of the Kola Peninsula, northwest Russia: Norsk Geologisk Tidsskrift, v. 77, p. 165–192.
Samuelsson, J., and Butterfield, N.J., 2001, Neoproterozoic fossils from the Franklin Mountains, northwestern Canada: stratigraphic and palaeobiological implications: Precambrian Research, v. 107, p. 235–251.
Samuelsson, J., Dawes, P.R., and Vidal, G., 1999, Organic-walled microfossils from the Proterozoic Thule Supergroup, northwest Greenland: Precambrian Research, v. 96, p. 1–23.
Schiffbauer, J.D., and Xiao, S., 2009, Novel application of focused ion beam electron microscopy (FIB-EM) in preparation and analysis of microfossil ultrastructures: a new view of complexity in early eukaryotic organisms: Palaios, v. 24, p. 616–626.
Schopf, J.W., 1968, Microflora of the Bitter Springs Formation, late Precambrian, central Australia: Journal of Paleontology, v. 42, p. 651–688.
Schopf, J.W., 1992, Atlas of representative Proterozoic microfossils, *in* Schopf, J.W., ed., The Proterozoic Biosphere. Cambridge, Cambridge University Press, p. 1055–1117.
Sergeev, V.N., and Schopf, J.W., 2010, Taxonomy, paleoecology and biostratigraphy of the late Neoproterozoic Chichkan microbiota of south Kazakhstan: the marine biosphere on the eve of the metazoan radiation: Journal of Paleontology, v. 84, p. 363–401.
Simonetti, C., and Fairchild, T.R., 2000, Proterozoic microfossils from subsurface siliciclastic rocks of the São Francisco Craton, south-central Brazil: Precambrian Research, v. 103, p. 1–29.
Singh, V.K., and Babu, R., 2013, Neoproterozoic chert permineralized silicified microbiota from the carbonate facies of Raipur Group, Chhattisgarh Basin, India: their biostratigraphic significance: Geological Society of India Special Publication, v. 1, p. 1–15.
Staplin, F.L., Jansonius, J., and Pocock, S.A.J., 1965, Evaluation of some acritarchous hystrichosphere genera: Neues Jarbuch für Geologie und Paläontologie Abhandlungen, v. 123, p. 167–201.
Strother, P.K, Battison, L., Brasier, M.D., and Wellman, C.H., 2011, Earth's earliest non-marine eukaryotes: Nature, v. 473, p. 505–509.
Su, W., Li, H., Xu, L., Jia, S., Geng, J., Zhou, H., Wang, Z., and Pu, H., 2012, Luoyu and Ruyang Group at the south margin of the North China Craton (NCC) should belong in the Mesoproterozoic Changchengian System: direct constraints from LA-MC-ICPMS U-Pb age on the tuffite in the Luoyukou Formation, Ruzhou, Henan, China: Geological Survey and Research, v. 35, p. 96–108.
Swanson-Hysell, N., Rose, C.V., Calmet, C.C., Halverson, G.P., Hurtgen, M.T., and Maloof, A.C., 2010, Cryogenian glaciations and the onset of carbon-isotope decoupling: Science, v. 328, p. 608–611.
Talyzina, N.M., and Moczydłowska, M., 2000, Morphological and ultrastructural studies of some acritarchs for the lower Cambrian Lükati Formation, Estonia: Review of Palaeobotany and Palynology, v. 112, p. 1–21.
Tang, Q., Pang, K., Xiao, S., Yuan, X., Ou, Z., and Wan., B., 2013, Organic-walled microfossils from the early Neoproterozoic Liulaobei Formation in the Huainan region of North China and their biostratigraphic significance: Precambrian Research, v. 236, p. 157–181.
Timofeev, B.V., 1959, Drevneishaia flora Pribaltiki i ee stratigraficheskoe znachenie [Ancient flora of the Baltic states and its stratigraphic value]: Vseoyuznyi Neftyanoi Naucho-Issledovatelskii Geologorazvedochnyi Institut, Leningrad Trudy VNIGRI, v. 129, p. 1–136, pl. 1–24 [in Russian].
Timofeev, B.V., 1966, Mikropaleofitologicheskoe Issledovanie Drevnikh Svit [Micropaleophytological study of Ancient Suite]: Moscow, Nauka, 147 p., 89 plates [in Russian].
Timofeev, B.V., 1969, Sferomorfidy Proterozoia [Proterozoic Sphaeromorphida]: Leningrad, Akademiia Nauk SSSR, 146 p. [in Russian].
Timofeev, B.V., and Hermann, T.N., 1979, Dokembriiskaia mikrobiota Lakhandinskoi svity [Precambrian microbiota of the Lakhanda Suite], *in* Sokolov, B.S., ed., Paleontologiia Dokembriia i Rannego Kembriia [Precambrian and Early Cambrian Paleontology]: Leningrad, Nauka, p. 137–147 [in Russian].
Timofeev, B.V., Hermann, T.N., and Mikhailova, N.S., 1976, Mikrofitofossilii Dokembriia, Kembriia i Ordovika [Microphytofossils of the Precambrian, Cambrian and Ordovician]: Leningrad, Akademiia Nauk SSSR, 107 p. [in Russian].
Tynni, R., and Uutela, A., 1984, Microfossils from the Precambrian Muhos Formation in western Finland: Geological Survey of Finland Bulletin, v. 330, 38 p., 20 pl.
Valensi, L., 1949, Sur quelques microorganisms planctoniques des silex du Jurassique moyen du Poitou et de Normandie: Bulletin de la Société géologique de France, série 5, v. 18, p. 537–550 [in French].
Veis, A.F, Petrov, P.U., and Vorob'eva, N.G., 1998, Miroedikhinskaia mikrobiota Verkhnego Rifeia Sibiri. Soobshchenie 1. Sostav i fatsial'no-ekologicheskoe raspredelenie organostennykh mikrofossilii [Miroyedikha microbiota of the upper Riphean, Siberia. Report 1. Compositions and facies-ecological distribution of organic-microfossils]: Stratigrafiya, Geologicheskaya Korreliatsiya, v. 6(5), p. 15–37 [in Russian].
Vidal, G., 1976, Late Precambrian microfossils from the Visingsö beds in southern Sweden: Fossils and Strata, v. no. 9, 37 p.
Vidal, G., 1979, Acritarchs form the upper Proterozoic and lower Cambrian of East Greenland: Grønlands Geologiske Undersøgelse Bulletin, v. 134, 40 p., 7 pl.
Vidal, G., 1981, Micropalaeontology and biostratigraphy of the upper Proterozoic and lower Cambrian sequence in East Finnmark, northern Norway: Norges Geologiske Undersøkelse Bulletin, v. 362, p. 1–53.
Vidal, G., and Ford, T.D., 1985, Microbiotas from the Late Proterozoic Chuar Group (Northern Arizona) and Uinta Mountain Group (Utah) and their chronostratigraphic implications: Precambrian Research, v. 28, p. 349–389.

https://doi.org/10.1017/jpa.2016.49 Published online by Cambridge University Press

Vidal, G., and Siedlecka, A., 1983, Planktonic, acid-resistant microfossils from the upper Proterozoic strata of the Barents Sea Region of Varanger Peninsula, East Finnmark, Northern Norway: Norges Geologiske Undersøkelse Bulletin, v. 382, p. 45–79.

Vorob'eva, N.G., Sergeev, V.N., and Knoll, A.H., 2009, Neoproterozoic microfossils from the northeastern margin of the East European Platform: Journal of Paleontology, v. 83, p. 161–196.

Walter, M.R., Veevers, J.J., Calver, C.R., and Grey, K., 1995, Neoproterozoic stratigraphy of the Centralian Superbasin: Precambrian Research, v. 73, p. 173–195.

Willman, S., 2009, Morphology and wall ultrastructure of leiosphaeric and acanthomorphic acritarchs from the Ediacaran of Australia: Geobiology, v. 7, p. 8–20.

Willman, S., and Moczydłowska, M., 2008, Ediacaran acritarch biota form the Giles 1 drillhole, Officer Basin, Australia, and its potential for biostratigraphic correlation: Precambrian Research, v. 162, p. 498–530.

Xiao, S., and Knoll, A.H., 1999, Fossil preservation in the Neoproterozoic Doushantuo phosphorite Lagerstätte, South China: Lethaia, v. 32, p. 219–240.

Xiao, S., Knoll, A.H., Kaufman, A.J., Yin, L., and Zhang, Y., 1997, Neoproterozoic fossils in Mesoproterozoic rocks? Chemostratigraphic resolution of a biostratigraphic conundrum from the North China Platform: Precambrian Research, v. 84, p. 197–220.

Xiao, S., Yuan, X., Steiner, M., and Knoll, A.H., 2002, Macroscopic carbonaceous compressions in a terminal Proterozoic shale: a systematic reassessment of the Miaohe biota, South China: Journal of Paleontology, v. 76, p. 347–376.

Yakshchin, M.S., and Luchinina, V.A., 1981, Novye Dannye po iskopaemym vodorosliam semeistva Oscillatoriaceae (Kirchn.) Elenkin [New data on fossil algae in Family Oscilliatoriacea (Kirchn.) Elenkin], *in* Meshkova, N.P., and Nikolaeva, E.B., eds., Pogranichnye otlozhenyia Dokembryia i Kembryia Cibirskoi platformi (biostratigrafiya, paleontologia, usloviya obrazovaniya) [Border Precambrian and Cambrian deposits of the Siberian platform (biostratigraphy, paleontology and conditions of formation)], Novosibirsk, Nauka, p. 28–34 [in Russian].

Yan, Y.-Z., and Liu, Z.-L., 1993, Significance of eucaryotic organisms in the microfossil flora of Changcheng System: Acta Micropalaeontologica Sinica, v. 10, p. 167–180 [in Chinese with English abstract].

Yan, Y.-Z., and Zhu, S.-X., 1992, Discovery of acanthomorphic acritarchs form the Baicaoping Formation in Yongjia, Shanxi and its geological significance: Acta Micropaleontologica Sinica, v. 9, p. 267–282.

Yin, L.-M., 1997, Acanthomorohic acritarchs form the Meso-Neoproterozoic shales of the Ruyang Group, Shanxi, China: Review of Palaeobotany and Palynology, v. 98, p. 15–25.

Yin, L.-M., and Sun, W.-G., 1994, Microbiota from the Neoproterozoic Liulaobei Formation in the Huainan region, northern Anhui, China: Precambrian Research, v. 65, p. 95–114.

Yuan, X., and Hofmann, H.J., 1998, New microfossils from the Neoproterozoic (Sinian) Doushantuo Formation, Wengan, Guizhou Province, southwestern China: Alcheringa, v. 22, p. 189–222.

Zang, W.-L., 1995, Early Neoproterozoic sequence stratigraphy and acritarch biostratigraphy, eastern Officer Basin, South Australia: Precambrian Research, v. 74, p. 119–175.

Zang, W.-L., and McKirdy, D.M., 1994, Microfossils and molecular fossils from the Neoproterozoic Alinya Formation—a possible new source rock in the eastern Officer Basin: PESA Journal, v. 22, p. 89–90.

Zang, W.-L., and Walter, M.R., 1992, Late Proterozoic and early Cambrian microfossils and biostratigraphy, northern Anhui and Jiangsu, central-eastern China: Precambrian Research, v. 57, p. 243–323.

Zimmer, A., Lang, D., Richardt, S., Frank, W., Reski, R., and Rensing, S., 2007, Dating the early evolution of plants: detection and molecular clock analyses of orthologs: Molecular Genetics and Genomics, v. 278, p. 393–402.

Accepted 7 October 2015